

Characterizing Inter-Layer Functional Mappings of Deep Learning Models

Donald Waagen, Katie Rainey, Jamie Gantert, David Gray, Megan King, M. Shane Thompson, Jonathan Barton, Will Waldron, Samantha Livingston, and Don Hulsey

Abstract—Deep learning architectures have demonstrated state-of-the-art performance for object classification and have become ubiquitous in commercial products. These methods are often applied without understanding (a) the difficulty of a classification task given the input data, and (b) how a specific deep learning architecture transforms that data. To answer (a) and (b), we illustrate the utility of a multivariate nonparametric estimator of class separation, the Henze-Penrose (HP) statistic, in the original as well as layer-induced representations. Given an N -class problem, our contribution defines the $C(N, 2)$ combinations of HP statistics as a sample from a distribution of class-pair separations. This allows us to characterize the distributional change to class separation induced at each layer of the model. Fisher permutation tests are used to detect statistically significant changes within a model. By comparing the HP statistic distributions between layers, one can statistically characterize: layer adaptation during training, the contribution of each layer to the classification task, and the presence or absence of consistency between training and validation data. This is demonstrated for a simple deep neural network using CIFAR10 with random-labels, CIFAR10, and MNIST datasets.

Index Terms—Neural networks, nonparametric statistics, divergence measures, classification, deep learning, model optimization



1 INTRODUCTION

DEEP learning architectures have become the new standard practice for solving pattern recognition and machine learning problems due to their predictive performance across a variety of datasets. However, the design process continues to be an ad hoc process considering these black box systems can have millions of free parameters. Most practitioners select a member of the standard set of architectures that have been shown to work well on related problems and make small adjustments or modifications to the respective architecture.

Beyond predictive performance, many questions remain. Interpretability and model explanation are becoming important requirements as deep learning architectures are increasingly incorporated into critical systems. We believe that understanding the nature of the data with respect to the task and the transformations induced by the model on the data are essential steps to facilitate trust and robustness for these systems.

Understanding the nature of deep learning functional mappings has been and continues to be an exciting area

of research. Visualization techniques abound (e.g. activation maps [1]) which attempt to identify the spatial regions and the associated neurons of importance in the classification of an image. Estimates of the sensitivity of the network to perturbations at each neuron [2] can provide insight into the relative importance of each neuron in the network to overall performance.

Zhang et al. [3] demonstrated that modern deep learning models (e.g. AlexNet [4]) have the capacity to memorize random labels. The generalization paradox describes the phenomenon that deep learning models have generalized well despite the high capacity. The mechanism of learning and associated generalization in the presence of high-capacity learning was posed by Bartlett et al. [5] who demonstrate margin gap analysis on the output layer in an attempt to address the paradox of generalization and capacity. The link between generalization and flat minima [6] is an area of current interest. Chaudhari et al. [7] exploit stochastic gradient descent (SGD) to favor flat minima and maximize the generalization of the derived solution. Dziugaite and Roy [8] utilize flat minima in a Probably Approximately Correct (PAC)-Bayes setting to derive numerical bounds for the generalization error of deep neural network models.

1.1 Our contribution

Our research is not attempting to quantify the resultant generalization of the output. Rather, we seek to characterize the utility of the functional mappings occurring within each layer of a deep learning network. Note that we focus on the functional mapping of a layer, not the individual neurons. This focus on layer induced mappings is also seen in earlier work by members of our team [9].

For our purposes, producing deep learning models that achieve *state-of-the-art* or *super-human* performance is *not* a

- Donald Waagen is with the Air Force Research Laboratory, Eglin Air Force Base, FL.
E-mail: donald.waagen@us.af.mil
- Katie Rainey is with the Space and Naval Warfare Systems Center Pacific, San Diego, CA.
E-mail: kate.rainey@navy.mil
- Jamie Gantert and David Gray are with the Air Force Research Laboratory, Eglin Air Force Base, FL.
- Megan King and Shane Thompson are with the Army Combat Capabilities Development Command, Aviation and Missile Center, Redstone Arsenal, AL.
- Jonathan Barton, Will Waldron, and Don Hulsey are with Dynetics, Inc., Huntsville, AL.
- Samantha Livingston is with Modern Technology Solutions, Inc., Alexandria, VA.

Distribution A: Approved for public release, distribution is unlimited, 96TW-2018-0343.

goal for this paper. Insight into the changes in class sample separation as the data are transformed through a deep learning model is the goal. Class-pair separation is estimated via the Henze-Penrose (HP) statistic. Given an N -class problem, we compute the $C(N, 2)$ combinations of HP statistics and treat them as a collection or sample from a distribution of separations. These statistics can also be computed for the data in the original measurement space (e.g. image), as well as at any location within a deep learning model. This allows us to statistically characterize the distributional change induced by each layer of the model with respect to the overall classification task. By computing and comparing these samples of separation statistics on deep models in different states, we can numerically quantify the changes to the data, as well as the changes to the data representations in the model.

The experiments are designed to compare and contrast the mappings learned under various data-label conditions: well separated data, poorly separated data, and identically distributed data. All experiments were performed using a single simple convolutional neural network architecture which is outlined in Section 3.2.

Given this simple motivational framework, we wish to investigate the following questions:

- How separable are the classes in the original measurement space (Section 4.1)?
- What happens to the data when passed through a model before training (Section 4.2)?
- How much adaptation has a representation produced by a layer undergone during training (Section 4.3)?
- How much is each layer contributing to the classification process (Section 4.4)?
- Which layers in the trained model transform the validation and training data equivalently, and conversely, differently? (Section 4.5)?

Answering these questions can provide a practitioner insight into model design, optimization, and robustness. In this paper, we provide a short and very myopic discussion on nonparametric tests and estimators of distributional separation in Section 2. We then discuss the datasets in Sections 3.1 and 4.1, a simple convolutional neural network model in Section 3.2, and the training process used in our experiments. Finally, we present the experiment results including nonparametric statistical hypothesis tests to address the questions above in Section 4. Note that a supplemental document is provided that includes the results in greater detail.

2 NONPARAMETRIC TWO SAMPLE TESTS

Statisticians have been and continue to be interested in defining procedures and tests for sameness. For example, given two random variables X and Y with cumulative distributions F_X and G_Y , define a procedure to test $H_0 : \phi(X) = \phi(Y)$ vs. $H_A : \phi(X) \neq \phi(Y)$, where $\phi(X)$ represents the distribution or a statistic (e.g. mean, variance) of the random variables X . Many tests make some strong assumptions about the distributional form of F_X and G_Y ,

while other procedures, called distribution-free or nonparametric tests, require minimal prior information on the nature of the distributions. For the purposes of this paper, we are interested in nonparametric measures of the distributional differences between X and Y , (i.e. under the $H_A : F_X \neq G_Y$ hypothesis).

Given two univariate and independent sample observations $X_n = (x_1, x_2, x_3, \dots, x_n)$ and $Y_m = (y_1, y_2, y_3, \dots, y_m)$ of random variables X and Y , Wald and Wolfowitz [10] defined the runs test, a nonparametric procedure to test the hypothesis $H_0 : F_X = G_Y$ vs. $H_A : F_X \neq G_Y$. The construction of the test consists of pooling the $N = n + m$ samples and sorting the pooled sample, generating an ordered list. From the ordered list, replace the values with their associated class labels C and count the number of runs, i.e., the number of consecutive sequences of identical labels, or equivalently, the number of times the i th and i th+1 class labels $c_{(i)}$ and $c_{(i+1)}$ disagree. Let R denote the number of runs and S be the number of times neighboring ordered labels disagree, giving $R = S + 1$ and $S = \sum_{i=1}^{N-1} |c_{(i)} \neq c_{(i+1)}|$.

The expected value and expected variance of R under H_0 are

$$\mathbb{E}(R) = \frac{2mn}{m+n} + 1 \quad (1)$$

$$\sigma^2(R) = \frac{2mn(2mn - m - n)}{(m+n)^2(m+n-1)}, \quad (2)$$

respectively. The null hypothesis $H_0 : F_X = G_Y$ can then be rejected or fail to be rejected using the Wald-Wolfowitz test statistic

$$W = \frac{R - \mathbb{E}(R)}{\sqrt{\sigma^2(R)}} \quad (3)$$

which asymptotically converges to a standard normal distribution $N(0, 1)$ as $m, n \rightarrow \infty$. Wald and Wolfowitz point out that the runs test is a one-sided test, that is, rejection of the null hypothesis occurs for small W .

In high dimensional spaces, the concept of defining a strict ordering via sorting of samples becomes ill-defined. This led Friedman and Rafsky [11] to develop a surrogate method for defining an ordering and generalizing Wald's runs test for multivariate data. Let $\mathbf{X}, \mathbf{Y} \in \mathbb{R}^d$ denote two multivariate random variables with distributions $F_{\mathbf{X}}$ and $G_{\mathbf{Y}}$, and let $X_n = (x_1, x_2, x_3, \dots, x_n)$ and $Y_m = (y_1, y_2, y_3, \dots, y_m)$ denote n and m *i.i.d.* observations of \mathbf{X} and \mathbf{Y} , respectively. To test $H_0 : F_{\mathbf{X}} = G_{\mathbf{X}}$ vs. $H_A : F_{\mathbf{X}} \neq G_{\mathbf{X}}$, Friedman pools the samples $Z_{n+m} = X_n \cup Y_m$ and constructs a minimal spanning tree $T = (E, V) = \text{MST}(Z)$ on the pooled sample Z . The sample observations from Z define the vertices V of the graph, and the ordering is defined by the set of edges E connecting the sample points. By construction, the number of edges $|E|$ in T is $n + m - 1$. Let $E_c \subset E$ denote the subset of edges of E connecting vertices $v_i, v_j \in V$ associated with differing class labels, that is, $\text{class}(v_i) \neq \text{class}(v_j)$. The Friedman-Rafsky test statistics S is defined as the number of edges in T which connect vertices with differing class labels, $S = |E_c|$. Closely related to S is the *runs* statistic R which is defined as the number of connected sets produced when the edges that connect vertices connecting different labels are removed, with $R = S + 1$. This statistic is a member of

complexity measures identified and used for characterizing the complexity of a classification problem [12].

Friedman and Rafsky also provide the asymptotic convergence of W for the multivariate case, for which (1) and (3) are shown to still hold. However, the variance has the form

$$\sigma^2(R|C) = \frac{2mn}{N(N-1)} \left[\frac{2mn - N}{N} + \frac{C - N + 2}{(N-2)(N-3)} [N(N-1) - 4mn + 2] \right] \quad (4)$$

where C is the number of edge pairs that share a common node. Thus the variance under H_0 is conditioned on the topology of the minimal spanning tree. Fixing the topology and performing a permutation test under H_0 sampling values of R with randomly permuted class labels allows one to empirically calculate $\sigma^2(R) \equiv \sigma^2(R|C)$.

2.1 Connections to the f -Divergence Function Family

The f -divergence functions [13] are a family of general measures of distributional separation between two probability distributions. Henze and Penrose [14] proved that a simple function of the Friedman-Rafsky statistic S asymptotically converges to a member of the f -divergence family. Given samples X_n and Y_m sampled from probability distributions f and g , they show that

$$\frac{S}{n+m} \rightarrow 2qp \int \frac{f(x)g(x)}{pf(x) + qg(x)} d\mathbf{x} = 1 - \delta(f, g, p) \quad (5)$$

where

$$\delta(f, g, p) = \int \frac{p^2 f^2(x) + q^2 g^2(x)}{pf(x) + qg(x)} dx \quad (6)$$

as $n, m \rightarrow \infty$ in a linked manner (*i.e.* $\frac{m}{m+n} \rightarrow p$ and $q = 1 - p$), with $\delta(f, g, p)$ in (6) being a member of the f -divergence family of functions. Therefore, given two multivariate samples X_n, Y_m , the Friedman-Rafsky test statistic S can provide a sample-based estimate of the distributional separation in high dimensions, that is,

$$\hat{\delta}(X_n, Y_m, p) = 1 - \frac{S}{n+m}. \quad (7)$$

Under the null hypothesis $H_0 : F = G$, $\delta(f, g, p) \equiv \delta(f, f, p) = p^2 + q^2$, and the distribution of the sample statistic $\hat{\delta}$ under H_0 is conditioned on the proportion of points from each class (the values of p and q). For example, when $p = 0.5$, $\mathbb{E}_{H_0}[\hat{\delta}(X_n, Y_n, 0.5)] = 0.5$.

Extending the work of Henze and Penrose, Berisha et al. [15] define a closely related distributional measure of separation, which they denote as $D_p(f, g)$, defined as

$$D_p(f, g) = \frac{1}{4pq} \left[\int \frac{(pf(x) - qg(x))^2}{pf(x) + qg(x)} dx - (p - q)^2 \right]. \quad (8)$$

Berisha demonstrates that under $H_0 : F_x = G_y$, $D_p(f, g) = D_p(f, f) = 0$. Thus, the expected value of D_p under H_0 is zero and is independent of the prior p .

Similar to Henze and Penrose and under the same linked conditions previously described, Berisha proves that

a simple function of the Friedman-Rafsky test statistic S converges asymptotically to (8),

$$1 - S \frac{n+m}{2nm} \rightarrow D_p(f, g). \quad (9)$$

As one can see from (9), a sample-based estimate of $D_p(f, g)$ can easily be computed using the Friedman-Rafsky statistic S . Given two multivariate samples X_n and Y_m , the sample estimate of $D_p(f, g)$, which we denote as \mathcal{H} , is given by

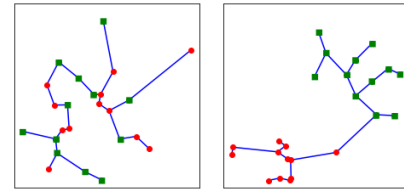
$$\mathcal{H} = 1 - S \frac{n+m}{2nm}. \quad (10)$$

We refer to \mathcal{H} in (10) as the Henze-Penrose-Berisha-Hero divergence sample statistic, or HP statistic for short. When the class sample sizes are equal (*i.e.* $m = n$)

$$\mathcal{H} = 1 - S \frac{n+m}{2nm} = 1 - 2 \frac{S}{n+m}, \quad (11)$$

which is equivalent to a rescaling of (7).

\mathcal{H} has the desirable property of providing consistent and easily interpretable results, generating values near zero when the two distributions are statistically indistinguishable, and near one when the distributions are well separated. Figure 1 provides an example of minimal spanning trees and associated Friedman-Rafsky and HP statistics (S, \mathcal{H}) under mixed and well separated distributional conditions.



(a) $S=11, \mathcal{H}=0.08$ (b) $S=1, \mathcal{H}=0.92$

Fig. 1: Friedman-Rafsky (S) and Henze-Penrose-Berisha-Hero (\mathcal{H}) statistics for (a) mixed and (b) separated samples.

Given a measure of proximity, the simple nonparametric statistic such as the \mathcal{H} is invariant to changes in rotation and scale. Additionally, since it can be computed in arbitrarily finite dimensional spaces, computing and comparing class separation in differently dimensioned representations is easily performed. One can therefore compare the distributional separation between classes before and after a functional transformation $f : \mathbb{R}^d \rightarrow \mathbb{R}^p$ is applied.

A caveat to this approach is that the measure of proximity applied to the measurements should be consistent with the algorithmic mappings under evaluation and/or thoughtfully selected by the practitioner. For instance, Euclidean distance may not be the best measure for comparing images or signals without an alignment or correlation of the data measurements. With this in mind and given an appropriate proximity/distance measure, one can meaningfully compare the distributional separation in the original representation space as well as the separation in the space induced by a mathematical mapping (*e.g.* feature transfor-

mation)¹. Distributional separation for multiple classes can be computed pairwise or as one against all. For our experiments, we will compute the pairwise separation between classes and compare/contrast the sample distributions of those statistics. Because Euclidean distance is the typically proximity measure applied with \mathcal{H} , our baseline analysis uses it.² An equivalent analysis was also performed with cosine distance as the measure for computing \mathcal{H} . It produced results consistent with the Euclidian distance case.³

For all the datasets under evaluation, this work will compare and contrast the \mathcal{H} computed between all pairs of classes. Let \mathcal{H} denote the set or distribution of all class pairwise \mathcal{H} values computed between all classes in the population, that is,

$$\mathcal{H} = \{\mathcal{H}(x_i, x_j) \quad \forall i, j = 1, 2, \dots, n, i < j\} \quad (12)$$

where $\mathcal{H}(x_i, x_j)$ is the HP divergence between samples from class x_i and x_j , and n is the number of classes in the data. And given a sample \mathcal{H} , let $\bar{\mathcal{H}}$ denote its sample mean,

$$\bar{\mathcal{H}} = \frac{2}{n(n-1)} \sum_i \sum_{j|i < j} \mathcal{H}(x_i, x_j) \quad (13)$$

In all of our experiments, there are 10 classes defined in each dataset, and therefore 45 pairwise \mathcal{H} (i.e. $C(10, 2)$) values define the set or distribution of \mathcal{H} values. This set quantifies the pairwise separation between all the classes in a space, which allows us to compare and statistically evaluate \mathcal{H} for the original measurement space, as well as the representations produced on the data by the transformations defined by the deep learning model.

For the discussions that follow, let $\mathcal{H}_{(L,M)}$ denote the distribution of HP statistics for the output of layer L of a model and at a prescribed model state M . We limit our analysis of model states M to two values, specifically $M = 0$ (when initialized) and $M = T$ (final or trained). Let $\mathcal{H}_{(L,M)}^{(t)}$ and $\mathcal{H}_{(L,M)}^{(v)}$ represent the sets of \mathcal{H} values for training and validation data, respectively. If the superscript is not explicitly provided, the set corresponds to the training set, that is, $\mathcal{H}_{(L,M)} \equiv \mathcal{H}_{(L,M)}^{(t)}$.

3 METHODOLOGY

3.1 The datasets a.k.a. the Good, the Bad, and the Ugly

Our experimental design matrix is given in Table 1. The experimental datasets we use for illustration and analysis include the public domain MNIST [16] and CIFAR10 [17] datasets, as well as the CIFAR10 dataset with randomly permuted labels. By permuting the CIFAR10 dataset labels, each sampled pseudo-class actually consists of examples from all classes, and therefore each class is sampling from the same underlying distribution.

We randomly subdivided the nominal training data for CIFAR10 (50,000 example image chips) and MNIST (60,000

1. Note that this classification-oriented comparative analysis is not just for analysis of deep learning models, but can be useful in evaluating the representations produced by any functional mapping for classification, including engineered features selected by experts.

2. Additional analysis results are included in the supplemental material.

3. The results of the analysis using cosine distance are included in the supplemental material.

TABLE 1: Model Instances

Dataset	Class Labels	Spaghetti Western
		Projection
MNIST	Truth	<i>the Good</i>
CIFAR10	Truth	<i>the Bad</i>
CIFAR10	Random	<i>the Ugly</i>

example image chips) into non-overlapping training and validation subsets. Our validation subsets for CIFAR10 and MNIST each contain 1,000 examples per class, leaving 50,000 and 40,000 images in the training subsets, respectively. The 10,000 image test datasets for CIFAR10 and MNIST were maintained as the source provided. For the CIFAR10 randomized label experiments, we copied the CIFAR10 training and validation subsets with their true labels and generated pseudo-class identifiers for the images by randomly permuting labels within each subset. The randomized labeling processes was repeated five times to generate five different instances of the CIFAR10 dataset with random labels for use in training multiple models.

For the statistical analysis of each neural network model, we randomly selected an analysis sample from each training subset such that the sample contained 10,000 images with 1,000 images per class to match the size and class composition of the images in the associated validation subset. By restricting the sample size, the analysis becomes more computationally tractable. The statistical characterization of data passing through a neural network was performed using the 10,000 sample subset of training data and the full 10,000 sample validation dataset.

For each experiment, we implemented and trained our reference convolutional neural network model with Tensorflow 1.8 [18] using the Keras 2.1 [19] interface. During training, we selected categorical cross entropy as the loss function and simple stochastic gradient descent for optimization with nominal hyperparameters (minibatch size of 32 and learning rate fixed at 0.01). No regularization or data augmentation was applied during training. In the experiments using true labels, we trained five different network instances per experiment, each starting with different random initializations of the layer weights (sampling from Glorot uniform distributions). Training was stopped when the peak accuracy was achieved on the validation set. For the random label case, five network instances were also trained with different random initializations of the layer weights. However, a different instance of the randomly-permuted image labels was used for each. The training ended at 200 epochs. This provided a sufficient number of epochs for the classification performance of the model to stabilize.

To test various hypotheses and evaluate the mappings of the network models with respect to the training and validation data, we apply a permutation test [20]. For each hypothesis test, the permutation tests are estimated via Monte Carlo sampling, with 50,000 samples generated to estimate each distribution under the null hypothesis. A critical value of $\alpha = 0.025$ is chosen for our threshold of statistical significance for all tests.

3.2 Our Black Box: a simple convolutional neural network

A single, simple representative convolutional neural network architecture is defined for our experiments to facilitate communication of the concepts and interpretation of the results. The model architecture is outlined in Table 2. We are not precluded from analyzing deeper and/or complex architectures, but our choice of a simple model is driven by a desire to maximize transparency in the approach and analysis.

TABLE 2: Experimental Convolutional Neural Network

Layer	Type	Configuration
0.Input	Input Space	Rows x Columns x Channels
1.Conv	2D Convolutional Layer	32 3x3xChannels
1.ReLU	ReLU Activation	
2.Conv	2D Convolutional Layer	32 3x3
2.ReLU	ReLU Activation	
2.MaxPool	Max-Pooling Operation	2x2
3.Conv	2D Convolutional Layer	64 3x3
3.ReLU	ReLU Activation	
4.Conv	2D Convolutional Layer	64 3x3
4.ReLU	ReLU Activation	
4.MaxPool	Max-Pooling Operation	2x2
5.Dense	Fully Connected Dense Layer	512
5.ReLU	ReLU Activation	
6.Dense	Fully Connected Dense Layer	10
6.SoftMax	Softmax Activation	

4 ANSWER ME, THESE QUESTIONS THREE – I MEAN FIVE

4.1 Class separability in the original measurement space

When a practitioner is supplied a set of measurements and a task, one of the first questions to be investigated should be in regards to how easy or difficult the task is given the measurements as represented in the original measurement space. For a classification task, this can be subdivided into two subproblems: (1) what is the ratio of the signals of interest to the not-signals of interest in the measurements, and (2) how different are the signals of interest. Signal conditioning or preprocessing is generally performed to retain as much of the differences of the signals of interest as possible while minimizing any non-signal content in the measurements in the process. However, this can require human intervention. It has been a goal of machine learning to eliminate the task of preprocessing as much as possible, allowing the system to learn what is signal and what is not. Therefore, we wish to understand what the intrinsic separation of classes are in the ambient (measurement) representation *before* any signal conditioning or algorithmic transformations are performed.

For each dataset, we compute the set of class-pairwise statistics $\mathcal{H}^{(t)}$ and $\mathcal{H}^{(v)}$ for training and validation samples, respectively. The lower-triangular breakdown of the individual \mathcal{H} values and a kernel density estimate of the

$\mathcal{H}^{(t)}$ and $\mathcal{H}^{(v)}$ distributions are presented in Figure 2. As can be seen, the corresponding training and validation distributions are visually similar (and will be statistically characterized in the subsections below), while the distributions for each task are all quite different.

As indicated in Figure 2, the class pairwise \mathcal{H} statistics for the MNIST dataset given the true class labels are all between 0.9 and 1.0, which indicate that measurements from each class are quite well separated from each other *in the original space*. The lowest \mathcal{H} value, corresponds to the 4 and 9 class problem (see Figure 2C), which is naturally the easiest pair to confuse. For the CIFAR10 dataset, given true class labels, the \mathcal{H} values vary widely, ranging from 0.05 to 0.8. From Figure 2B, the HP statistics are lowest for the Cat-Dog and Bird-Deer image class distributions, while Ship-Frog images have the highest value. CIFAR10 is obviously more difficult than MNIST due to the less processed nature of data (exemplars are not necessarily centered, etc.) which is captured by the HP statistics.

The matrix of pairwise values for the CIFAR10 with random class labels (Figure 2A) provides more insight into the behavior of the HP-statistic. In this case, the distributional separation of the pseudo-labels should be near zero, since each pseudo-class is sampled from the union of classes. This is indeed the case, as the histogram of statistics (Figure 2D) is centered around 0 for these pairs, with the HP test statistics indicating that the class labels are well mixed (which is by experimental design). By applying the HP statistic to a classification task, a practitioner can learn about the difficulty or impossibility of data classification using the unaltered/initial data representations. The information about the difficulty of the task will provide valuable guidance in signal conditioning or potential model designs to perform the given classification task.

The utility of estimating the difficulty of a problem given a set of measurements should not be underestimated. As shown in Figure 2D, the distribution of \mathcal{H} statistics for each task are linearly separable from each other. Therefore, under the Euclidean measure of proximity and the original representations (i.e. pixels), we have discovered a natural and unambiguous easy-harder-hardest ordering for the classification tasks, with MNIST being the easiest and CIFAR10 with random class labels being extremely difficult. Furthermore, we now have baseline estimates of separation which we can compare with estimates of separation generated by the layers of the deep learning models. Given these distributions, we can now evaluate the interlayer representations produced by the deep learning model.

4.2 Inside the Black Box: before training

We wish to characterize the transformations produced by the neural network layers at model initialization as well as after training. Characterizing the model at initialization allows one to define a baseline to compare with the model produced via the training process, enabling quantification of the adaptation (or learning) that each model layer undergoes as a model is trained.

For deep learning model initialization, a lesson every practitioner is taught early in their machine learning education is that their model layers are to be initialized with small

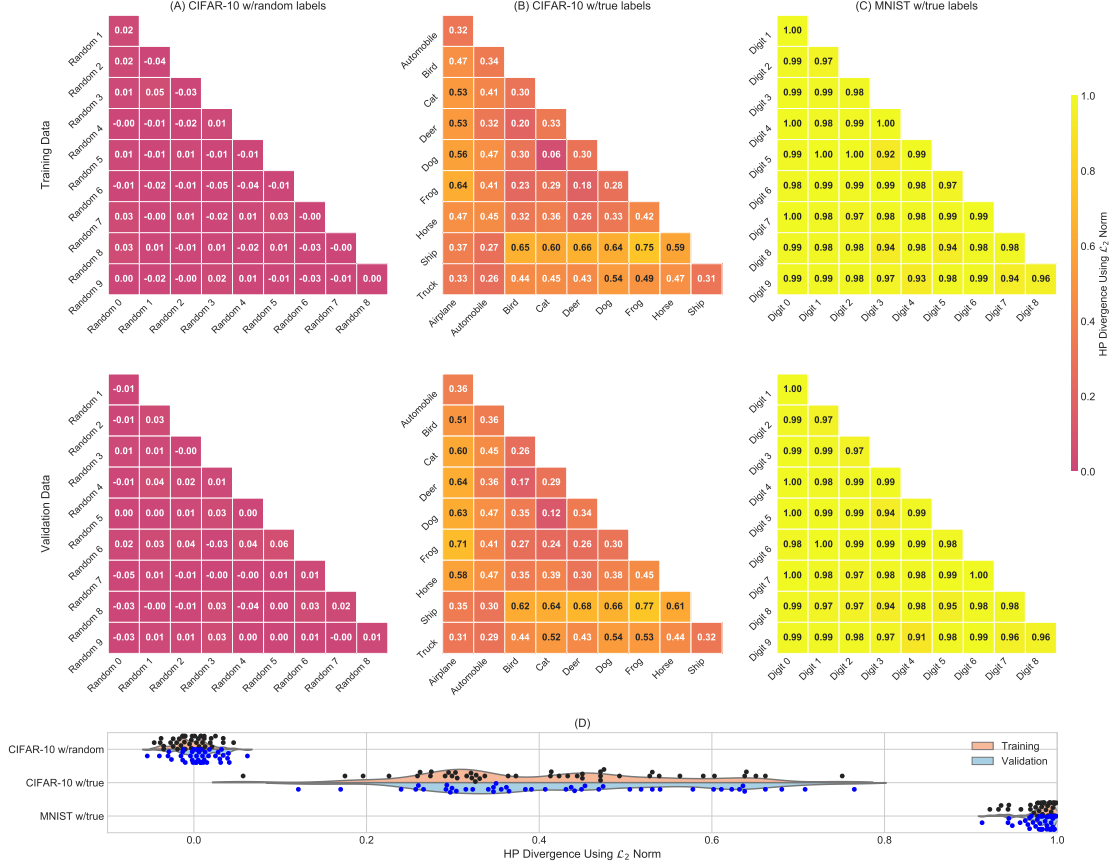


Fig. 2: Pairwise class HP statistics (training data above, validation data below) computed on (A) CIFAR10 with random labels, (B) CIFAR10 with true labels, and (C) MNIST with true labels. (D) The $\mathcal{H}^{(t)}$ (black dots, above), $\mathcal{H}^{(v)}$ (blue dots, below) values and respective kernel-based density functions (orange = training, blue = validation) for each task, which illustrate that the estimated class separation for each task in their respective ambient representations are quite distinct.

random values. These values are generally drawn from a normal distribution and appropriately scaled by a function of the number of filters in the layer.

This random initialization has an interesting property. In 1984, Johnson and Lindenstrauss [21] proved that any n point subset of Euclidean space can be mapped into a random subspace of $k = \mathcal{O}(\log n/\epsilon^2)$ dimensions, and the interpoint distances of the points projected in that subspace differ from the distances in the original space only by $(1 \pm \epsilon)$. Increasing k , the number of random projections, decreases the expected interpoint distance error. Thus, the process of randomly initializing the weights of each layer can possibly act as a set of random projections and retain the interpoint distances in the original space within some distortion value ϵ . That is, a deep learning layer may retain the interpoint distances of the training and validation sets via the random initialization alone. This is a motivational factor in the design of *extreme learning machines* [22], which randomly initialize and fix the single hidden layer input weights. In effect, random projections can provide ‘data-agnostic transfer learning’ as they can retain interpoint distances independent of the input data distributions. This is something to note, as it provides the mechanism for the initial state of a deep learning system to ‘do no harm’. It also would allow arbitrarily large networks to operate on relatively easy problems within the bounds of the product of

the distortions induced at each layer $(1 \pm \epsilon) = \prod_{i=1}^N (1 \pm \epsilon_i)$.

For each layer of the neural network model, we compute the class-pair HP statistics for the induced representations of the training and validation data. Figure 3 illustrates the \mathcal{H} distributions at the output of each layer of randomly initialized networks. In each figure, the HP statistics for the training data are represented by top/black dots and an orange kernel density at each layer of the network, and the HP statistics generated by the test data are represented by bottom/blue dots and a corresponding blue kernel density estimate.

The motivation for this discussion is two-fold. First, demonstrating that random initialization of deep learning models can maintain the interpoint distances between classes. Second, this initialized behavior provides us a baseline to quantify the effective changes in the distribution of class-pair separation \mathcal{H} produced in training the models. Figure 3 illustrates the distribution of \mathcal{H} statistics produced by each layer for the initialized models before any adaptation or training. We are interested to test if the initialized state of each layer is behaving as a set of distance-preserving random projections, or given an appropriate number of random projections, if the average class-pair separation between input and output spaces are statistically equivalent. A nonparametric two-sided permutation test of the statistical equivalence of the mean class separation $\bar{\mathcal{H}}$ (13) between

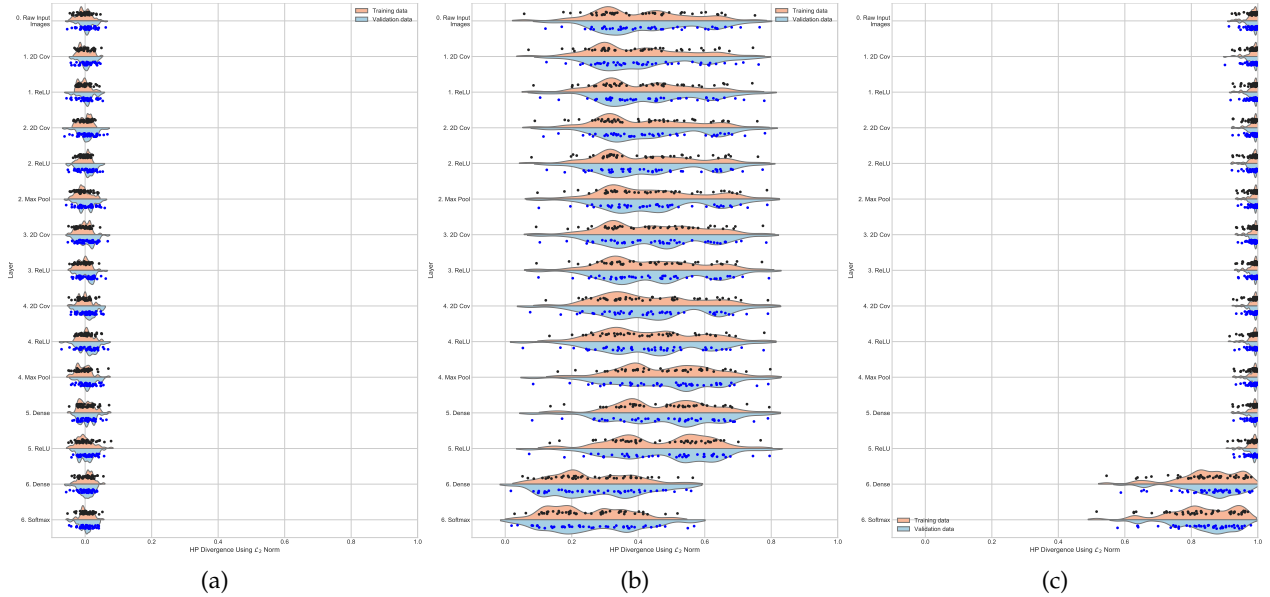


Fig. 3: \mathcal{H} class-pair statistics at each layer for the randomly initialized model state (epoch 0) for (a) CIFAR10 with random class labels, (b) CIFAR10 with true class labels, and (c) MNIST with true class labels.

the input and output spaces of each layer is applied. For each layer, the hypotheses under test corresponds to the following:

$$\mathbf{H}_0 : \bar{\mathcal{H}}_{(k-1,0)} = \bar{\mathcal{H}}_{(k,0)} \quad vs. \quad \mathbf{H}_A : \bar{\mathcal{H}}_{(k-1,0)} \neq \bar{\mathcal{H}}_{(k,0)} \quad (14)$$

For each layer, we select an $\alpha = 0.025$ level of significance for the two-sided test, and compute the p -values for the model instances of each task. These results are summarized in Table 3.

Table 3 demonstrates that even the simple convolutional neural network model (as defined in Table 2) has sufficient number of convolutional filters such that the random values in each layer preserve the intrinsic separation between the three datasets. The notable exception is the 6.Dense layer, for which the null hypothesis is rejected in 12 of the 15 experiments. Note that the input space of the 6.Dense layer is 512, but the output space is the number of classes, which in each case is 10 dimensional. Hence the change in class interpoint distances is easily explained by the expected distortion induced by randomly projecting the originally high dimensional data into a 10 dimensional subspace.

In our view, this distance preserving property of the initialization phase has positive and negative consequences. On the positive side, any adequately sized initialized model has the demonstrable ability to retain interpoint distances between classes. On the negative side, this ‘do no harm’ property allows a machine learning practitioner to blindly apply any deep learning model to a task at hand without spending time understanding the data and underlying phenomenon being operating on, treating the model as a black box. While the ability to apply any deep learning model to multiple tasks is not necessarily negative, we caution application without an understanding and deep analysis of the original task versus any new task and the potential hidden affects of doing so.

4.3 Inside the Black Box: layer adaptation

As described in the previous section, five model instantiations are trained on each task, where training is stopped (a) when training performance vs the validation performance is maximal, or (b) in the random label case, after 200 epochs. Figure 4 illustrates the training (orange, above) and validation (blue, below) \mathcal{H} statistics at each layer of a trained model for each dataset.

As previously discussed, one would hope that what is learned by a model via training manifests itself as a concentration of class measure, that is, some combination of within-class distances decreasing and/or between-class distances increasing. The HP statistics would capture this concentration with a corresponding higher value as a result of fewer edges in a minimal spanning tree connecting disparate class samples. Therefore, using the training set we compare the class separation statistics in each layer before and after training, and test if there is a statistical significant change to mean class separation $\bar{\mathcal{H}}$ (13). Using a permutation test, we test the following hypotheses:

$$\mathbf{H}_0 : \bar{\mathcal{H}}_{(k,T)} - \bar{\mathcal{H}}_{(k,0)} \leq 0 \quad vs. \quad \mathbf{H}_A : \bar{\mathcal{H}}_{(k,T)} - \bar{\mathcal{H}}_{(k,0)} > 0 \quad (15)$$

For each model instantiation, the mean differences and associated p -values for (15) are given in Table 4.

In reviewing the mean difference statistics and associated p -values in Table 4, one will note that for all datasets the mean separation as estimated by $\bar{\mathcal{H}}$ for the first convolutional and ReLU layers have not significantly improved between initialized and trained states. Moreover, in four out of five models for the CIFAR10 dataset trained with random labels and all five MNIST trained models, we fail to reject that all the convolutional layers of the trained network are producing statistically equivalent or less class separation statistics. These two cases are extreme, one being quite easy, and the other impossible. In neither case are the models required or able to improve class separation in the con-

TABLE 3: Two-sided permutation test to detect change in $\bar{\mathcal{H}}$ between layers (before training) with critical value $\alpha = 0.025$. **Red font** denotes layer instances for which we reject \mathbf{H}_0 , and black font denotes layers for which we fail to reject \mathbf{H}_0 (14). (Note: $\Delta\bar{\mathcal{H}} = \bar{\mathcal{H}}_{(k,0)}^{(t)} - \bar{\mathcal{H}}_{(k-1,0)}^{(t)}$)

Input Space	Output Space	CIFAR10 w Random		CIFAR10 w True		MNIST w True	
		$\Delta\bar{\mathcal{H}}$	p -values	$\Delta\bar{\mathcal{H}}$	p -values	$\Delta\bar{\mathcal{H}}$	p -values
0.Input	1.Conv	.003; .002; -.004; .003; -.003	.460; .649; .445; .556; .515	-.012; .005; -.017; -.003; -.004	.714; .864; .593; .923; .912	.002; .001; -.001; .000; .000	.672; .792; .864; .934; .900
1.Conv	1.ReLU	-.002; -.003; .004; .002; .003	.531; .523; .434; .675; .641	.016; -.022; -.003; .001; -.000	.607; .463; .933; .969; .991	.001; .000; .001; .002; .000	.875; .906; .713; .648; .918
1.ReLU	2.Conv	.003; .001; -.001; -.002; -.001	.375; .801; .856; .650; .906	.003; -.006; -.001; -.009; -.005	.924; .842; .964; .771; .878	.000; -.000; -.001; -.001; -.000	.970; .981; .878; .826; .933
2.Conv	2.ReLU	-.001; -.002; .003; -.002; .001	.671; .626; .526; .667; .906	.002; -.017; .005; -.003; .003	.959; .562; .869; .929; .912	-.001; -.000; -.001; -.001; .001	.730; .962; .803; .748; .839
2.ReLU	2.MaxPool	-.005; .004; -.001; -.007; -.004	.202; .390; .832; .195; .576	.019; .035; .015; .020; .015	.563; .241; .623; .505; .624	.003; .003; .005; .004; .002	.365; .394; .202; .294; .565
2.MaxPool	3.Conv	.001; -.001; .004; -.006; -.003	.873; .876; .428; .286; .695	.003; -.001; .003; -.002; -.009	.936; .978; .931; .948; .755	.000; .000; -.000; -.000; .000	.998; 1.00; .998; .956; .973
3.Conv	3.ReLU	-.001; -.000; -.003; .002; .007	.747; .969; .574; .629; .246	.002; .003; .007; .004; -.002	.960; .914; .827; .895; .957	-.001; -.001; -.001; -.001; -.001	.872; .849; .721; .768; .895
3.ReLU	4.Conv	.005; .004; -.000; .000; -.005	.231; .345; .932; .954; .379	-.006; -.001; -.001; -.004; -.004	.861; .967; .975; .897; .904	.000; .001; .001; .001; .001	.998; .860; .823; .777; .842
4.Conv	4.ReLU	.005; -.000; .001; .003; .001	.220; .945; .842; .551; .821	-.003; -.003; -.006; -.008; .005	.936; .913; .851; .797; .878	-.001; .000; -.000; -.000; .000	.750; .945; .954; .893; .983
4.ReLU	4.MaxPool	-.009; .008; -.004; -.004; .004	.059; .092; .364; .425; .444	.049; .054; .040; .051; .038	.113; .061; .204; .096; .212	-.000; .000; .001; .001; .001	.962; .987; .840; .778; .777
4.MaxPool	5.Dense	.009; .000; .000; .000; .001	.061; .976; .925; .996; .838	-.005; -.001; .002; .003; -.003	.858; .976; .962; .920; .908	-.001; -.001; -.001; -.001; -.001	.758; .746; .633; .880; .682
5.Dense	5.ReLU	-.004; .004; .005; .001; -.006	.424; .385; .283; .925; .199	-.007; -.014; -.008; -.003; .003	.813; .596; .789; .908; .915	-.002; -.002; -.001; -.002; -.002	.696; .654; .723; .549; .666
5.ReLU	6.Dense	.005; -.017; -.017 ; .005; .003	.330; .001; .000 ; .305; .549	-.202; -.226; -.182 ; -.189; -.198	.000; .000; .000 ; .000; .000	-.135; -.173; -.202 ; -.219; -.177	.000; .000; .000 ; .000; .000
6.Dense	6.Softmax	-.001; -.002; -.002; -.007; -.000	.891; .665; .688; .145; .933	-.018; -.011; -.010; -.013; -.017	.473; .457; .690; .618; .446	-.018; -.030; -.030; -.014; -.016	.419; .280; .296; .652; .582

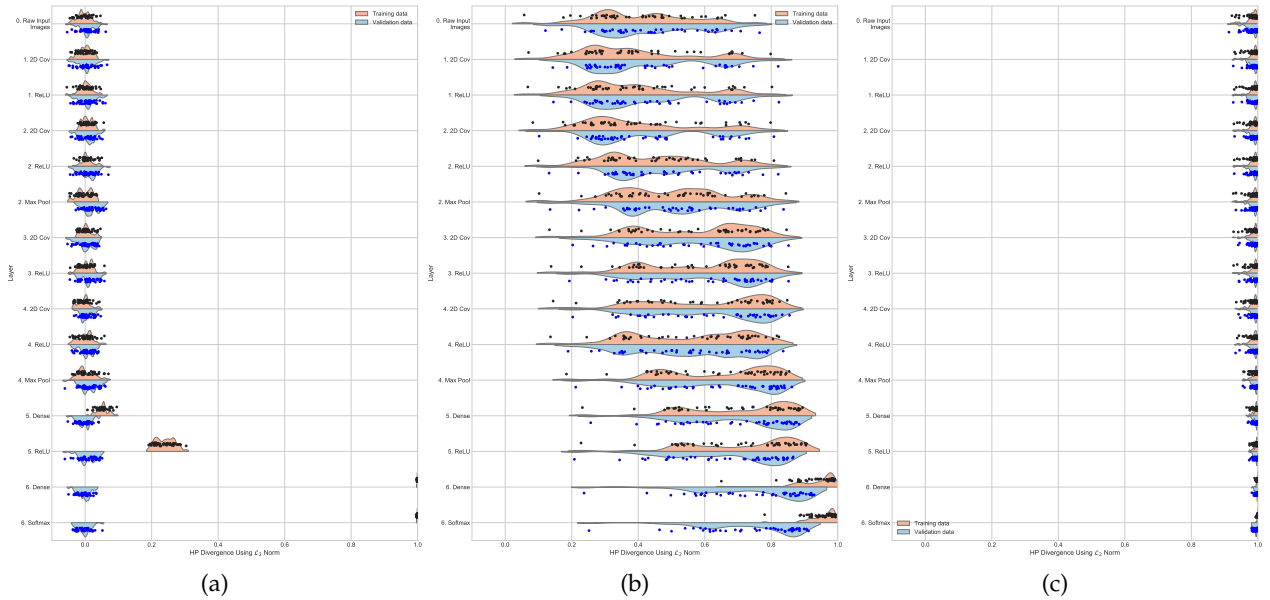


Fig. 4: Illustrative HP class-pair statistics of (a) CIFAR10 with random labels, (b) CIFAR10 with true labels, and (c) MNIST with true labels, computed on respective models after training is complete.

volitional layers to optimize its performance. Conversely, the models trained with true CIFAR10 labels demonstrate statistically significant changes in separation statistics in the third and fourth convolutional layers. In all cases, statistically significant differences in mean class separation occur by the time the representations are mapped in the dense layers, indicating that the dense layers have adapted and

the corresponding learned mappings significantly improve \mathcal{H} class statistics for the training data.

4.4 Inside the Black Box: individual layer contribution

To quantitatively estimate the improvement in class separation for each layer in the trained models, we again compute the difference between the class-pair statistics \mathcal{H} , but now

TABLE 4: Differences between the trained and initialized \mathcal{H} class-pair statistics of a layer, and respective p -values for the corresponding one-sided permutation test (15). **Red font** denotes layer instances for which we reject \mathbf{H}_0 , and **black font** denotes layers for which we fail to reject \mathbf{H}_0 . (Note: $\Delta\bar{\mathcal{H}} = \bar{\mathcal{H}}_{(k,T)}^{(t)} - \bar{\mathcal{H}}_{(k,0)}^{(t)}$)

Output Space	CIFAR10 w Random		CIFAR10 w True		MNIST w True	
	$\Delta\bar{\mathcal{H}}$	p -values	$\Delta\bar{\mathcal{H}}$	p -values	$\Delta\bar{\mathcal{H}}$	p -values
1.Conv	-.000; -.002; .000; -.007; .000	.507; .645; .472; .888; .482	-.007; .005; -.008; .004; -.004	.580; .435; .591; .453; .542	.001; .002; .004; .003; .003	.346; .277; .126; .209; .248
1.ReLU	.004; .004; -.004; -.009; -.001	.137; .225; .775; .955; .587	-.012; .029; .005; .015; .005	.646; .183; .440; .320; .448	.001; .002; .003; .001; .002	.417; .316; .208; .354; .274
2.Conv	.007; -.009; -.011; -.014; -.004	.032; .973; .976; .995; .812	-.017; .039; -.006; .028; .001	.690; .121; .570; .200; .491	.001; .002; .004; .003; .003	.422; .247; .161; .243; .202
2.ReLU	.008 ; -.003; -.012; -.015; -.008	.017 ; .706; .989; .998; .913	.032; .095 ; .051; .066 ; .051	.174; .002 ; .068; .024 ; .068	.002; .003; .005; .004; .002	.281; .233; .105; .161; .271
2.MaxPool	-.005; .004; -.015; -.010; -.004	.126; .161; .999; .967; .725	-.065; .100 ; .094 ; .081 ; .073	.030; .002 ; .003 ; .008 ; .016	-.002; -.002; -.001; -.001; -.001	.722; .669; .647; .655; .603
3.Conv	.009 ; .001; -.021; .000; .004	.011 ; .388; 1.00; .498; .233	.127 ; .117 ; .168 ; .097 ; .118	.000 ; .000 ; .000 ; .002 ; .000	-.000; .001; .001; .001; .001	.525; .433; .328; .355; .440
3.ReLU	.010 ; .001; -.020; -.006; -.008	.010 ; .365; 1.00; .896; .926	.140 ; .135 ; .184 ; .117 ; .149	.000 ; .000 ; .000 ; .000 ; .000	-.000; .001; .002; .002; .001	.500; .431; .264; .281; .390
4.Conv	-.002; .006; -.014; -.011; .008	.669; .111; .999; .989; .053	.168 ; .131 ; .205 ; .129 ; .148	.000 ; .000 ; .000 ; .000 ; .000	.000; .001; .002; .001; .001	.444; .381; .278; .330; .358
4.ReLU	-.001; .007; -.006; -.007; -.003	.610; .084; .919; .909; .704	.128 ; .098 ; .190 ; .011; .106	.000 ; .002 ; .000 ; .366; .001	.001; .001; .002; .003; .002	.336; .397; .228; .210; .314
4.MaxPool	.009; -.007; -.016; .006; -.011	.045; .928; .999; .127; .988	.161 ; .163 ; .207 ; .125 ; .181	.000 ; .000 ; .000 ; .000 ; .000	.006 ; .005; .006 ; .005; .004	.023 ; .049; .015 ; .038; .068
5.Dense	.049 ; .024 ; .036 ; .035 ; .029	.000 ; .000 ; .000 ; .000 ; .000	.227 ; .231 ; .257 ; .225 ; .258	.000 ; .000 ; .000 ; .000 ; .000	.009 ; .008 ; .009 ; .007 ; .007	.001 ; .001 ; .000 ; .001 ; .002
5.ReLU	.241 ; .234 ; .233 ; .238 ; .246	.000 ; .000 ; .000 ; .000 ; .000	.248 ; .256 ; .279 ; .237 ; .270	.000 ; .000 ; .000 ; .000 ; .000	.012 ; .011 ; .012 ; .010 ; .011	.000 ; .000 ; .000 ; .000 ; .000
6.Dense	.994 ; 1.002 ; 1.00 ; .989 ; .996	.000 ; .000 ; .000 ; .000 ; .000	.669 ; .681 ; .610 ; .718 ; .668	.000 ; .000 ; .000 ; .000 ; .000	.152 ; .188 ; .218 ; .234 ; .192	.000 ; .000 ; .000 ; .000 ; .000
6.Softmax	.995 ; 1.004 ; 1.002 ; .996 ; .996	.000 ; .000 ; .000 ; .000 ; .000	.706 ; .711 ; .634 ; .741 ; .706	.000 ; .000 ; .000 ; .000 ; .000	.171 ; .219 ; .250 ; .249 ; .209	.000 ; .000 ; .000 ; .000 ; .000

between the input and output representations of each layer after training. That is,

$$\bar{\mathcal{H}}_{(k,T)} - \bar{\mathcal{H}}_{(k-1,T)}. \quad (16)$$

The results for each dataset and their five trained models are given in Table 5 for one-sided, permutation-based null hypothesis tests of the form

$$\begin{aligned} \mathbf{H}_0 &: \bar{\mathcal{H}}_{(k,T)} - \bar{\mathcal{H}}_{(k-1,T)} \leq 0 \quad vs. \\ \mathbf{H}_A &: \bar{\mathcal{H}}_{(k,T)} - \bar{\mathcal{H}}_{(k-1,T)} > 0. \end{aligned} \quad (17)$$

Unlike Table 4, the results in Table 5 are not characterizing the cumulative changes due to training, but rather looking at the individual change in separation statistics given the input and output representations of a layer. We should caveat that failure to reject the null hypothesis does not mean that a layer is not mapping the data into an improved (more separated) representation, but that the differences are not statistically significant enough. The behavior of the second dense layer (6.Dense) is unique, where in all 15 cases we reject the null hypothesis with very small p -values. Significant changes to the data representations are occurring on that layer. Nowhere is that more true than for the CIFAR10 dataset with random labels, where both dense layers effectively translate the training data from a totally mixed state with the \mathcal{H} values centered at zero, to completely separated with \mathcal{H} statistics extremely close to one. Since this separation is meaningless because the classes are sampled from the same distribution, the learning in this case is just overfitting or memorization of the training set. In

this example, the statistics have clearly identified the layers in this model responsible for memorization.

4.5 Inside the Black Box: comparing model behavior on training vs. validation data

Finally, we wish to investigate the layer-wise change in class separation induced on validation data, that is, data that has not been explicitly used for model training, but in theory have the same labeling distribution as the training data. To remind the reader, Figure 4 illustrates $\mathcal{H}^{(t)}$ training (above, orange) and $\mathcal{H}^{(v)}$ validation (below, blue) class-pair distributions that have been computed at each layer for each trained model. Additionally, we will look at detecting whether the change in statistics for validation and training \mathcal{H} distributions are significantly different. For the randomized CIFAR10 dataset, any difference in layer training and validation behavior are by design due to the model overfitting and outright memorization. This has allowed us to identify the layers responsible for memorization. For the datasets with non-randomized class labels, we will not attempt to tease out the root causes for differences in behavior between training and validation data. Differences can be due not only to overfitting by the deep learning model, but also from potential domain-shifts between training and validation data. See [2], [23] for more information on domain-shifted datasets and derived relationships between error bounds. For the true-labeled data, identifying contributions due to domain-shifts and overfitting will be the focus for a future paper or an exercise for an intrepid reader. To restate, our purpose is to

TABLE 5: Training data difference between input and output of each layer \mathcal{H} class-pair statistics for the trained models, and respective p -values for the one sided permutation test (17). **Red font** denotes layer instances for which we reject \mathbf{H}_0 , and black font denotes layers for which we fail to reject \mathbf{H}_0 . (Note: $\Delta\bar{\mathcal{H}} = \bar{\mathcal{H}}_{(k,T)}^{(t)} - \bar{\mathcal{H}}_{(k-1,T)}^{(t)}$)

Input Space	Output Space	CIFAR10 w Random		CIFAR10 w True		MNIST w True	
		$\Delta\bar{\mathcal{H}}$	p -values	$\Delta\bar{\mathcal{H}}$	p -values	$\Delta\bar{\mathcal{H}}$	p -values
0.Input	1.Conv	.003; .000; -.004; -.003; -.003	.243; .474; .741; .729; .721	-.019; .011; -.025; .001; -.007	.708; .378; .767; .492; .582	.003; .003; .004; .003; .003	.200; .199; .169; .181; .208
1.Conv	1.ReLU	.002; .002; -.000; -.001; .001	.312; .303; .531; .542; .421	.010; .002; .010; .013; .008	.386; .481; .389; .356; .410	-.000; .000; .000; .000; .000	.506; .492; .481; .480; .493
1.ReLU	2.Conv	.006; -.012; -.008; -.007; -.003	.070; .990; .911; .896; .756	-.002; .004; -.013; .004; -.009	.525; .455; .635; .453; .591	.000; .001; .000; .000; .001	.494; .425; .502; .468; .433
2.Conv	2.ReLU	-.001; .004; .002; -.003; -.003	.573; .210; .330; .740; .752	.051; .039; .062; .035; .053	.080; .142; .052; .164; .076	.000; .000; .000; .000; .000	.481; .496; .482; .500; .494
2.ReLU	2.MaxPool	-.007; .010 ; -.005; -.005; .000	.955; .015 ; .827; .682; .471	.051; .040; .058; .035; .037	.071; .130; .055; .164; .152	-.001; -.001; -.001; -.001; -.001	.599; .609; .629; .632; .608
2.MaxPool	3.Conv	.005; -.003; -.001; .004; .005	.127; .775; .603; .193; .146	.065; .017; .077 ; .015; .036	.035; .318; .020 ; .334; .158	.002; .002; .003; .003; .002	.301; .274; .210; .235; .323
3.Conv	3.ReLU	-.001; -.000; -.002; -.004; -.005	.610; .503; .616; .776; .840	.014; .021; .023; .024; .029	.346; .285; .270; .251; .210	-.000; -.001; -.001; -.000; -.000	.534; .581; .568; .543; .513
3.ReLU	4.Conv	-.007; .009; .005; -.005; .011	.947; .039; .132; .865; .010	.023; -.005; .020; .008; -.004	.276; .550; .307; .412; .545	.000; .001; .001; .000; .001	.444; .371; .425; .440; .374
4.Conv	4.ReLU	.006; .000; .009 ; .007; -.009	.107; .462; .007 ; .058; .975	-.043; -.036; -.020; -.126; -.038	.866; .839; .701; 1.00; .845	-.000; .000; .000; .001; .001	.522; .476; .458; .404; .428
4.ReLU	4.MaxPool	.001; -.005; -.015; .009; -.004	.397; .869; .999; .041; .806	.081 ; .119 ; .057; .165 ; .113	.015 ; .001; .068; .000 ; .002	.004; .004; .004; .003; .004	.051; .068; .059; .089; .085
4.MaxPool	5.Dense	.049 ; .031 ; .053 ; .029 ; .040	.000 ; .000 ; .000 ; .000 ; .000	.061; .067; .051; .103 ; .074	.042; .028; .080; .002 ; .020	.002; .002; .002; .002; .002	.111; .136; .192; .165; .195
5.Dense	5.ReLU	.188 ; .214 ; .202 ; .203 ; .212	.000 ; .000 ; .000 ; .000 ; .000	.013; .010; .015; .009; .015	.351; .380; .338; .396; .332	.001; .001; .002; .001; .002	.176; .190; .126; .292; .091
5.ReLU	6.Dense	.758 ; .752 ; .750 ; .756 ; .753	.000 ; .000 ; .000 ; .000 ; .000	.220 ; .199 ; .148 ; .292 ; .201	.000 ; .000 ; .000 ; .000 ; .000	.005 ; .004 ; .004 ; .005 ; .004	.000 ; .000 ; .000 ; .000 ; .000
6.Dense	6.Softmax	-.000; -.000; .000; .000; -.000	.985; .581; .250; .145; .858	.019; .019; .015; .010 ; .020	.049; .124; .221; .000 ; .070	.001 ; .001 ; .001 ; .001 ; .001	.001 ; .000 ; .000 ; .028; .000

demonstrate techniques that evoke and enable the reader to gain insights into the behavior of individual layers of an optimized/trained deep learning model. For the discussion that follows, we explicitly use $\mathcal{H}^{(t)}$ and $\mathcal{H}^{(v)}$ to denote the distribution of class-pair statistics computed on the training and validation data, respectively.

We will now attempt to address the following questions:

- Q1: Is there a statistically significant change in $\mathcal{H}^{(v)}$ between the input and output spaces of each layer?
Q2: Is the induced change in distributional separation of training and validation data statistically equivalent?

To investigate Q1, we compute the difference in mean distributional separation and test if this difference is statistically significant via a one-sided permutation test, that is,

$$\begin{aligned} \mathbf{H}_0 &: \bar{\mathcal{H}}_{(k,T)}^{(v)} - \bar{\mathcal{H}}_{(k-1,T)}^{(v)} \leq 0 \quad vs. \\ \mathbf{H}_A &: \bar{\mathcal{H}}_{(k,T)}^{(v)} - \bar{\mathcal{H}}_{(k-1,T)}^{(v)} > 0. \end{aligned} \quad (18)$$

We are using a one-sided permutation test of means with our arbitrary critical value $\alpha = 0.025$. The results for each dataset and their five trained models are given in Table 6.

In reviewing Table 6 on the CIFAR10 dataset with random labels, no layers are consistently significant in increasing the average interclass separation across the five models, which is in contrast to the behavior of the training data in the dense layers (Table 5). This across the board discrepancy is a clear indicator of model overfitting. On the other hand, two layers of the models trained on CIFAR10 with true labels demonstrate statistically significant change in mean

separation on the validation data, namely the 4.MaxPooling and 6.Dense layers. This indicates that the mappings learned for these layers have provided a statistically significant improvement to the interpoint separation on unseen data.

The final question and statistical test is whether or not the change in \mathcal{H} on each layer is statistically equivalent for training and validation data (Q2, above). In other words, is the measured change in the mean separation produced by the layer on the training data statistically equivalent to the change induced on the validation data, as quantified by $\bar{\mathcal{H}}^{(t)}$ and $\bar{\mathcal{H}}^{(v)}$?

Define $\Delta\mathcal{H}$ to be the set of paired differences between two class-paired separability statistics from different layers, that is,

$$\Delta\mathcal{H}_{(k_1,k_2)}^{(D)} = \{\mathcal{H}(y_i^{(k_1)}, y_j^{(k_1)}) - \mathcal{H}(y_i^{(k_2)}, y_j^{(k_2)}) \mid \forall(i, j), i < j\} \quad (19)$$

where D indicates the data set (training data, t , or the validation data, v) being used, and $y_m^{(k)}$ is the set of feature vectors associated with class m of data set D produced by the model at layers k_1 and k_2 . Thus, $\Delta\mathcal{H}_{(k,k-1)}^{(t)}$ and $\Delta\mathcal{H}_{(k,k-1)}^{(v)}$ are the distributions of changes produced by the k th layer on the training and validation datasets, respectively.

We attempt to quantify whether the means of the differences or differences are statistically equivalent or not

$$\begin{aligned} \mathbf{H}_0 &: \overline{\Delta\mathcal{H}}_{(k,k-1)}^{(t)} - \overline{\Delta\mathcal{H}}_{(k,k-1)}^{(v)} = 0 \quad vs. \\ \mathbf{H}_A &: \overline{\Delta\mathcal{H}}_{(k,k-1)}^{(t)} - \overline{\Delta\mathcal{H}}_{(k,k-1)}^{(v)} \neq 0. \end{aligned} \quad (20)$$

TABLE 6: Validation data differences in mean class-pair separation statistics between the input and output representations of a layer, and respective one-sided permutation test p -values. **Red font** denotes layer instances for which we reject H_0 , and **black font** denotes layers for which we fail to reject H_0 (18). (Note: $\Delta\bar{H} = \bar{H}_{(k,T)}^{(v)} - \bar{H}_{(k-1,T)}^{(v)}$)

Input Space	Output Space	CIFAR10 w Random		CIFAR10 w True		MNIST w True	
		$\Delta\bar{H}$	p -values	$\Delta\bar{H}$	p -values	$\Delta\bar{H}$	p -values
0.Input	1.Conv	-.002; .006; -.003; -.001; -.004	.639; .035; .728; .543; .822	-.014; .017; -.021; .005; -.003	.662; .308; .729; .441; .533	.004; .004; .004; .004; .004	.094; .113; .137; .119; .103
1.Conv	1.ReLU	.002; .000; -.002; .001; .001	.348; .488; .676; .418; .412	.009; .001; .010; .012; .008	.402; .490; .395; .372; .415	.000; .000; .000; .000; -.000	.482; .488; .481; .466; .509
1.ReLU	2.Conv	.000; -.003; -.001; -.004; -.003	.499; .729; .583; .752; .789	-.006; -.003; -.019; -.004; -.006	.569; .531; .700; .544; .563	.000; .001; .001; .000; .001	.470; .429; .412; .449; .424
2.Conv	2.ReLU	.002; .005; .000; .004; -.001	.314; .138; .479; .251; .585	.054; .038; .064; .038; .046	.065; .136; .043; .138; .095	-.000; .000; .000; -.000; .000	.516; .498; .504; .510; .496
2.ReLU	2.MaxPool	.010; -.006; -.012; .002; -.001	.030; .919; .994; .323; .608	.041; .029; .053; .030; .031	.113; .198; .068; .195; .186	-.000; -.000; -.000; -.000; -.001	.517; .516; .536; .533; .568
2.MaxPool	3.Conv	-.014; .008; .012 ; -.007; .004	.996; .042; .016 ; .947; .150	.067; .027; .073 ; .019; .040	.028; .219; .024 ; .290; .122	.001; .001; .002; .001; .002	.332; .353; .284; .307; .281
3.Conv	3.ReLU	.005; -.002; .003; .006; .000	.157; .622; .301; .093; .495	.014; .021; .021; .022; .022	.346; .277; .286; .266; .260	-.000; -.000; -.001; -.000; -.001	.570; .542; .582; .551; .581
3.ReLU	4.Conv	-.005; -.005; -.009; -.002; -.002	.888; .858; .970; .689; .723	.022; -.006; .019; .002; -.002	.274; .570; .305; .476; .522	.001; .001; .001; .001; .001	.400; .409; .408; .374; .390
4.Conv	4.ReLU	.001; -.003; .008 ; .004; -.002	.405; .705; .023 ; .180; .640	-.057; -.045; -.026; -.120; -.053	.941; .906; .750; 1.00; .941	-.000; .000; .000; .000; .000	.523; .480; .455; .476; .434
4.ReLU	4.MaxPool	.007; .007; .005; .002; .013	.077; .050; .138; .348; .002	.089 ; .115 ; .061; .154 ; .119	.007 ; .000 ; .050; .000 ; .000	.003; .004; .004; .003; .003	.086; .042; .050; .077; .084
4.MaxPool	5.Dense	-.015; .003; -.009; -.010; -.008	.999; .237; .952; .973; .977	.049; .054; .035; .084 ; .058	.076; .056; .162; .008 ; .046	.002; .001; .001; .001; .002	.163; .225; .234; .217; .171
5.Dense	5.ReLU	.010 ; .000; -.002; .005; -.007	.018 ; .456; .693; .134; .944	-.027; -.016; .000; -.054; -.014	.782; .677; .500; .949; .662	.001; .001; .001; .001; .001	.288; .274; .168; .251; .147
5.ReLU	6.Dense	-.010; -.016; .006; -.011; .007	.987; 1.00; .071; .976; .089	.086 ; .084 ; .058; .118 ; .076	.006 ; .008 ; .043; .000 ; .012	.003 ; .002; .002; .002 ; .001	.008 ; .041; .081; .018 ; .103
6.Dense	6.Softmax	.001; .017 ; .010 ; .007; -.006	.407; .000 ; .011 ; .096; .880	-.009; .000; -.004; -.026; -.016	.611; .496; .557; .783; .692	-.003; -.003; -.004; -.005; -.005	.999; .999; 1.00; 1.00; 1.00

We test the hypothesis on the instances of our models via the random permutation test of means. The results for each model/dataset are given in Table 7. The results of this hypothesis test provide an indication of which individual layers are disproportionately improving class separation for the training data with respect to the improvement to the validation data. In all three cases, a portion of the back-end dense layers are showing a statistically significant bias in training data separation improvement vs. the validation data. These results provide the practitioner actionable information with respect to targeting these layers via regularization or other approaches to mitigate the training bias.

5 CONCLUSIONS

Advancements in hierarchical approaches can be accelerated given the statistical approach discussed. Using the Henze-Penrose-Berisha-Hero statistic, we have demonstrated the statistical characterization of the functional mappings of deep learning models trained on disparate datasets. These characterizations include the identification of layers that (a) are memorizing, (b) acting as distance-preserving random projections, or (c) inducing a domain mismatch between training and validation sets. Actionable insights include optimization of network topology, identification of layers which require additional regularization, and testing of data domain consistency or mismatch.

It has been demonstrated that estimating the distributional characteristics of the data with respect to a vector space can provide insight into the difficulty of the task as

well as the mechanisms and utility of each functional mapping applied. The comparative analysis between datasets illustrates that the required complexity of the model depends on the measurements and the class relationships therein and is not intrinsic to the architecture.

REFERENCES

- [1] M. D. Zeiler and R. Fergus, "Visualizing and understanding convolutional networks," *CoRR*, vol. abs/1311.2901, 2013.
- [2] V. Berisha and A. O. Hero, "Empirical non-parametric estimation of the fisher information," *IEEE Signal Processing Letters*, vol. 22, pp. 988–992, July 2015.
- [3] C. Zhang, S. Bengio, M. Hardt, B. Recht, and O. Vinyals, "Understanding deep learning requires rethinking generalization," *CoRR*, vol. abs/1611.03530, 2016.
- [4] A. Krizhevsky, I. Sutskever, and G. E. Hinton, "Imagenet classification with deep convolutional neural networks," in *Proceedings of the 25th International Conference on Neural Information Processing Systems - Volume 1*, NIPS'12, (USA), pp. 1097–1105, Curran Associates Inc., 2012.
- [5] P. L. Bartlett, D. J. Foster, and M. Telgarsky, "Spectrally-normalized margin bounds for neural networks," *CoRR*, vol. abs/1706.08498, 2017.
- [6] S. Hochreiter and J. Schmidhuber, "Long short-term memory," *Neural Computation*, vol. 9, no. 8, pp. 1735–1780, 1997.
- [7] P. Chaudhari, A. Choromanska, S. Soatto, Y. LeCun, C. Baldassi, C. Borgs, J. T. Chayes, L. Sagun, and R. Zecchina, "Entropy-sgd: Biasing gradient descent into wide valleys," *CoRR*, vol. abs/1611.01838, 2016.
- [8] G. Karolina Dziugaite and D. M. Roy, "Computing Nonvacuous Generalization Bounds for Deep (Stochastic) Neural Networks with Many More Parameters than Training Data," *ArXiv e-prints*, Mar. 2017.
- [9] M. Dotter, K. Rainey, and D. Waagen, "Visualization of high dimensional image features for classification," in *2016 IEEE Applied Imagery Pattern Recognition Workshop (AIPR)*, pp. 1–6, Oct 2016.

TABLE 7: Two-sided permutation test (20) comparing the differences in the mean change induced on the training and validation statistics ($\Delta\mathcal{H}_{(k,k-1)}^{(t)}$ and $\Delta\mathcal{H}_{(k,k-1)}^{(v)}$). **Red font** denotes layer instances for which we reject \mathbf{H}_0 , and **black font** denotes layers for which we fail to reject \mathbf{H}_0 . (Note: $\Delta\mu = \overline{\Delta\mathcal{H}}_{(k,k-1)}^{(t)} - \overline{\Delta\mathcal{H}}_{(k,k-1)}^{(v)}$)

Input Space	Output Space	CIFAR10 w Random		CIFAR10 w True		MNIST w True	
		$\Delta\mu$	p -values	$\Delta\mu$	p -values	$\Delta\mu$	p -values
0.Input	1.Conv	.005; -.006; -.001; -.003; .001	.156; .052; .769; .332; .811	-.004; -.006; -.004; -.004; -.005	.682; .225; .691; .457; .547	-.001; -.001; -.000; -.001; -.001	.212; .307; .852; .497; .242
1.Conv	1.ReLU	-.000; .002; .002; -.002; .000	.966; .204; .406; .376; .891	.001; .001; .001; .001; .000	.549; .569; .780; .598; .963	-.000; .000; .000; -.000; .000	.308; 1.00; 1.00; .459; .347
1.ReLU	2.Conv	.006; -.009 ; -.007; -.003; -.000	.250; .020 ; .192; .467; .980	.004; .007; .006; .008; -.003	.390; .172; .184; .146; .541	-.000; .000; -.001; -.000; .000	.735; .825; .079; .923; .936
2.Conv	2.ReLU	-.003; -.001; .002; -.007 ; -.002	.362; .809; .509; .011 ; .592	-.003; .001; -.001; -.003; -.002	.719; .892; .861; .575; .248	.000 ; .000; .000; .000; .000	.007 ; .832; .350; .672; .858
2.ReLU	2.MaxPool	-.017 ; .016 ; .008; -.004; .002	.000 ; .000 ; .088; .258; .701	.010; .011; .005; .004; .007	.130; .031; .434; .350; .154	-.001; -.001; -.001; -.001; -.001	.217; .188; .219; .227; .473
2.MaxPool	3.Conv	.018 ; -.012; -.013 ; .011 ; .000	.000 ; .027 ; .009 ; .014 ; .929	-.002; -.010; .004; -.004; -.004	.848; .049; .791; .321; .513	.001; .001; .001; .001; -.000	.421; .258; .332; .323; .974
3.Conv	3.ReLU	-.006; .002; -.005; -.010 ; -.005	.095; .616; .219; .011 ; .251	.000; .000; .002; .002; .007	.886; .970; .470; .614; .108	.000; -.000; -.000; .000; .000	.630; .335; 1.00; 1.00; .150
3.ReLU	4.Conv	-.001; .014 ; .015 ; -.003; .013	.805; .005 ; .005 ; .598; .007	.001; .001; .000; .006; -.002	.861; .772; .951; .281; .623	-.000; .000; -.000; -.000; .000	.672; .621; .948; .483; .717
4.Conv	4.ReLU	.005; .003; .001; .003; -.008	.406; .589; .783; .634; .177	.015; .009; .005; -.006; .016	.088; .267; .403; .695; .048	.000; .000; .000; .001; .000	1.00; .985; .969; .275; .890
4.ReLU	4.MaxPool	-.006; -.012 ; -.020 ; .007; -.017	.300; .012 ; .000 ; .247; .000	-.008; .004; -.004; .011; -.006	.332; .710; .516; .453; .581	.001; .000; .000; .000; .000	.348; .975; .789; .892; .731
4.MaxPool	5.Dense	.064 ; .028 ; .062 ; .039 ; .049	.000 ; .000 ; .000 ; .000 ; .000	.012 ; .013 ; .016 ; .020; .016	.013 ; .020 ; .001 ; .030; .006	.001; .001; .000; .001; .000	.431; .210; .387; .392; .938
5.Dense	5.ReLU	.179 ; .213 ; .204 ; .198 ; .218	.000 ; .000 ; .000 ; .000 ; .000	.040 ; .026 ; .015 ; .063 ; .029	.000 ; .000 ; .000 ; .000 ; .000	.001; .000; .000; -.000; .001	.217; .472; .511; .856; .239
5.ReLU	6.Dense	.768 ; .768 ; .744 ; .767 ; .746	.000 ; .000 ; .000 ; .000 ; .000	.134 ; .115 ; .090 ; .174 ; .124	.000 ; .000 ; .000 ; .000 ; .000	.002 ; .002 ; .003 ; .003 ; .003	.014 ; .015 ; .001 ; .003 ; .000
6.Dense	6.Softmax	-.001; -.017 ; -.010 ; -.007; .006	.750; .000 ; .025 ; .223; .266	.028 ; .019 ; .020 ; .036 ; .036	.000 ; .004 ; .000 ; .000 ; .000	.004 ; .005 ; .005 ; .006 ; .006	.000 ; .000 ; .000 ; .000 ; .000

- [10] A. Wald and J. Wolfowitz, "On a test whether two samples are from the same population," *Ann. Math. Statist.*, vol. 11, pp. 147–162, 06 1940.
- [11] J. H. Friedman and L. C. Rafsky, "Multivariate generalizations of the wald-wolfowitz and smirnov two-sample tests," *Ann. Statist.*, vol. 7, pp. 697–717, 07 1979.
- [12] T. K. Ho and M. Basu, "Complexity measures of supervised classification problems," *IEEE Transactions on Pattern Analysis and Machine Intelligence*, vol. 24, pp. 289–300, March 2002.
- [13] I. Csiszár, P. C. Shields, *et al.*, "Information theory and statistics: A tutorial," *Foundations and Trends® in Communications and Information Theory*, vol. 1, no. 4, pp. 417–528, 2004.
- [14] N. Henze and M. D. Penrose, "On the multivariate runs test," *Ann. Statist.*, vol. 27, pp. 290–298, 03 1999.
- [15] V. Berisha, A. Wisler, A. O. Hero, and A. Spanias, "Empirically estimable classification bounds based on a nonparametric divergence measure," *IEEE Transactions on Signal Processing*, vol. 64, pp. 580–591, Feb 2016.
- [16] Y. Lecun, L. Bottou, Y. Bengio, and P. Haffner, "Gradient-based learning applied to document recognition," *Proceedings of the IEEE*, vol. 86, pp. 2278–2324, Nov 1998.
- [17] A. Krizhevsky, V. Nair, and G. Hinton, "Cifar-10," <http://www.cs.toronto.edu/~kriz/cifar.html>.
- [18] M. Abadi, A. Agarwal, P. Barham, E. Brevdo, Z. Chen, C. Citro, G. S. Corrado, A. Davis, J. Dean, M. Devin, S. Ghemawat, I. Goodfellow, A. Harp, G. Irving, M. Isard, Y. Jia, R. Jozefowicz, L. Kaiser, M. Kudlur, J. Levenberg, D. Mané, R. Monga, S. Moore, D. Murray, C. Olah, M. Schuster, J. Shlens, B. Steiner, I. Sutskever, K. Talwar, P. Tucker, V. Vanhoucke, V. Vasudevan, F. Viégas, O. Vinyals, P. Warden, M. Wattenberg, M. Wicke, Y. Yu, and X. Zheng, "TensorFlow: Large-scale machine learning on heterogeneous systems," 2015. Software available from tensorflow.org, <https://www.tensorflow.org/>.
- [19] F. Chollet *et al.*, "Keras," 2015. <https://github.com/fchollet/keras>.
- [20] B. Efron and R. J. Tibshirani, *An introduction to the bootstrap*. CRC press, 1994.
- [21] W. B. Johnson, J. Lindenstrauss, and G. Schechtman, "Extensions of lipschitz maps into banach spaces," *Israel Journal of Mathematics*, vol. 54, pp. 129–138, Jun 1986.
- [22] G.-B. Huang, Q.-Y. Zhu, and C.-K. Siew, "Extreme learning machine: Theory and applications," *Neurocomputing*, vol. 70, no. 1, pp. 489 – 501, 2006. Neural Networks.
- [23] S. Ben-David, J. Blitzer, K. Crammer, A. Kulesza, F. Pereira, and J. W. Vaughan, "A theory of learning from different domains," *Machine Learning*, vol. 79, pp. 151–175, May 2010.

Supplement to Paper: Characterizing Inter-Layer Functional Mappings of Deep Learning Models

Donald Waagen¹, Katie Rainey², Jamie Gantert¹, David Gray¹, Megan King³, M. Shane Thompson³, Johnathan Barton⁴, Will Waldron⁴, Samantha Livingston⁵ and Don Hulsey⁴

¹Air Force Research Laboratory

²Space and Naval Warfare Systems Center Pacific

³U.S. Army CCDC Aviation and Missile Center

⁴Dynetics, Inc.

⁵Modern Technology Solutions, Inc.

S.1 Statistical analysis using Euclidean distance as measure of proximity

This supplemental material presents more detailed results from the three experiments (CIFAR10 with random labels, CIFAR10 with true labels, and MNIST with true labels) using the Euclidean distance metric for the proximity measure of the HP statistics.

Figure S-1 shows the between-class HP statistics of the raw images, or class separability in the original measurement space. The comparisons were made using the analysis subset of the training data (1000 images per class) and the validation data (1000 images per class). As described in Section 3 of the paper, for the case using CIFAR10 with random labels there are five different versions of the randomly permuted labels; one per instance of the training network. The results for only one of these versions is tabulated and plotted in Figures S-1 (A) and (D), respectively.

Figures S-2 through S-6 present the class-wise HP statistics of the training and validation samples of the CIFAR10 data with random labels as they pass through an associated model. Each figure plots the results for one of the five training instances discussed in Section 3 of the paper. The (a) subfigures show the data passing through the untrained models and the (b) subfigures show the data passing through the trained version of the models. Similarly, Figures S-7 through S-11 present plots for the 5 model instances trained on the CIFAR10 data with true labels, and Figures S-12 through S-16 show the plots for the 5 MNIST-trained models.

Tables S-1 through S-9 present a superset of the results of two-sample null hypothesis tests of means presented in the main body of the paper. In particular Tables S-4, S-5, S-7, and S-8 show the test performed between multi-layer components of the networks. The tables flag cases where the estimated p -values are < 0.025 . Note that the tests were performed using the random permutation algorithm with 50,000 Monte Carlo trials.

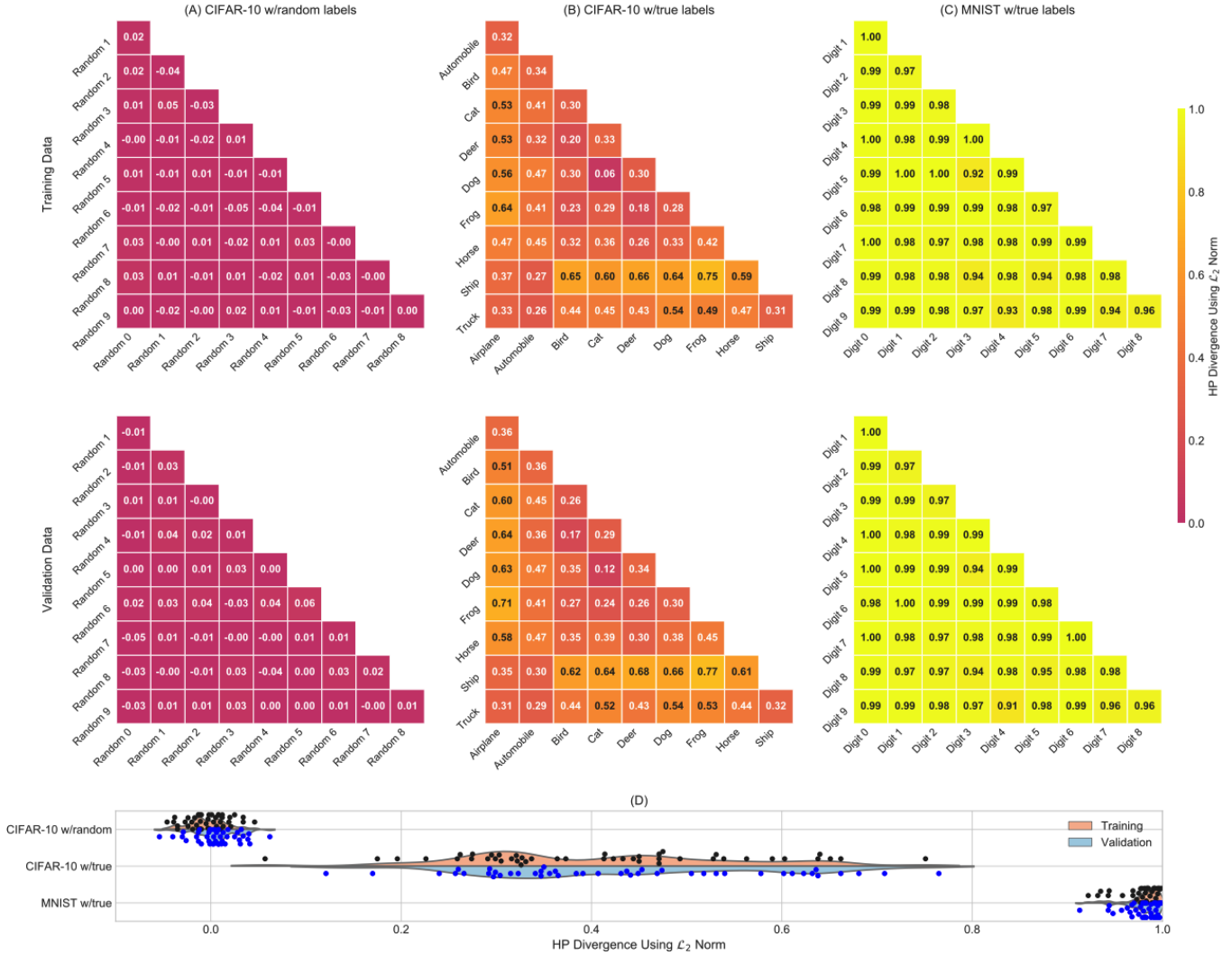


Figure S-1: Pairwise class HP statistics using Euclidean distance (training data above, validation data below) computed on (A) CIFAR10 with random labels, (B) CIFAR10 with true labels, and (C) MNIST with true labels. (D) The $\mathcal{H}^{(t)}$ (black dots above) and $\mathcal{H}^{(v)}$ (blue dots, below) values and respective kernel-based density functions (orange = training, blue = validation) for each task which illustrate that the estimated class separation for each task in their respective ambient representations are quite distinct.

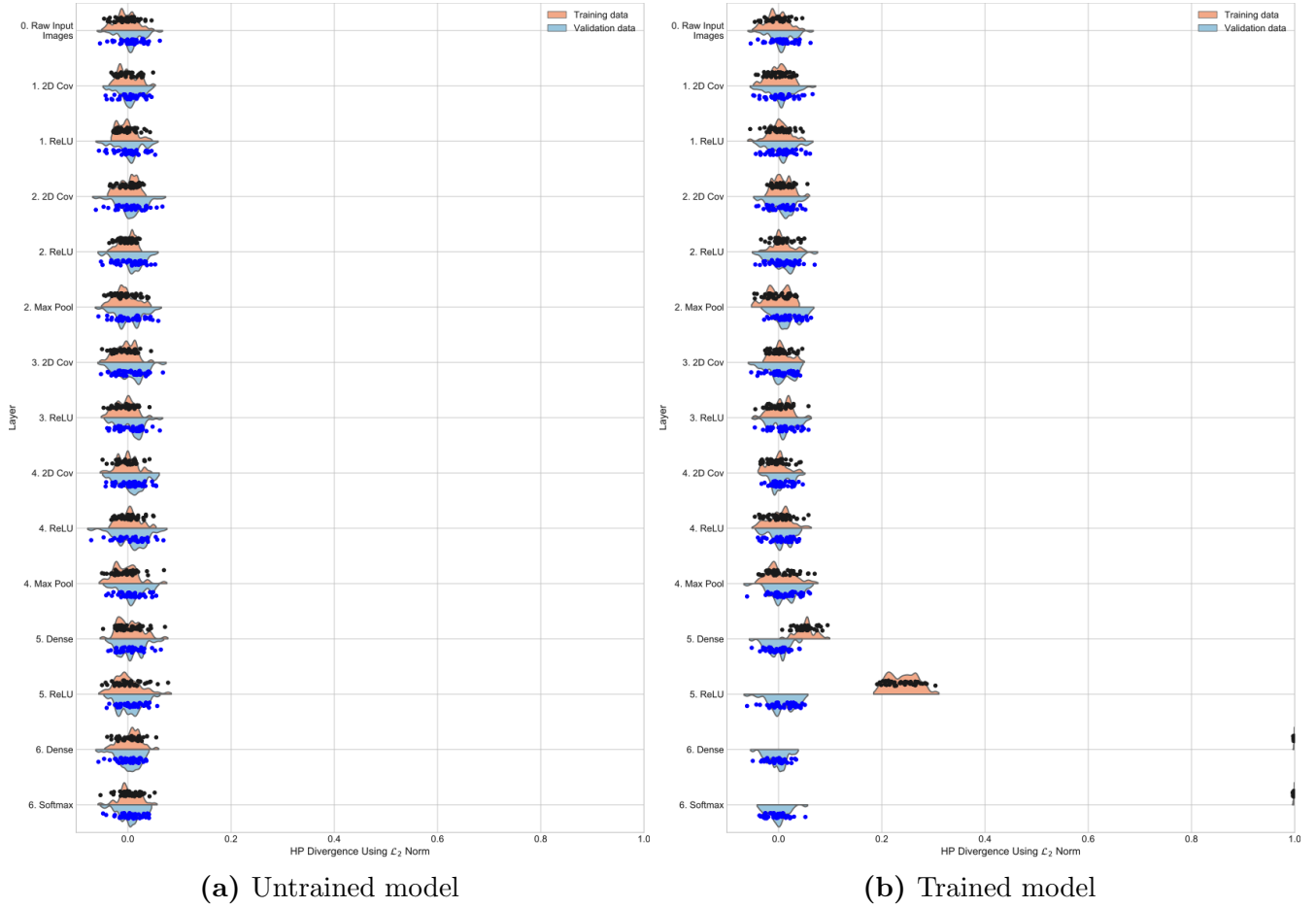


Figure S-2: \mathcal{H} class-pair statistics at each layer for instance 1 of the model for CIFAR10 with random class labels. (a) shows results for the data for passing through the randomly initialized model (epoch 0 state). (b) shows the results for the data passing through the fully trained model (epoch 200 state). (Note: Euclidean distance is used as the proximity measure.)

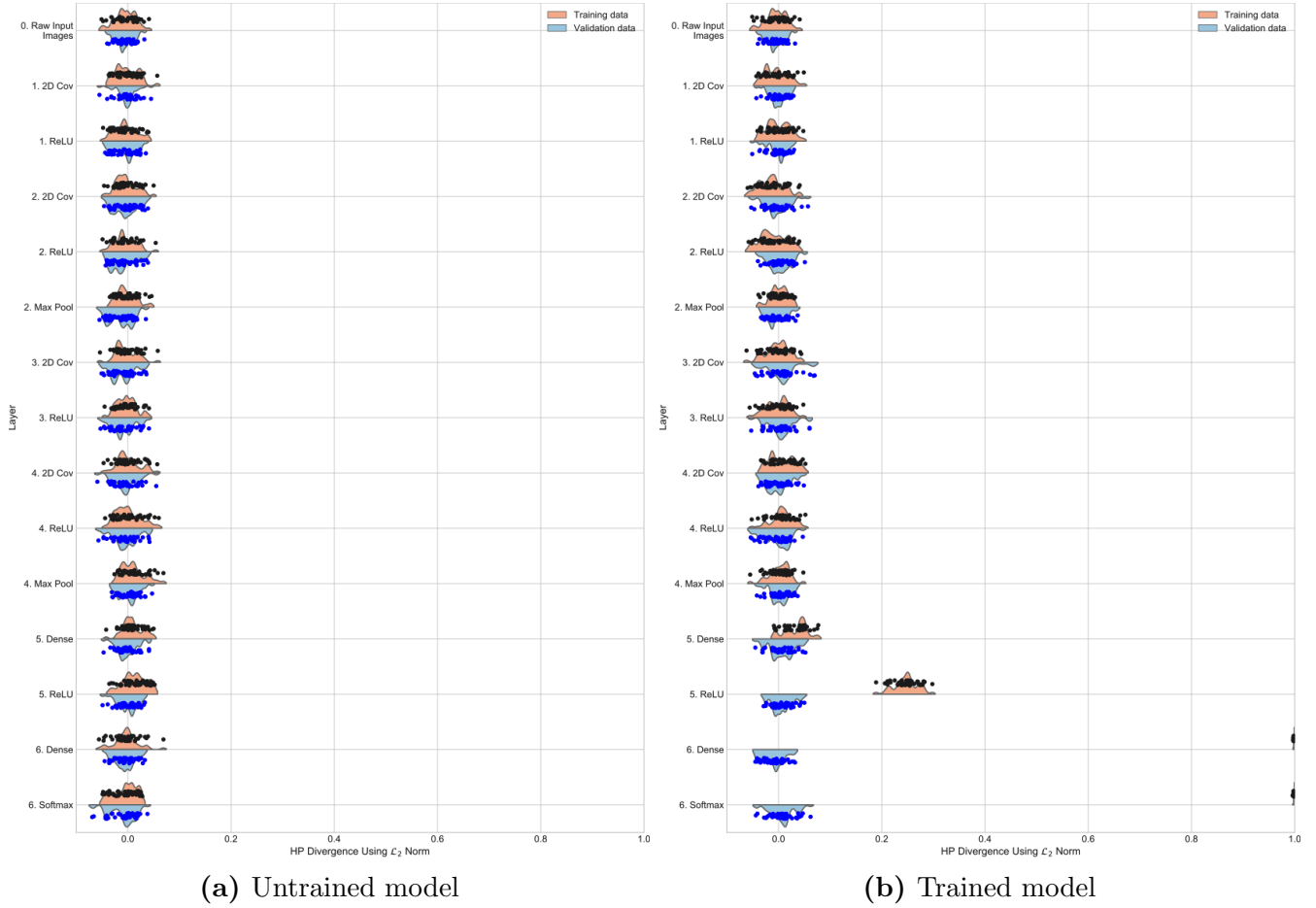


Figure S-3: \mathcal{H} class-pair statistics at each layer for instance 2 of the model for CIFAR10 with random class labels. (a) shows results for the data for passing through the randomly initialized model (epoch 0 state). (b) shows the results for the data passing through the fully trained model (epoch 200 state). (Note: Euclidean distance is used as the proximity measure.)

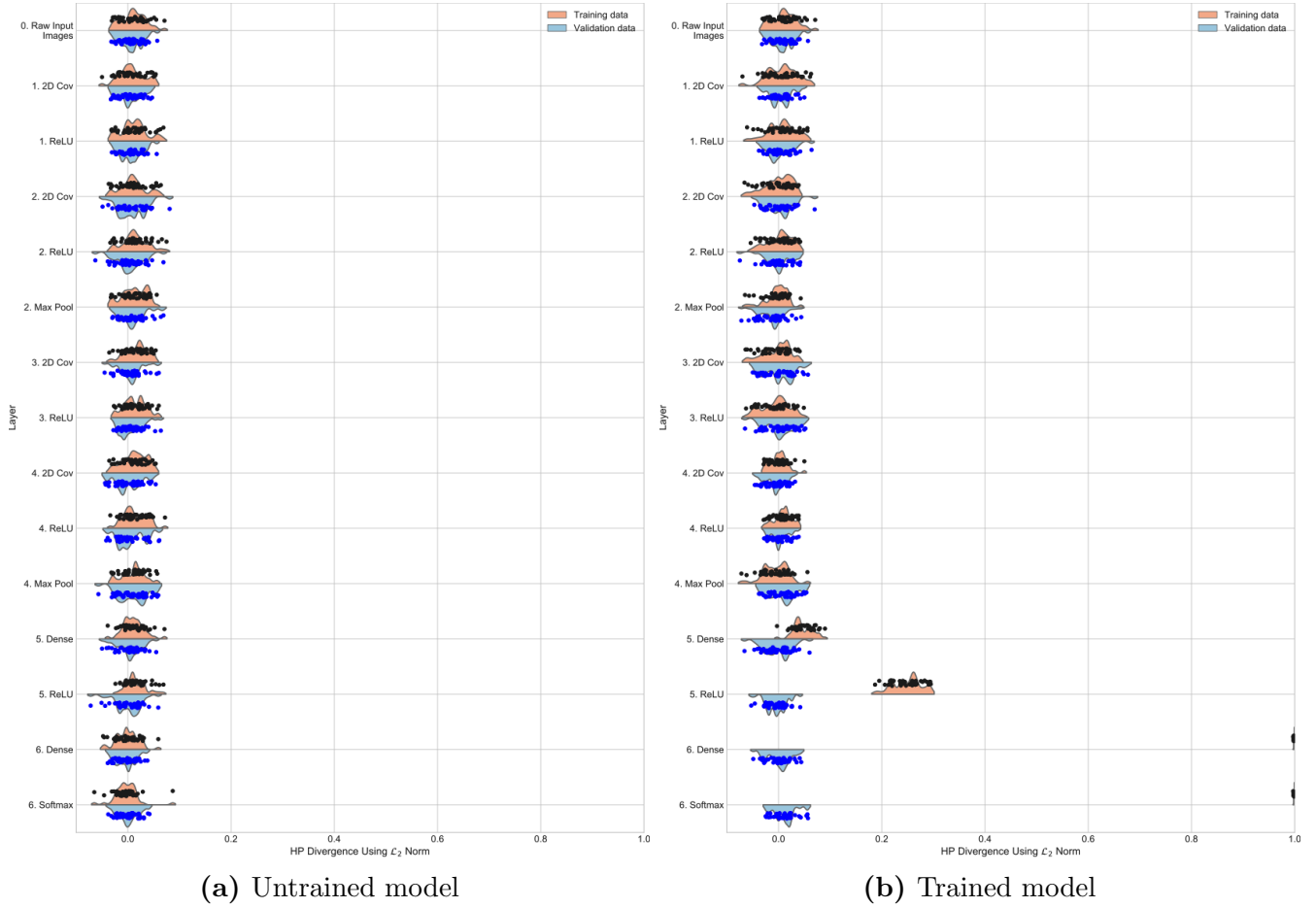


Figure S-4: \mathcal{H} class-pair statistics at each layer for instance 3 of the model for CIFAR10 with random class labels. (a) shows results for the data for passing through the randomly initialized model (epoch 0 state). (b) shows the results for the data passing through the fully trained model (epoch 200 state). (Note: Euclidean distance is used as the proximity measure.)

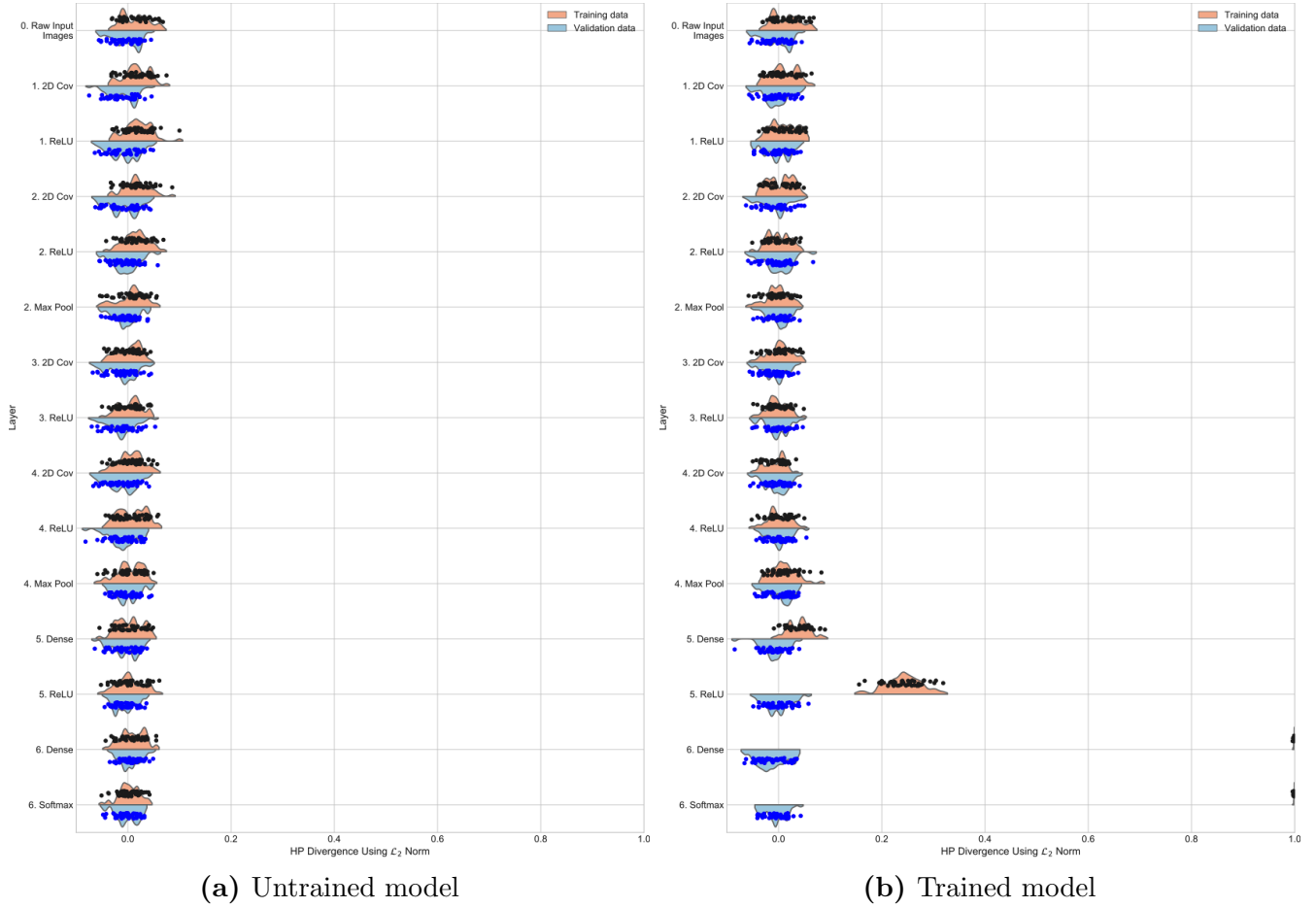


Figure S-5: \mathcal{H} class-pair statistics at each layer for instance 4 of the model for CIFAR10 with random class labels. (a) shows results for the data for passing through the randomly initialized model (epoch 0 state). (b) shows the results for the data passing through the fully trained model (epoch 200 state). (Note: Euclidean distance is used as the proximity measure.)

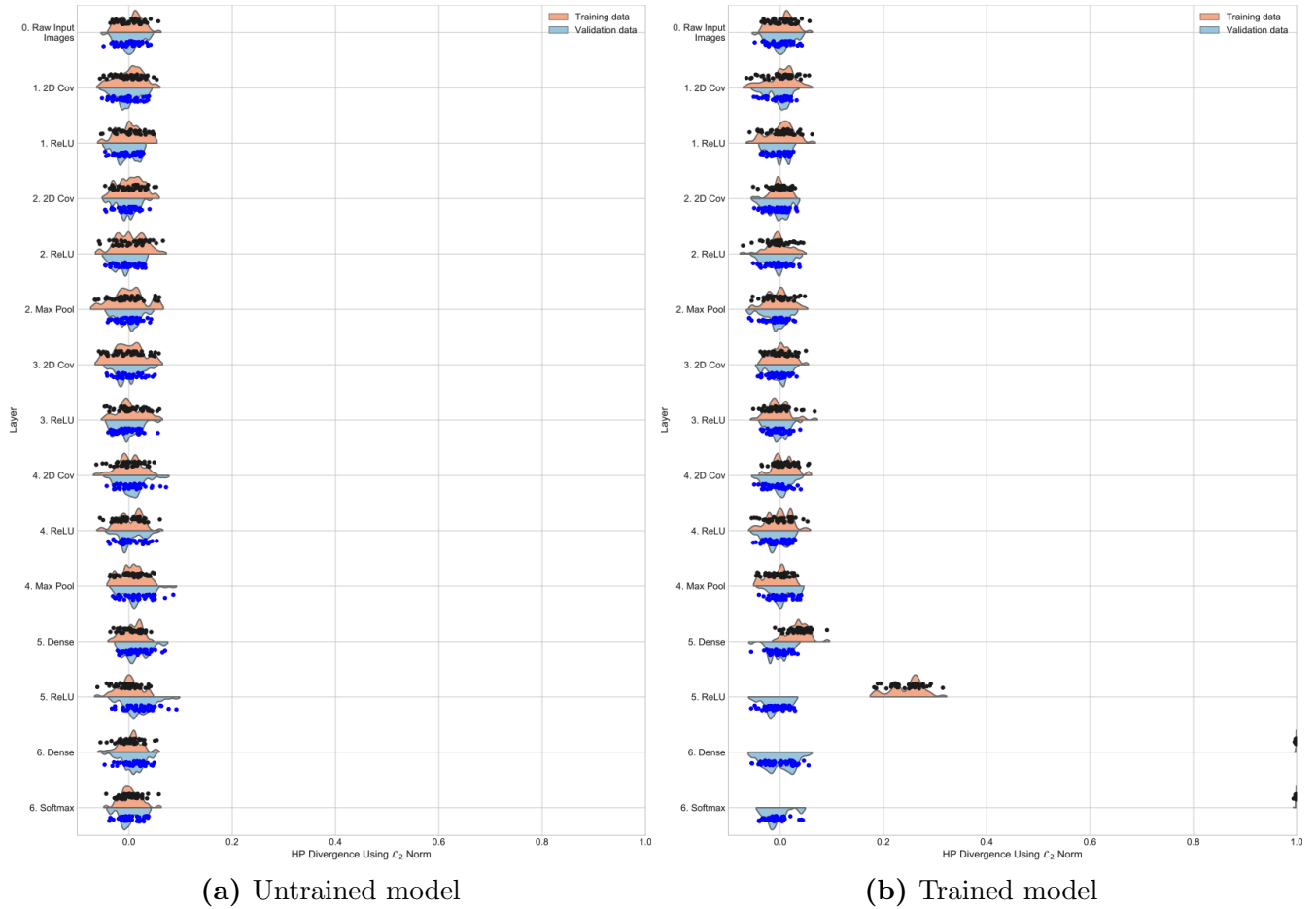


Figure S-6: \mathcal{H} class-pair statistics at each layer for instance 5 of the model for CIFAR10 with random class labels. (a) shows results for the data for passing through the randomly initialized model (epoch 0 state). (b) shows the results for the data passing through the fully trained model (epoch 200 state). (Note: Euclidean distance is used as the proximity measure.)

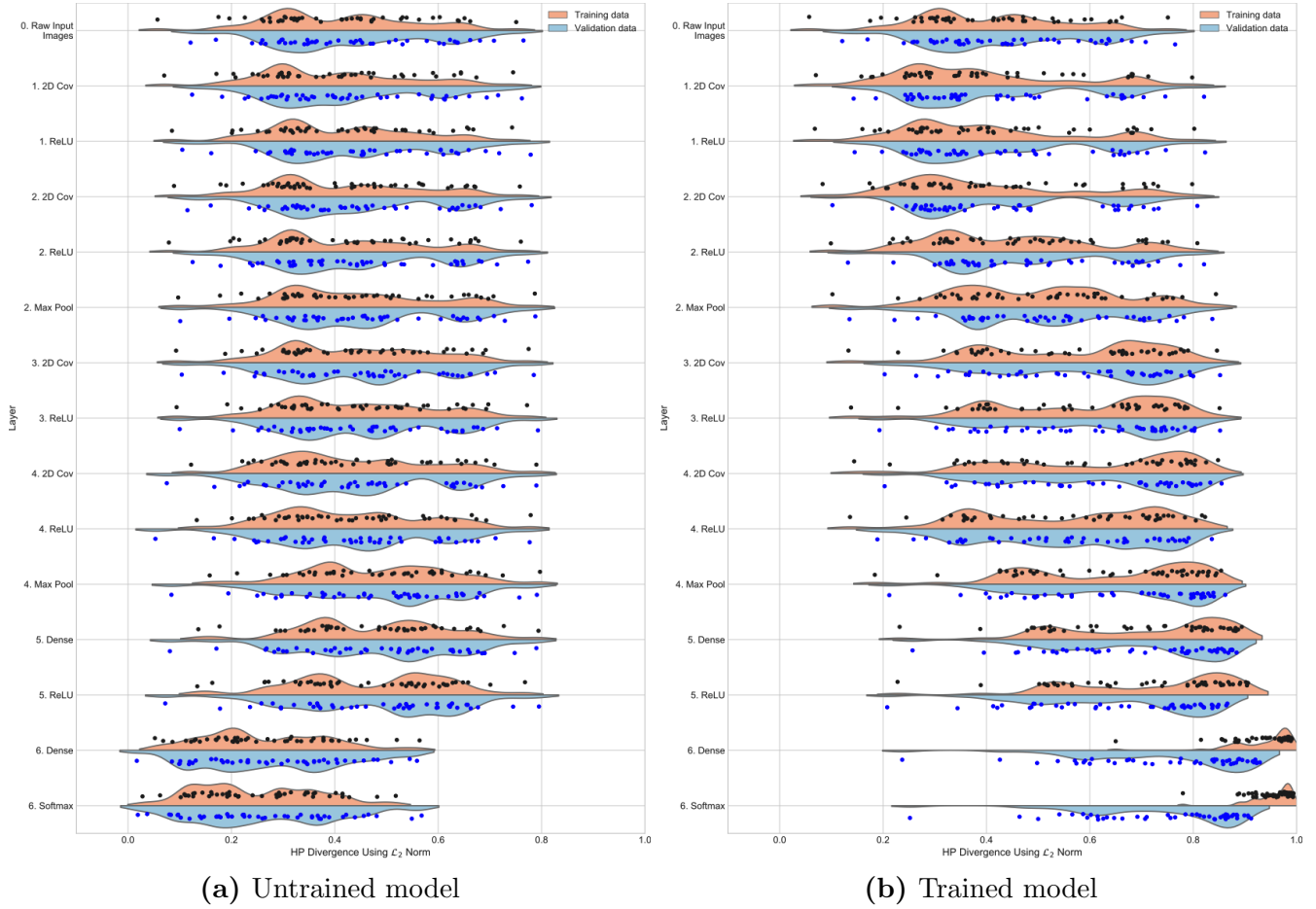


Figure S-7: \mathcal{H} class-pair statistics at each layer for instance 1 of the model for CIFAR10 with true class labels. (a) shows results for the data for passing through the randomly initialized model (epoch 0 state). (b) shows the results for the data passing through the fully trained model (stopping at peak validation set accuracy). (Note: Euclidean distance is used as the proximity measure.)

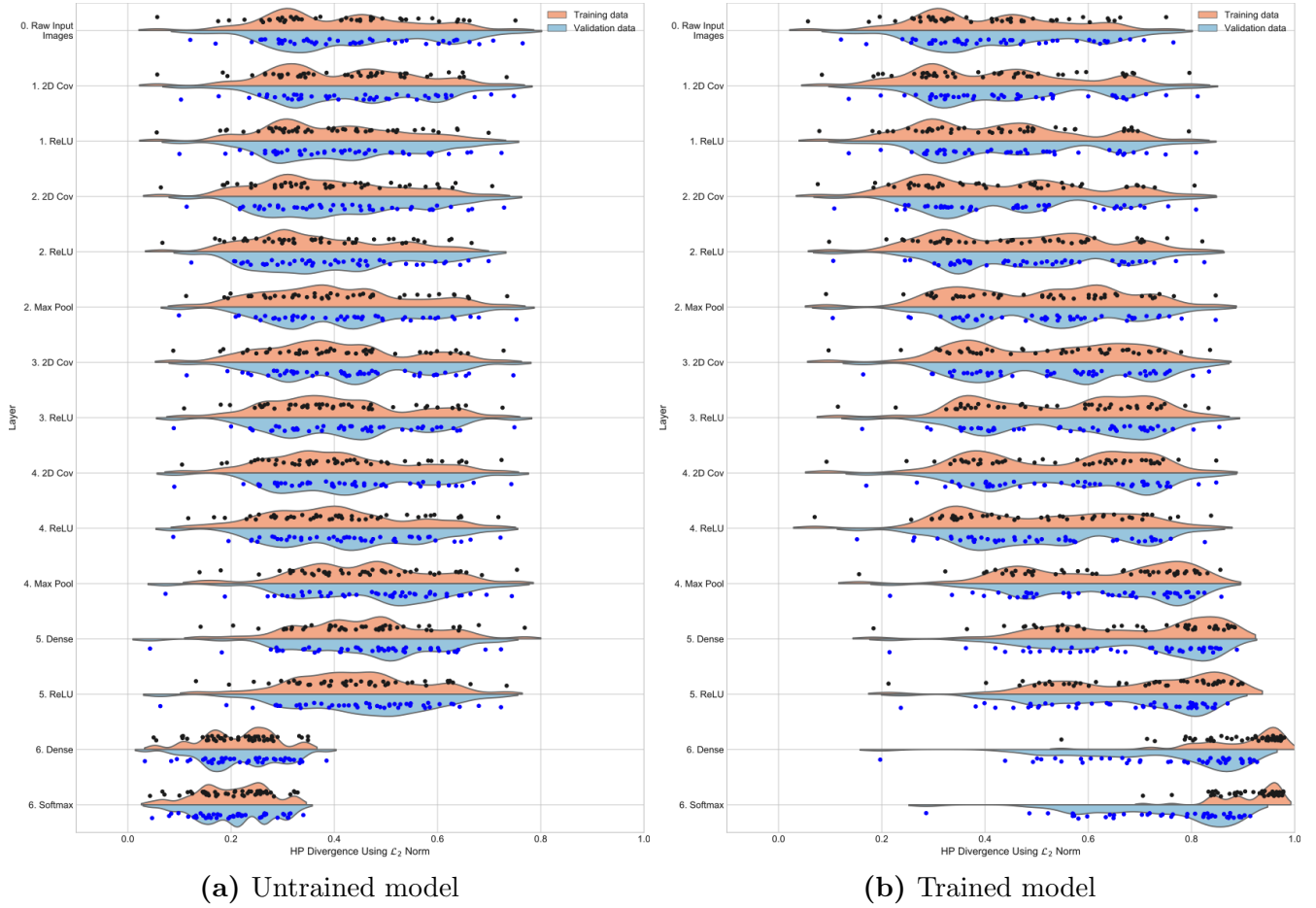


Figure S-8: \mathcal{H} class-pair statistics at each layer for instance 2 of the model for CIFAR10 with true class labels. (a) shows results for the data for passing through the randomly initialized model (epoch 0 state). (b) shows the results for the data passing through the fully trained model (stopping at peak validation set accuracy). (Note: Euclidean distance is used as the proximity measure.)

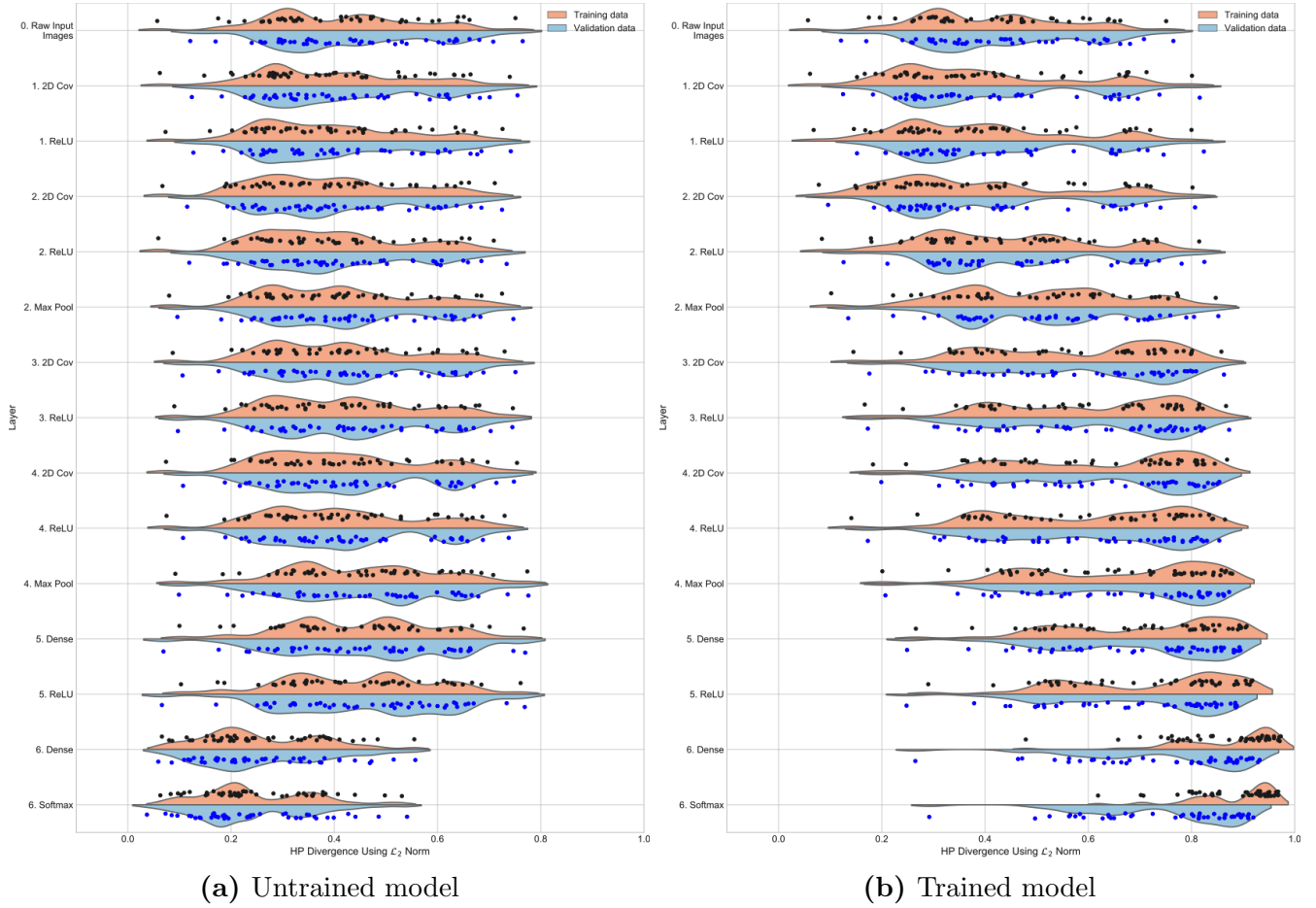


Figure S-9: \mathcal{H} class-pair statistics at each layer for instance 3 of the model for CIFAR10 with true class labels. (a) shows results for the data for passing through the randomly initialized model (epoch 0 state). (b) shows the results for the data passing through the fully trained model (stopping at peak validation set accuracy). (Note: Euclidean distance is used as the proximity measure.)

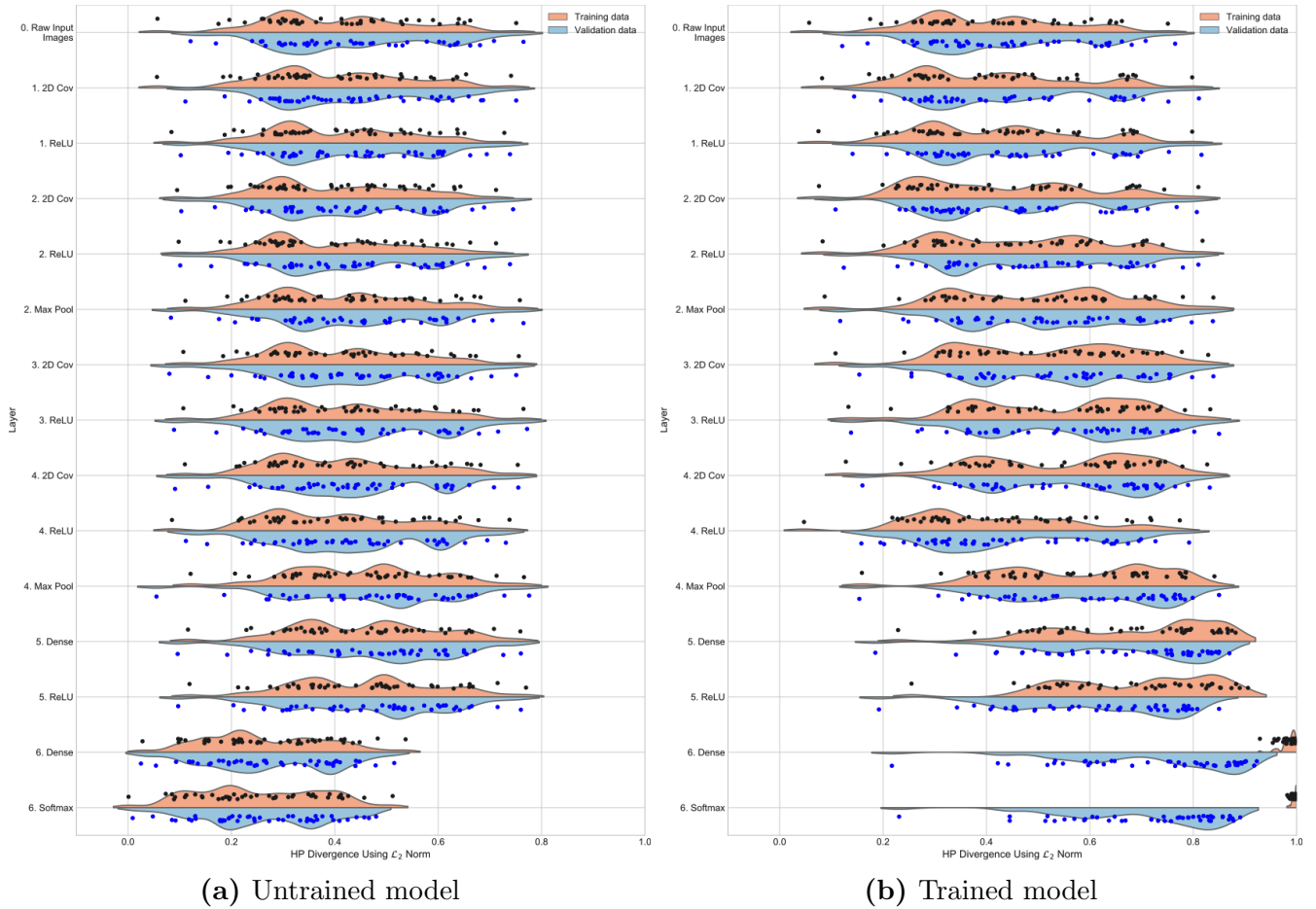


Figure S-10: \mathcal{H} class-pair statistics at each layer for instance 4 of the model for CIFAR10 with true class labels. (a) shows results for the data for passing through the randomly initialized model (epoch 0 state). (b) shows the results for the data passing through the fully trained model (stopping at peak validation set accuracy). (Note: Euclidean distance is used as the proximity measure.)

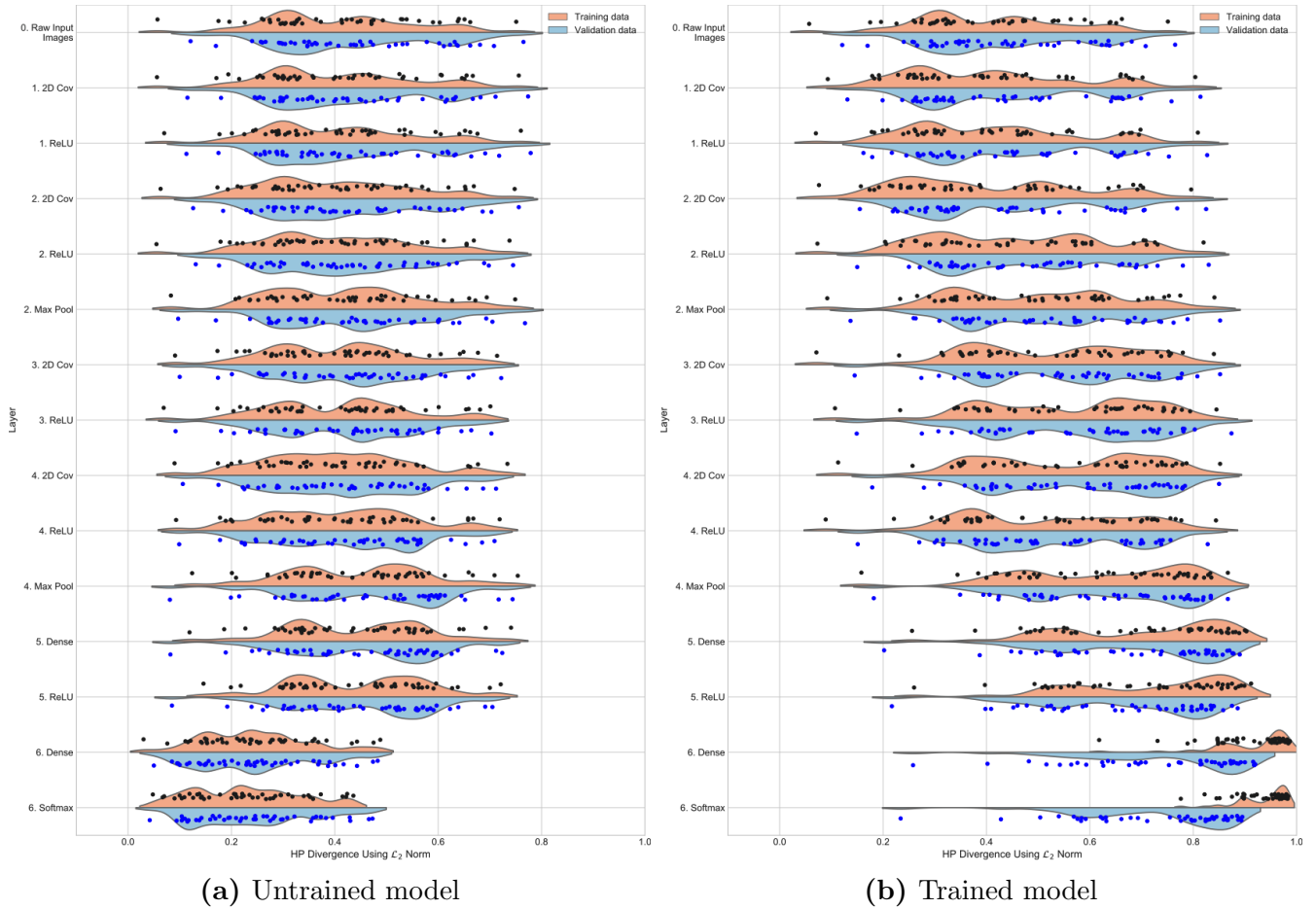


Figure S-11: \mathcal{H} class-pair statistics at each layer for instance 5 of the model for CIFAR10 with true class labels. (a) shows results for the data for passing through the randomly initialized model (epoch 0 state). (b) shows the results for the data passing through the fully trained model (stopping at peak validation set accuracy). (Note: Euclidean distance is used as the proximity measure.)

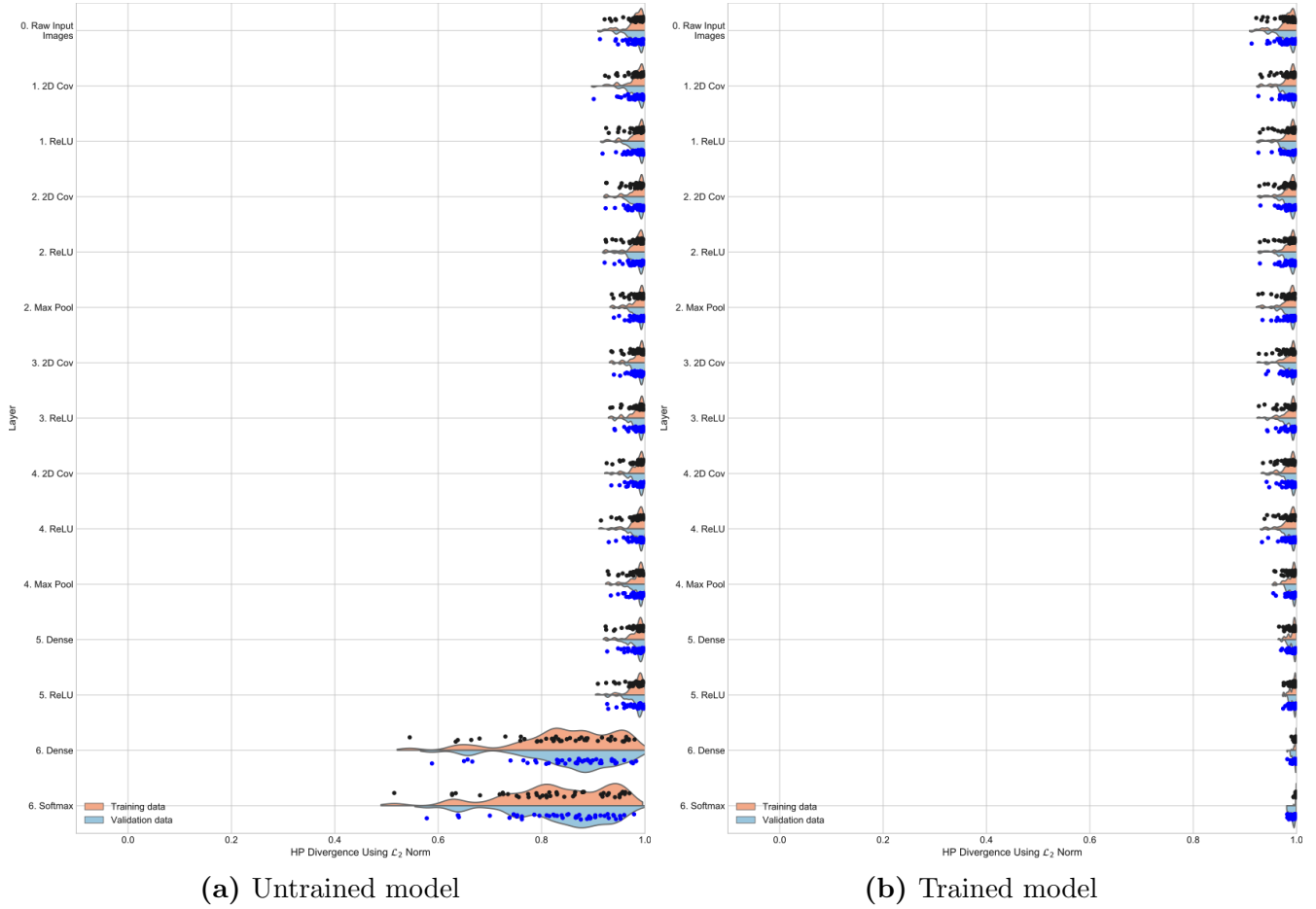


Figure S-12: \mathcal{H} class-pair statistics at each layer for instance 1 of the model for MNIST with true class labels. (a) shows results for the data for passing through the randomly initialized model (epoch 0 state). (b) shows the results for the data passing through the fully trained model (stopping at peak validation set accuracy). (Note: Euclidean distance is used as the proximity measure.)

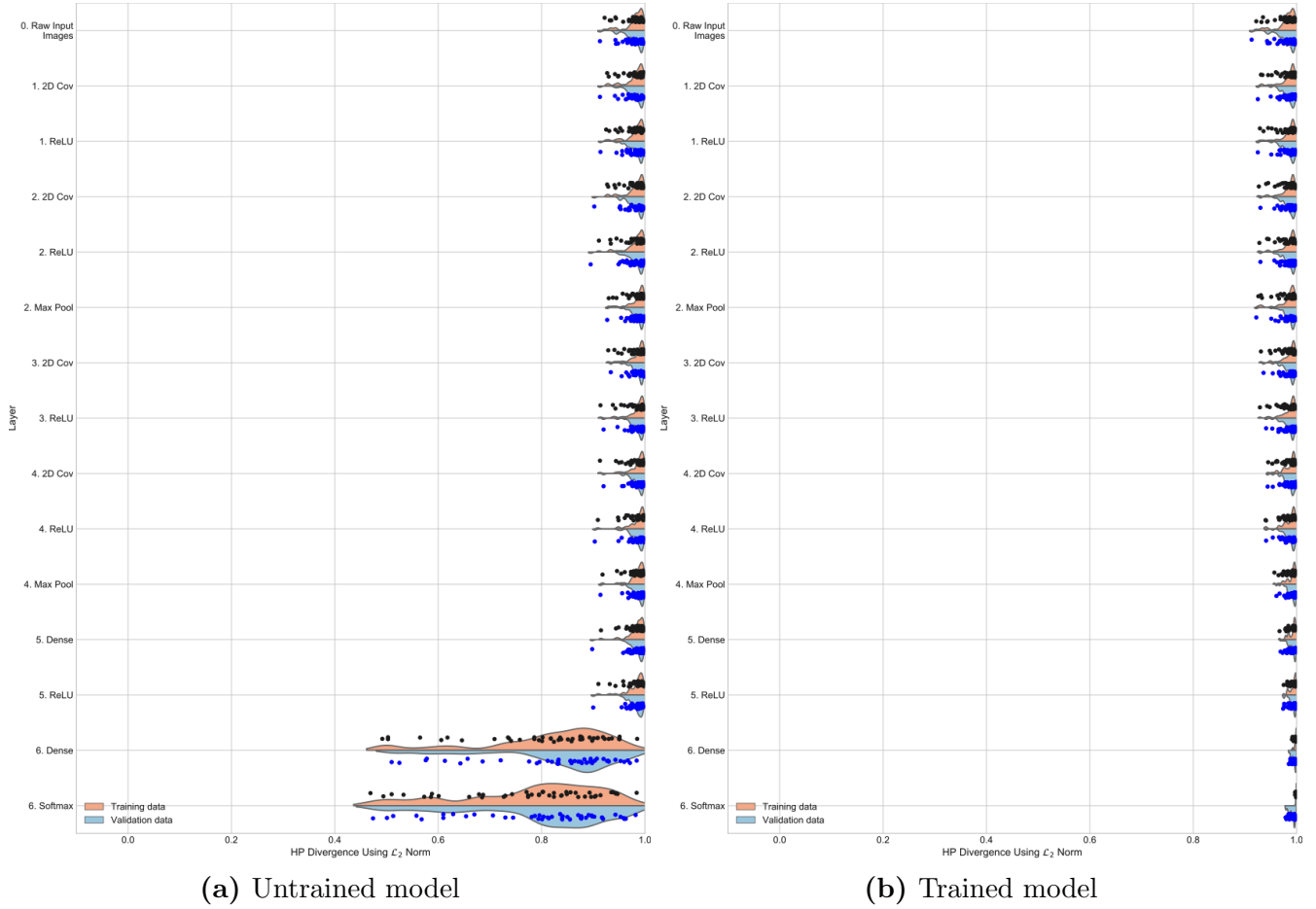


Figure S-13: \mathcal{H} class-pair statistics at each layer for instance 2 of the model for MNIST with true class labels. (a) shows results for the data for passing through the randomly initialized model (epoch 0 state). (b) shows the results for the data passing through the fully trained model (stopping at peak validation set accuracy). (Note: Euclidean distance is used as the proximity measure.)

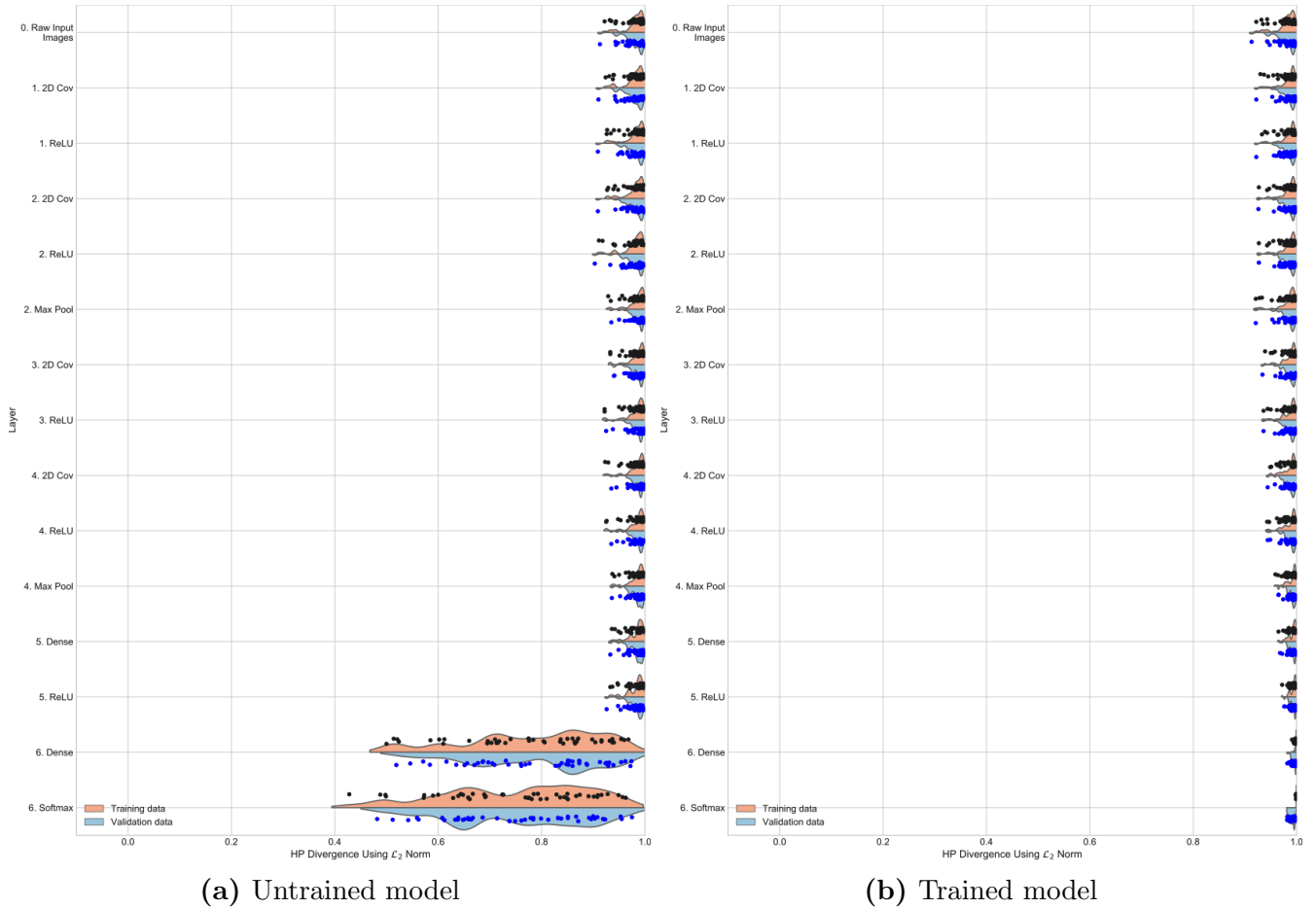


Figure S-14: \mathcal{H} class-pair statistics at each layer for instance 3 of the model for MNIST with true class labels. (a) shows results for the data for passing through the randomly initialized model (epoch 0 state). (b) shows the results for the data passing through the fully trained model (stopping at peak validation set accuracy). (Note: Euclidean distance is used as the proximity measure.)

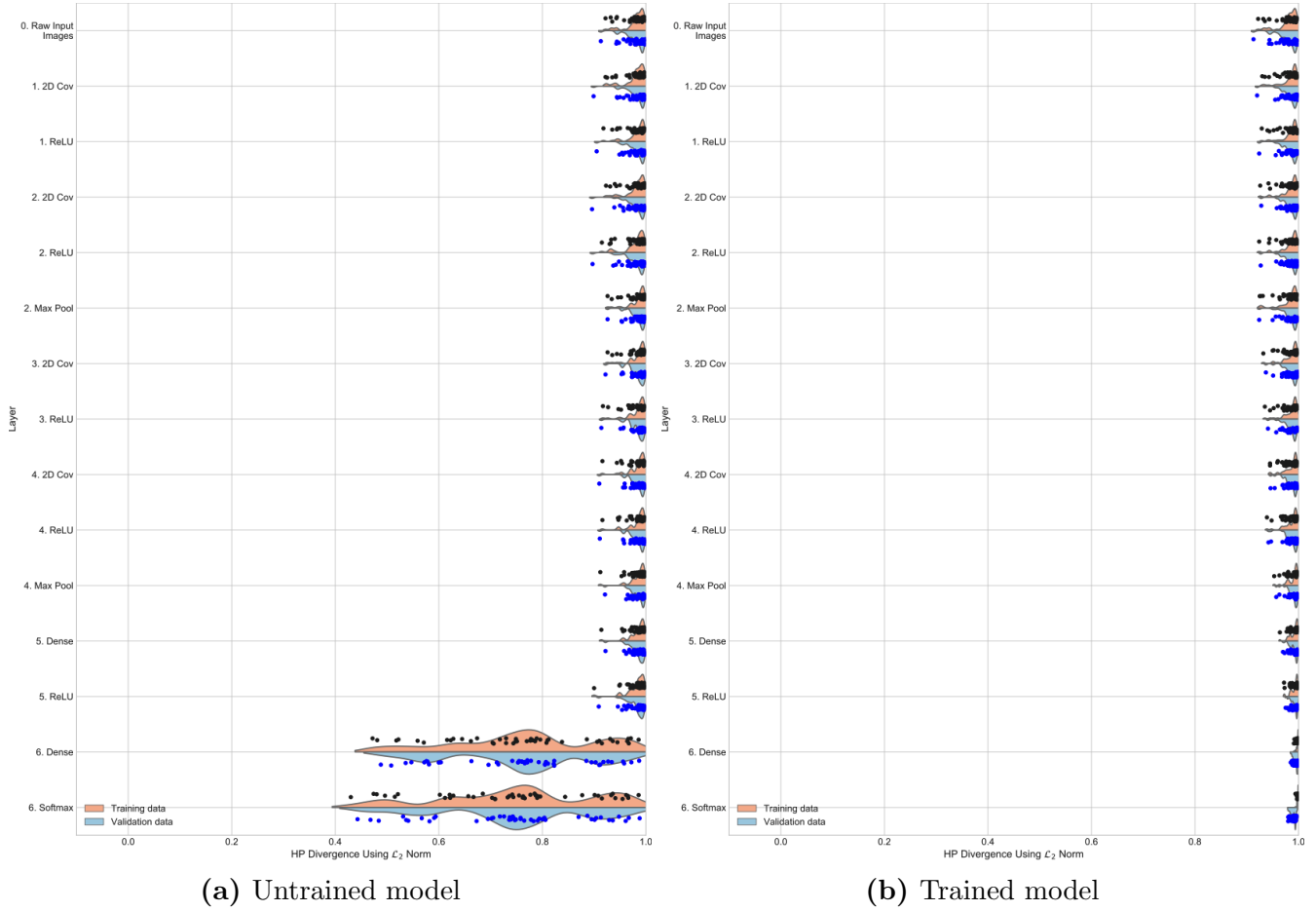


Figure S-15: \mathcal{H} class-pair statistics at each layer for instance 4 of the model for MNIST with true class labels. (a) shows results for the data for passing through the randomly initialized model (epoch 0 state). (b) shows the results for the data passing through the fully trained model (stopping at peak validation set accuracy). (Note: Euclidean distance is used as the proximity measure.)

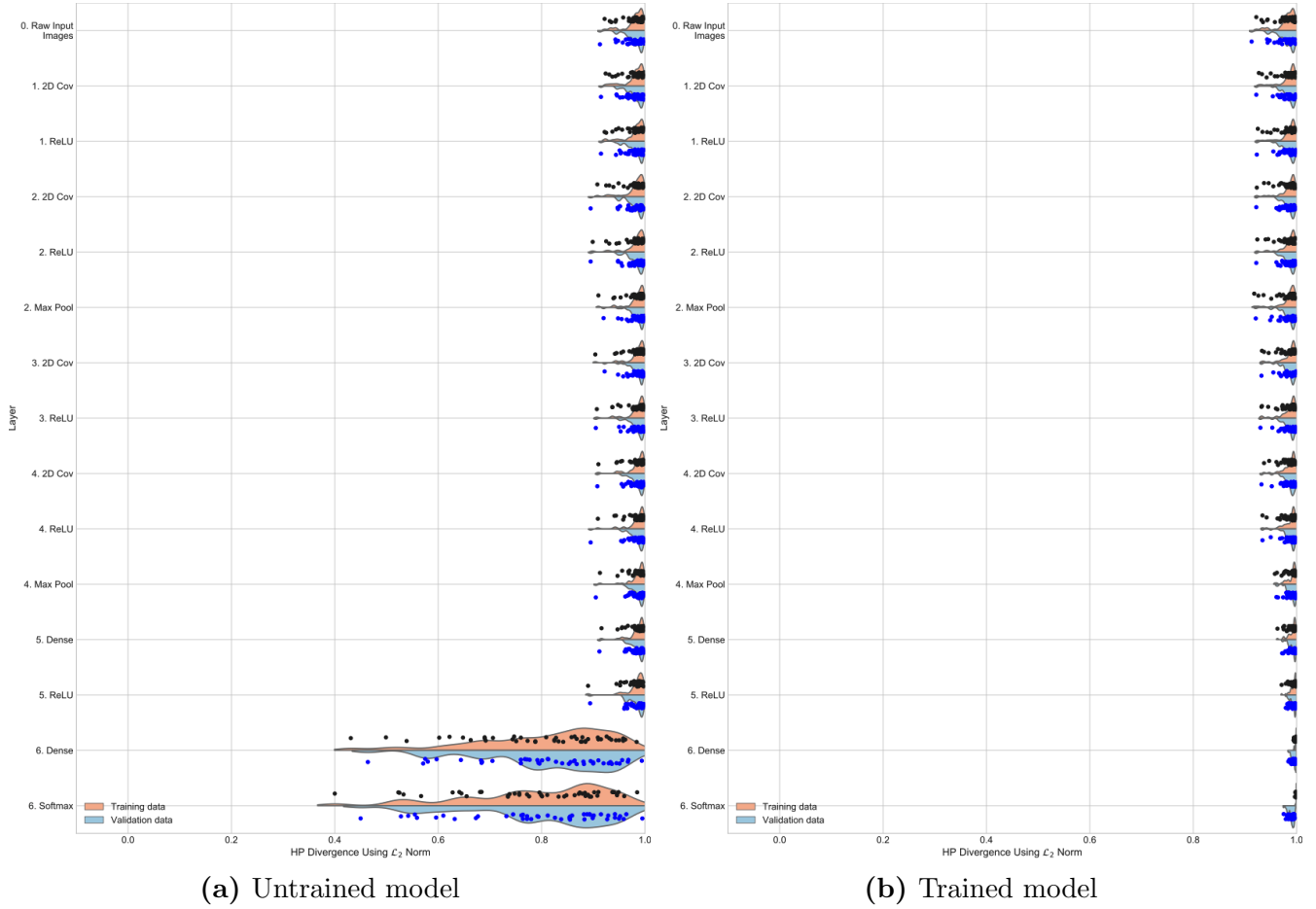


Figure S-16: \mathcal{H} class-pair statistics at each layer for instance 5 of the model for MNIST with true class labels. (a) shows results for the data for passing through the randomly initialized model (epoch 0 state). (b) shows the results for the data passing through the fully trained model (stopping at peak validation set accuracy). (Note: Euclidean distance is used as the proximity measure.)

Table S-1: Two-sided permutation test of training data to detect change in $\bar{\mathcal{H}}$ between layers (before training) with critical value $\alpha = 0.025$. **Red font** denote layer instances for which we reject \mathbf{H}_0 , black font denotes layers for which we fail to reject \mathbf{H}_0 . (Eq. 14 in paper) (Note: Euclidean distance is used as the proximity measure. 50,000 Monte Carlo trials were used to estimate the p -values. $\Delta\bar{\mathcal{H}} = \bar{\mathcal{H}}_{(k,0)}^{(t)} - \bar{\mathcal{H}}_{(k-1,0)}^{(t)}$)

Input Space	Output Space	CIFAR10 w Random		CIFAR10 w True		MNIST w True	
		$\Delta\bar{\mathcal{H}}$	p -values	$\Delta\bar{\mathcal{H}}$	p -values	$\Delta\bar{\mathcal{H}}$	p -values
0.Input	1.Conv	.003; .002; -.004; .003; -.003	.460; .649; .445; .556; .515	-.012; .005; -.017; -.003; -.004	.714; .864; .593; .923; .912	-.002; .001; -.001; .000; .000	.672; .792; .864; .934; .900
1.Conv	1.ReLU	-.002; -.003; .004; .002; .003	.531; .523; .434; .675; .641	.016; -.022; -.003; .001; -.000	.607; .463; .933; .969; .991	-.001; .000; .001; .002; .000	.875; .906; .713; .648; .918
1.ReLU	2.Conv	-.003; .001; -.001; -.002; -.001	.375; .801; .856; .650; .906	.003; -.006; -.001; -.009; -.005	.924; .842; .964; .771; .878	.000; -.000; -.001; -.001; -.000	.970; .981; .878; .826; .933
2.Conv	2.ReLU	-.001; -.002; .003; -.002; .001	.671; .626; .526; .667; .906	.002; -.017; .005; -.003; .003	.959; .562; .869; .929; .912	-.001; -.000; -.001; -.001; .001	.730; .962; .803; .748; .839
2.ReLU	2.MaxPool	-.005; .004; -.001; -.007; -.004	.202; .390; .832; .195; .576	.019; .035; .015; .020; .015	.563; .241; .623; .505; .624	.003; .003; .005; .004; .002	.365; .394; .202; .294; .565
2.MaxPool	3.Conv	-.001; -.001; .004; -.006; -.003	.873; .876; .428; .286; .695	.003; -.001; .003; -.002; -.009	.936; .978; .931; .948; .755	-.000; .000; -.000; -.000; .000	.998; 1.000; .998; .956; .973
3.Conv	3.ReLU	-.001; -.000; -.003; .002; .007	.747; .969; .574; .629; .246	.002; .003; .007; .004; -.002	.960; .914; .827; .895; .957	-.001; -.001; -.001; -.001; -.001	.872; .849; .721; .768; .895
3.ReLU	4.Conv	.005; .004; -.000; .000; -.005	.231; .345; .932; .954; .379	-.006; -.001; -.001; -.004; -.004	.861; .967; .975; .897; .904	.000; .001; .001; .001; .001	.998; .860; .823; .777; .842
4.Conv	4.ReLU	.005; -.000; .001; .003; .001	.220; .945; .842; .551; .821	-.003; -.003; -.006; -.008; .005	.936; .913; .851; .797; .878	-.001; .000; -.000; -.000; .000	.750; .945; .954; .893; .983
4.ReLU	4.MaxPool	-.009; .008; -.004; -.004; .004	.059; .092; .364; .425; .444	.049; .054; .040; .051; .038	.113; .061; .204; .096; .212	-.000; .000; .001; .001; .001	.962; .987; .840; .778; .777
4.MaxPool	5.Dense	.009; .000; .000; .000; .001	.061; .976; .925; .996; .838	-.005; -.001; .002; .003; -.003	.858; .976; .962; .920; .908	-.001; -.001; -.001; -.001; -.001	.758; .746; .633; .880; .682
5.Dense	5.ReLU	-.004; .004; .005; .001; -.006	.424; .385; .283; .925; .199	-.007; -.014; -.008; -.003; .003	.813; .596; .789; .908; .915	-.002; -.002; -.001; -.002; -.002	.696; .654; .723; .549; .666
5.ReLU	6.Dense	-.005; -.017 ; -.017 ; .005; .003	.330; .001 ; .000 ; .305; .549	-.202 ; -.226 ; -.182 ; -.189 ; -.198	.000 ; .000 ; .000 ; .000 ; .000	-.135 ; -.173 ; -.202 ; -.219 ; -.177	.000 ; .000 ; .000 ; .000 ; .000
6.Dense	6.Softmax	-.001; -.002; -.002; -.007; -.000	.891; .665; .688; .145; .933	-.018; -.011; -.010; -.013; -.017	.473; .457; .690; .618; .446	-.018; -.030; -.030; -.014; -.016	.419; .280; .296; .652; .582

Table S-2: Differences between the trained and initialized \mathcal{H} class-pair statistics of a layer, and respective p -values for the corresponding one-sided permutation test (Eq. 15 in paper). **Red font** denotes layer instances for which we reject \mathbf{H}_0 , and **black font** denotes layers for which we fail to reject \mathbf{H}_0 . (Note: Euclidean distance is used as the proximity measure. 50,000 Monte Carlo trials to estimate the p -values. $\Delta\bar{\mathcal{H}} = \bar{\mathcal{H}}_{(k,T)}^{(t)} - \bar{\mathcal{H}}_{(k,0)}^{(t)}$)

Output Space	CIFAR10 w Random		CIFAR10 w True		MNIST w True	
	$\Delta\bar{\mathcal{H}}$	p -values	$\Delta\bar{\mathcal{H}}$	p -values	$\Delta\bar{\mathcal{H}}$	p -values
1.Conv	-.000; -.002; .000; -.007; .000	.507; .645; .472; .888; .482	-.007; .005; -.008; .004; -.004	.580; .435; .591; .453; .542	.001; .002; .004; .003; .003	.346; .277; .126; .209; .248
1.ReLU	-.004; .004; -.004; -.009; -.001	.137; .225; .775; .955; .587	-.012; .029; .005; .015; .005	.646; .183; .440; .320; .448	.001; .002; .003; .001; .002	.417; .316; .208; .354; .274
2.Conv	.007; -.009; -.011; -.014; -.004	.032; .973; .976; .995; .812	-.017; .039; -.006; .028; .001	.690; .121; .570; .200; .491	.001; .002; .004; .003; .003	.422; .247; .161; .243; .202
2.ReLU	-.008 ; -.003; -.012; -.015; -.008	.017 ; .706; .989; .998; .913	.032 ; .095 ; .051 ; .066 ; .051	.174 ; .002 ; .068 ; .024 ; .068	.002; .003; .005; .004; .002	.281; .233; .105; .161; .271
2.MaxPool	.005; .004; -.015; -.010; -.004	.126; .161; .999; .967; .725	.065 ; .100 ; .094 ; .081 ; .073	.030 ; .002 ; .003 ; .008 ; .016	-.002; -.002; -.001; -.001; -.001	.722; .669; .647; .655; .603
3.Conv	-.009 ; .001; -.021; .000; .004	.011 ; .388; 1.000; .498; .233	.127 ; .117 ; .168 ; .097 ; .118	.000 ; .000 ; .000 ; .002 ; .000	-.000; .001; .001; .001; .001	.525; .433; .328; .355; .440
3.ReLU	.010 ; .001; -.020; -.006; -.008	.010 ; .365; 1.000; .896; .926	.140 ; .135 ; .184 ; .117 ; .149	.000 ; .000 ; .000 ; .000 ; .000	-.000; .001; .002; .002; .001	.500; .431; .264; .281; .390
4.Conv	-.002; .006; -.014; -.011; .008	.669; .111; .999; .989; .053	.168 ; .131 ; .205 ; .129 ; .148	.000 ; .000 ; .000 ; .000 ; .000	.000; .001; .002; .001; .001	.444; .381; .278; .330; .358
4.ReLU	-.001; .007; -.006; -.007; -.003	.610; .084; .919; .909; .704	.128 ; .098 ; .190 ; .011; .106	.000 ; .002 ; .000 ; .366; .001	.001; .001; .002; .003; .002	.336; .397; .228; .210; .314
4.MaxPool	.009; -.007; -.016; .006; -.011	.045; .928; .999; .127; .988	.161 ; .163 ; .207 ; .125 ; .181	.000 ; .000 ; .000 ; .000 ; .000	.006 ; .005; .006 ; .005; .004	.023 ; .049; .015 ; .038; .068
5.Dense	.049 ; .024 ; .036 ; .035 ; .029	.000 ; .000 ; .000 ; .000 ; .000	.227 ; .231 ; .257 ; .225 ; .258	.000 ; .000 ; .000 ; .000 ; .000	.009 ; .008 ; .009 ; .007 ; .007	.001 ; .001 ; .000 ; .001 ; .002
5.ReLU	.241 ; .234 ; .233 ; .238 ; .246	.000 ; .000 ; .000 ; .000 ; .000	.248 ; .256 ; .279 ; .237 ; .270	.000 ; .000 ; .000 ; .000 ; .000	.012 ; .011 ; .012 ; .010 ; .011	.000 ; .000 ; .000 ; .000 ; .000
6.Dense	.994 ; 1.002 ; 1.000 ; .989 ; .996	.000 ; .000 ; .000 ; .000 ; .000	.669 ; .681 ; .610 ; .718 ; .668	.000 ; .000 ; .000 ; .000 ; .000	.152 ; .188 ; .218 ; .234 ; .192	.000 ; .000 ; .000 ; .000 ; .000
6.Softmax	.995 ; 1.004 ; 1.002 ; .996 ; .996	.000 ; .000 ; .000 ; .000 ; .000	.706 ; .711 ; .634 ; .741 ; .706	.000 ; .000 ; .000 ; .000 ; .000	.171 ; .219 ; .250 ; .249 ; .209	.000 ; .000 ; .000 ; .000 ; .000

Table S-3: Training data difference between input and output of each layer’s \mathcal{H} class-pair statistics for the trained models, and respective p -values for the one sided permutation test (Eq. 17 in paper). **Red font** denotes layer instances for which we reject \mathbf{H}_0 , and black font denotes layers for which we fail to reject \mathbf{H}_0 . (Note: Euclidean distance is used as the proximity measure. 50,000 Monte Carlo trials used to estimate the p -values. $\Delta\bar{\mathcal{H}} = \bar{\mathcal{H}}_{(k,T)}^{(t)} - \bar{\mathcal{H}}_{(k-1,T)}^{(t)}$)

Input Space	Output Space	CIFAR10 w Random		CIFAR10 w True		MNIST w True	
		$\Delta\bar{\mathcal{H}}$	p -values	$\Delta\bar{\mathcal{H}}$	p -values	$\Delta\bar{\mathcal{H}}$	p -values
0.Input	1.Conv	.003; .000; -.004; -.003; -.003	.243; .474; .741; .729; .721	-.019; .011; -.025; .001; -.007	.708; .378; .767; .492; .582	.003; .003; .004; .003; .003	.200; .199; .169; .181; .208
1.Conv	1.ReLU	.002; .002; -.000; -.001; -.001	.312; .303; .531; .542; .421	.010; .002; .010; .013; .008	.386; .481; .389; .356; .410	-.000; .000; .000; .000; .000	.506; .492; .481; .480; .493
1.ReLU	2.Conv	.006; -.012; -.008; -.007; -.003	.070; .990; .911; .896; .756	-.002; .004; -.013; .004; -.009	.525; .455; .635; .453; .591	.000; .001; .000; .000; .001	.494; .425; .502; .468; .433
2.Conv	2.ReLU	-.001; .004; .002; -.003; -.003	.573; .210; .330; .740; .752	.051; .039; .062; .035; .053	.080; .142; .052; .164; .076	.000; .000; .000; .000; .000	.481; .496; .482; .500; .494
2.ReLU	2.MaxPool	-.007; .010; -.005; -.002; .000	.955; .015; .827; .682; .471	.051; .040; .058; .035; .037	.071; .130; .055; .164; .152	-.001; -.001; -.001; -.001; -.001	.599; .609; .629; .632; .608
2.MaxPool	3.Conv	.005; -.003; -.001; .004; .005	.127; .775; .603; .193; .146	.065; .017; .077; .015; .036	.035; .318; .020; .334; .158	.002; .002; .003; .003; .002	.301; .274; .210; .235; .323
3.Conv	3.ReLU	-.001; -.000; -.002; -.004; -.005	.610; .503; .616; .776; .840	.014; .021; .023; .024; .029	.346; .285; .270; .251; .210	-.000; -.001; -.001; -.000; -.000	.534; .581; .568; .543; .513
3.ReLU	4.Conv	-.007; .009; .005; -.005; .011	.947; .039; .132; .865; .010	.023; -.005; .020; .008; -.004	.276; .550; .307; .412; .545	.000; .001; .001; .000; .001	.444; .371; .425; .440; .374
4.Conv	4.ReLU	.006; .000; .009; .007; -.009	.107; .462; .007; .058; .975	-.043; -.036; -.020; -.126; -.038	.866; .839; .701; 1.000; .845	-.000; .000; .000; .001; .001	.522; .476; .458; .404; .428
4.ReLU	4.MaxPool	.001; -.005; -.015; .009; -.004	.397; .869; .999; .041; .806	.081; .119; .057; .165; .113	.015; .001; .068; .000; .002	.004; .004; .004; .003; .004	.051; .068; .059; .089; .085
4.MaxPool	5.Dense	.049; .031; .053; .029; .040	.000; .000; .000; .000; .000	.061; .067; .051; .103; .074	.042; .028; .080; .002; .020	.002; .002; .002; .002; .002	.111; .136; .192; .165; .195
5.Dense	5.ReLU	.188; .214; .202; .203; .212	.000; .000; .000; .000; .000	.013; .010; .015; .009; .015	.351; .380; .338; .396; .332	.001; .001; .002; .001; .002	.176; .190; .126; .292; .091
5.ReLU	6.Dense	.758; .752; .750; .756; .753	.000; .000; .000; .000; .000	.220; .199; .148; .292; .201	.000; .000; .000; .000; .000	-.005; .004; -.004; .005; .004	.000; .000; .000; .000; .000
6.Dense	6.Softmax	-.000; -.000; .000; .000; -.000	.985; .581; .250; .145; .858	.019; .019; .015; .010; .020	.049; .124; .221; .000; .070	.001; .001; .001; .001; .001	.001; .000; .000; .028; .000

Table S-4: Training data difference between between multi-layer component input and output \mathcal{H} class-pair statistics for the trained models, and respective p -values for the one sided permutation test (Eq. 17 in paper). **Red font** denotes layer instances for which we reject \mathbf{H}_0 , and black font denotes layers for which we fail to reject \mathbf{H}_0 . (Note: Euclidean distance is used as the proximity measure. 50,000 Monte Carlo trials used to estimate the p -values. $\Delta\bar{\mathcal{H}} = \bar{\mathcal{H}}_{(k_2,T)}^{(t)} - \bar{\mathcal{H}}_{(k_1,T)}^{(t)}$)

Input Space	Output Space	CIFAR10 w Random		CIFAR10 w True		MNIST w True	
		$\Delta\bar{\mathcal{H}}$	p -values	$\Delta\bar{\mathcal{H}}$	p -values	$\Delta\bar{\mathcal{H}}$	p -values
0.Input	1.ReLU	.005; .003; -.004; -.004; -.002	.120; .283; .765; .757; .649	-.008; .013; -.015; .013; .001	.598; .353; .668; .341; .492	.003; .003; .004; .004; .003	.203; .195; .151; .171; .201
1.ReLU	2.ReLU	.005; -.007; -.005; -.010; -.006	.101; .920; .833; .973; .880	.049; .043; .049; .040; .045	.083; .114; .090; .132; .110	.000; .001; .000; .000; .001	.476; .424; .474; .467; .421
2.ReLU	2.MaxPool	-.007; .010; -.005; -.002; .000	.956; .014; .828; .688; .471	.051; .040; .058; .035; .037	.072; .131; .057; .167; .152	-.001; -.001; -.001; -.001; -.001	.606; .611; .631; .633; .608
2.MaxPool	3.ReLU	.004; -.003; -.003; .001; .000	.204; .781; .715; .443; .473	.079; .038; .100; .039; .065	.015; .142; .005; .133; .037	.002; .001; .002; .002; .002	.330; .344; .265; .262; .338
3.ReLU	4.ReLU	-.001; .009; .014; .002; .001	.585; .027; .002; .308; .389	-.020; -.041; -.001; -.118; -.042	.703; .871; .506; 1.000; .876	.000; .001; .001; .001; .002	.461; .358; .384; .347; .315
4.ReLU	4.MaxPool	.001; -.005; -.015; .009; -.004	.396; .872; .999; .041; .806	.081; .119; .057; .165; .113	.015; .001; .068; .000; .001	.004; .004; .004; .003; .004	.051; .067; .058; .089; .087
4.MaxPool	5.ReLU	.238; .245; .255; .232; .252	.000; .000; .000; .000; .000	.075; .078; .065; .112; .089	.018; .014; .035; .000; .005	-.004; .003; -.003; .003; .004	.020; .030; .024; .067; .017
5.ReLU	6.Softmax	.758; .752; .750; .757; .753	.000; .000; .000; .000; .000	.238; .218; .163; .303; .221	.000; .000; .000; .000; .000	.006; .006; .005; .006; .005	.000; .000; .000; .000; .000

Table S-5: Training data difference between between multi-layer component input and output \mathcal{H} class-pair statistics for the trained models, and respective p -values for the one sided permutation test (Eq. 17 in paper). **Red font** denotes layer instances for which we reject \mathbf{H}_0 , and black font denotes layers for which we fail to reject \mathbf{H}_0 . (Note: Euclidean distance is used as the proximity measure. 50,000 Monte Carlo trials used to estimate the p -values.

$$\Delta \bar{\mathcal{H}} = \bar{\mathcal{H}}_{(k_2, T)}^{(t)} - \bar{\mathcal{H}}_{(k_1, T)}^{(t)}$$

Input Space	Output Space	CIFAR10 w Random		CIFAR10 w True		MNIST w True	
		$\Delta \bar{\mathcal{H}}$	p -values	$\Delta \bar{\mathcal{H}}$	p -values	$\Delta \bar{\mathcal{H}}$	p -values
0.Input	2.MaxPool	.003; .006; -.014; -.016; -.008	.275; .078; .998; .998; .949	.093; .095; .093; .087; .083	.003; .003; .003; .006; .008	.002; .003; .003; .003; .003	.271; .227; .240; .252; .231
2.MaxPool	4.MaxPool	.004; .001; -.003; .012; -.002	.213; .402; .760; .011; .699	.141; .116; .157; .085; .136	.000; .000; .000; .007; .000	.006; .006; .007; .007; .007	.021; .016; .011; .014; .017
4.MaxPool	5.ReLU	.238; .245; .255; .232; .252	.000; .000; .000; .000; .000	.075; .078; .065; .112; .089	.018; .013; .037; .000; .005	.004; .003; .003; .003; .004	.020; .029; .025; .066; .018
5.ReLU	6.Softmax	.758; .752; .750; .757; .753	.000; .000; .000; .000; .000	.238; .218; .163; .303; .221	.000; .000; .000; .000; .000	.006; .006; .005; .006; .005	.000; .000; .000; .000; .000

Table S-6: Validation data differences in mean of \mathcal{H} class-pair statistics between the input and output representations of a layer, and respective one-sided permutation test p -values. **Red font** denotes layer instances for which we reject \mathbf{H}_0 , and black font denotes layers for which we fail to reject \mathbf{H}_0 (Eq. 18 in paper). (Note: Note: Euclidean distance is used as the proximity measure. 50,000 Monte Carlo trials used to estimate the p -values.

$$\Delta \bar{\mathcal{H}} = \bar{\mathcal{H}}_{(k, T)}^{(v)} - \bar{\mathcal{H}}_{(k-1, T)}^{(v)}$$

Input Space	Output Space	CIFAR10 w Random		CIFAR10 w True		MNIST w True	
		$\Delta \bar{\mathcal{H}}$	p -values	$\Delta \bar{\mathcal{H}}$	p -values	$\Delta \bar{\mathcal{H}}$	p -values
0.Input	1.Conv	-.002; .006; -.003; -.001; -.004	.639; .035; .728; .543; .822	-.014; .017; -.021; .005; -.003	.662; .308; .729; .441; .533	.004; .004; .004; .004; .004	.094; .113; .137; .119; .103
1.Conv	1.ReLU	.002; .000; -.002; .001; .001	.348; .488; .676; .418; .412	.009; .001; .010; .012; .008	.402; .490; .395; .372; .415	.000; .000; .000; .000; -.000	.482; .488; .481; .466; .509
1.ReLU	2.Conv	.000; -.003; -.001; -.004; -.003	.499; .729; .583; .752; .789	-.006; -.003; -.019; -.004; -.006	.569; .531; .700; .544; .563	.000; .001; .001; .000; .001	.470; .429; .412; .449; .424
2.Conv	2.ReLU	.002; .005; .000; .004; -.001	.314; .138; .479; .251; .585	.054; .038; .064; .038; .046	.065; .136; .043; .138; .095	-.000; .000; .000; -.000; .000	.516; .498; .504; .510; .496
2.ReLU	2.MaxPool	.010; -.006; -.012; .002; -.001	.030; .919; .994; .323; .608	.041; .029; .053; .030; .031	.113; .198; .068; .195; .186	-.000; -.000; -.000; -.000; -.001	.517; .516; .536; .533; .568
2.MaxPool	3.Conv	-.014; .008; .012; -.007; .004	.996; .042; .016; .947; .150	.067; .027; .073; .019; .040	.028; .219; .024; .290; .122	.001; .001; .002; .001; .002	.332; .353; .284; .307; .281
3.Conv	3.ReLU	.005; -.002; .003; .006; .000	.157; .622; .301; .093; .495	.014; .021; .021; .022; .022	.346; .277; .286; .266; .260	-.000; -.000; -.001; -.000; -.001	.570; .542; .582; .551; .581
3.ReLU	4.Conv	-.005; -.005; -.009; -.002; -.002	.888; .858; .970; .689; .723	.022; -.006; .019; .002; -.002	.274; .570; .305; .476; .522	.001; .001; .001; .001; .001	.400; .409; .408; .374; .390
4.Conv	4.ReLU	.001; -.003; .008; .004; -.002	.405; .705; .023; .180; .640	-.057; -.045; -.026; -.120; -.053	.941; .906; .750; 1.000; .941	-.000; .000; .000; .000; .000	.523; .480; .455; .476; .434
4.ReLU	4.MaxPool	.007; .007; .005; .002; .013	.077; .050; .138; .348; .002	.089; .115; .061; .154; .119	.007; .000; .050; .000; .000	.003; .004; .004; .003; .003	.086; .042; .050; .077; .084
4.MaxPool	5.Dense	-.015; .003; -.009; -.010; -.008	.999; .237; .952; .973; .977	.049; .054; .035; .084; .058	.076; .056; .162; .008; .046	.002; .001; .001; .001; .002	.163; .225; .234; .217; .171
5.Dense	5.ReLU	.010; .000; -.002; .005; -.007	.018; .456; .693; .134; .944	-.027; -.016; .000; -.054; -.014	.782; .677; .500; .949; .662	.001; .001; .001; .001; .001	.288; .274; .168; .251; .147
5.ReLU	6.Dense	-.010; -.016; .006; -.011; .007	.987; 1.000; .071; .976; .089	.086; .084; .058; .118; .076	.006; .008; .043; .000; .012	.003; .002; .002; .002; .001	.008; .041; .081; .018; .103
6.Dense	6.Softmax	.001; .017; .010; .007; -.006	.407; .000; .011; .096; .880	-.009; .000; -.004; -.026; -.016	.611; .496; .557; .783; .692	-.003; -.003; -.004; -.005; -.005	.999; .999; 1.000; 1.000; 1.000

Table S-7: Validation data differences in mean of \mathcal{H} class-pair statistics between the input and output representations of multilayer layer components, and respective one-sided permutation test p -values. **Red font** denotes layer instances for which we reject \mathbf{H}_0 , and black font denotes layers for which we fail to reject \mathbf{H}_0 (Eq. 18 in paper). (Note: Note: Euclidean distance is used as the proximity measure. 50,000 Monte Carlo trials used to estimate the p -values. $\Delta\bar{\mathcal{H}} = \bar{\mathcal{H}}_{(k_2,T)}^{(v)} - \bar{\mathcal{H}}_{(k_1,T)}^{(v)}$)

Input Space	Output Space	CIFAR10 w Random		CIFAR10 w True		MNIST w True	
		$\Delta\bar{\mathcal{H}}$	p -values	$\Delta\bar{\mathcal{H}}$	p -values	$\Delta\bar{\mathcal{H}}$	p -values
0.Input	1.ReLU	.000; .006; -.005; .000; -.003	.482; .041; .850; .466; .776	-.005; .017; -.011; .017; .005	.561; .297; .631; .307; .440	.005; .004; .004; .004; .004	.086; .108; .121; .098; .104
1.ReLU	2.ReLU	.002; .002; -.001; .000; -.004	.316; .274; .558; .501; .846	.048; .035; .044; .035; .040	.086; .150; .110; .159; .126	-.000; .001; .001; .000; .001	.484; .426; .405; .458; .420
2.ReLU	2.MaxPool	-.010; -.006; -.012; .002; -.001	.030; .917; .992; .325; .607	.041; .029; .053; .030; .031	.114; .200; .070; .193; .186	-.000; -.000; -.000; -.000; -.001	.515; .525; .533; .531; .567
2.MaxPool	3.ReLU	-.009; .007; .015; -.001; .005	.960; .063; .003; .583; .135	.081; .047; .094; .041; .062	.011; .087; .006; .118; .037	.001; .001; .001; .001; .001	.403; .386; .349; .346; .351
3.ReLU	4.ReLU	-.004; -.008; -.002; .002; -.004	.827; .938; .654; .345; .835	-.036; -.051; -.006; -.118; -.055	.840; .932; .567; 1.000; .946	.001; .001; .001; .001; .001	.422; .393; .365; .354; .335
4.ReLU	4.MaxPool	.007; .007; .005; .002; .013	.078; .051; .138; .350; .002	.089; .115; .061; .154; .119	.007; .001; .049; .000; .000	.003; .004; .004; .003; .003	.089; .044; .049; .076; .084
4.MaxPool	5.ReLU	-.005; .004; -.012; -.004; -.015	.831; .175; .992; .806; 1.000	.022; .038; .035; .029; .044	.261; .127; .163; .188; .094	-.003; .002; .002; .002; .003	.066; .087; .050; .083; .028
5.ReLU	6.Softmax	-.009; .001; .017; -.004; .001	.979; .426; .000; .820; .415	.077; .084; .054; .093; .060	.011; .005; .048; .002; .029	-.000; -.001; -.002; -.003; -.003	.662; .860; .972; .987; .999

Table S-8: Validation data differences in mean of \mathcal{H} class-pair statistics between the input and output representations of multilayer layer components, and respective one-sided permutation test p -values. **Red font** denotes layer instances for which we reject \mathbf{H}_0 , and black font denotes layers for which we fail to reject \mathbf{H}_0 (Eq. 18 in paper). (Note: Euclidean distance is used as the proximity measure. 50,000 Monte Carlo trials used to estimate the p -values. $\Delta\bar{\mathcal{H}} = \bar{\mathcal{H}}_{(k_2,T)}^{(v)} - \bar{\mathcal{H}}_{(k_1,T)}^{(v)}$)

Input Space	Output Space	CIFAR10 w Random		CIFAR10 w True		MNIST w True	
		$\Delta\bar{\mathcal{H}}$	p -values	$\Delta\bar{\mathcal{H}}$	p -values	$\Delta\bar{\mathcal{H}}$	p -values
0.Input	2.MaxPool	.012; .003; -.018; .003; -.009	.007; .203; 1.000; .284; .969	.084; .082; .086; .082; .076	.007; .009; .007; .009; .012	.005; .005; .004; .004; .004	.087; .085; .100; .098; .102
2.MaxPool	4.MaxPool	-.006; .006; .018; .003; .014	.879; .045; .000; .288; .001	.135; .111; .149; .077; .126	.000; .001; .000; .013; .000	-.005; .005; .006; .005; .006	.032; .016; .011; .018; .014
4.MaxPool	5.ReLU	-.005; .004; -.012; -.004; -.015	.829; .172; .992; .806; 1.000	.022; .038; .035; .029; .044	.260; .122; .163; .187; .094	.003; .002; .002; .002; .003	.063; .087; .050; .081; .029
5.ReLU	6.Softmax	-.009; .001; .017; -.004; .001	.979; .426; .000; .823; .413	.077; .084; .054; .093; .060	.011; .004; .049; .002; .031	-.000; -.001; -.002; -.003; -.003	.667; .861; .972; .988; .999

Table S-9: Two-sided permutation test (Eq. 20 in paper) comparing the differences in the mean change induced on the training and validation statistics ($\Delta\mathcal{H}_{(k,k-1)}^{(t)}$ and $\Delta\mathcal{H}_{(k,k-1)}^{(v)}$). **Red font** denotes layer instances for which we reject \mathbf{H}_0 , and **black font** denotes layers for which we fail to reject \mathbf{H}_0 . (Note: Euclidean distance is used as the proximity measure. 50,000 Monte Carlo trials used to estimate the p -values. $\Delta\mu = \overline{\Delta\mathcal{H}}_{(k,k-1)}^{(t)} - \overline{\Delta\mathcal{H}}_{(k,k-1)}^{(v)}$)

Input Space	Output Space	CIFAR10 w Random		CIFAR10 w True		MNIST w True	
		$\Delta\mu$	p -values	$\Delta\mu$	p -values	$\Delta\mu$	p -values
0.Input	1.Conv	.005; -.006; -.001; -.003; .001	.156; .052; .769; .332; .811	-.004; -.006; -.004; -.004; -.005	.682; .225; .691; .457; .547	-.001; -.001; -.000; -.001; -.001	.212; .307; .852; .497; .242
1.Conv	1.ReLU	-.000; .002; .002; -.002; .000	.966; .204; .406; .376; .891	.001; .001; .001; .001; .000	.549; .569; .780; .598; .963	-.000; .000; .000; -.000; .000	.308; 1.000; 1.000; .459; .347
1.ReLU	2.Conv	-.006; -.009 ; -.007; -.003; -.000	.250; .020 ; .192; .467; .980	.004; .007; .006; .008; -.003	.390; .172; .184; .146; .541	-.000; .000; -.001; -.000; .000	.735; .825; .079; .923; .936
2.Conv	2.ReLU	-.003; -.001; .002; -.007 ; -.002	.362; .809; .509; .011 ; .592	-.003; .001; -.001; -.003; .007	.719; .892; .861; .575; .248	.000 ; .000; .000; .000; .000	.007 ; .832; .350; .672; .858
2.ReLU	2.MaxPool	-.017 ; .016 ; .008; -.004; .002	.000 ; .000 ; .088; .258; .701	.010; .011; .005; .004; .007	.130; .031; .434; .350; .154	-.001; -.001; -.001; -.001; -.001	.217; .188; .219; .227; .473
2.MaxPool	3.Conv	.018 ; -.012; -.013 ; .011 ; .000	.000 ; .027; .009 ; .014 ; .929	-.002; -.010; .004; -.004; -.004	.848; .049; .791; .321; .513	.001; .001; .001; .001; -.000	.421; .258; .332; .323; .974
3.Conv	3.ReLU	-.006; .002; -.005; -.010 ; -.005	.095; .616; .219; .011 ; .251	.000; .000; .002; .002; .007	.886; .970; .470; .614; .108	.000; -.000; -.000; .000; .000	.630; .335; 1.000; 1.000; .150
3.ReLU	4.Conv	-.001; .014 ; .015 ; -.003; .013	.805; .005 ; .005 ; .598; .007	.001; .001; .000; .006; -.002	.861; .772; .951; .281; .623	-.000; .000; -.000; -.000; .000	.672; .621; .948; .483; .717
4.Conv	4.ReLU	.005; .003; .001; .003; -.008	.406; .589; .783; .634; .177	.015; .009; .005; -.006; .016	.088; .267; .403; .695; .048	.000; .000; .000; .001; .000	1.000; .985; .969; .275; .890
4.ReLU	4.MaxPool	-.006; -.012 ; -.020 ; .007; -.017	.300; .012 ; .000 ; .247; .000	-.008; .004; -.004; .011; -.006	.332; .710; .516; .453; .581	.001; .000; .000; .000; .000	.348; .975; .789; .892; .731
4.MaxPool	5.Dense	.064 ; .028 ; .062 ; .039 ; .049	.000 ; .000 ; .000 ; .000 ; .000	.012 ; .013 ; .016 ; .020 ; .016	.013 ; .020 ; .001 ; .030 ; .006	.001; .001; .000; .001; .000	.431; .210; .387; .392; .938
5.Dense	5.ReLU	.179 ; .213 ; .204 ; .198 ; .218	.000 ; .000 ; .000 ; .000 ; .000	.040 ; .026 ; .015 ; .063 ; .029	.000 ; .000 ; .000 ; .000 ; .000	.001; .000; .000; -.000; .001	.217; .472; .511; .856; .239
5.ReLU	6.Dense	.768 ; .768 ; .744 ; .767 ; .746	.000 ; .000 ; .000 ; .000 ; .000	.134 ; .115 ; .090 ; .174 ; .124	.000 ; .000 ; .000 ; .000 ; .000	.002 ; .002 ; .003 ; .003 ; .003	.014 ; .015 ; .001 ; .003 ; .000
6.Dense	6.Softmax	-.001; -.017 ; -.010 ; -.007; .006	.750; .000 ; .025 ; .223; .266	.028 ; .019 ; .020 ; .036 ; .036	.000 ; .004 ; .000 ; .000 ; .000	.004 ; .005 ; .005 ; .006 ; .006	.000 ; .000 ; .000 ; .000 ; .000

S.2 Statistical analysis using cosine distance as measure of proximity

This supplemental material presents results for the three experiments (CIFAR10 with random labels, CIFAR10 with true labels, and MNIST with true labels) using the cosine distance for the proximity measure of the HP statistics. Note that the cosine distance between two vectors x and y is defined as

$$R_{\text{cosine}}(x, y) = 1 - \frac{x \cdot y}{\|x\| \|y\|} \quad (1)$$

Figure S-17 shows the between-class HP statistics of the raw images, or class separability in the original measurement space using the cosine distance. The comparisons were made using the analysis subset of the training data (1000 images per class) and the validation data (1000 images per class). As previously noted, there are five different versions of the randomly permuted labels; one per instance of the training network model. The results for only one of these versions is tabulated and plotted in Figures S-17 (A) and (D), respectively.

Figures S-18 through S-22 present the class-wise HP statistics of the training and validation samples of the CIFAR10 data with random labels as they pass through an associated model. Each figure plots the results for one of the five training instances discussed in Section 3 of the paper. The (a) subfigures show the data passing through the untrained models and the (b) subfigures show the data passing through the trained version of the models. Similarly, Figures S-23 through S-27 present plots for the 5 model instances trained on the CIFAR10 data with true labels, and Figures S-28 through S-32 show the plots for the 5 MNIST-trained models. As mentioned above, the cosine distance is used for all of these cases¹.

Tables S-10 through S-18 present results of two-sample null hypothesis test of the difference of means, where cosine distance is used in the HP divergence calculations. The tables flag cases where the estimated p -values are < 0.025 ².

¹Note that that the results using cosine distance and the Euclidian distance show similar trends.

²Note that the tests were performed using the random permutation algorithm with 50,000 Monte Carlo trials.

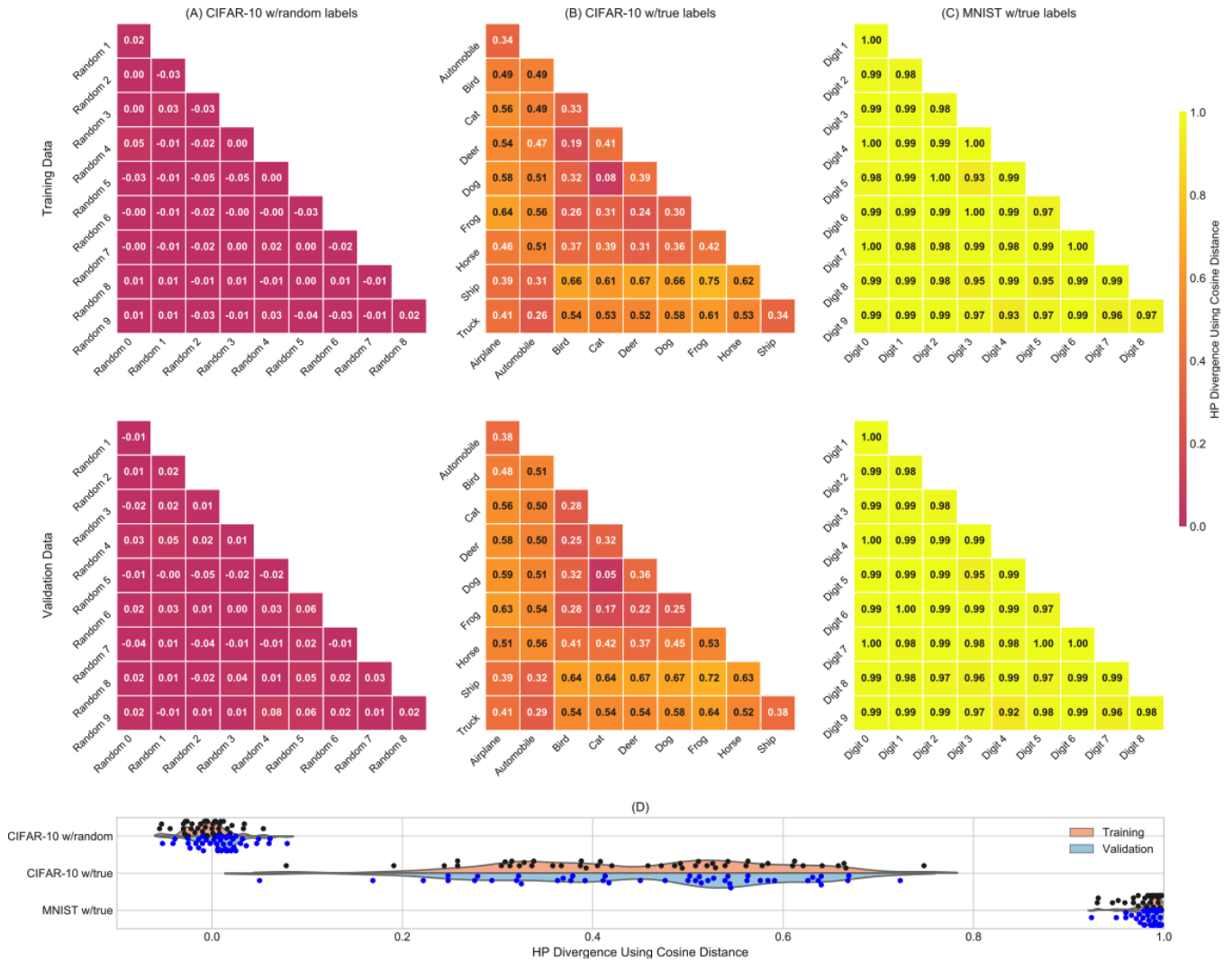


Figure S-17: Pairwise class HP statistics using cosine distance (training data above, validation data below) computed on (A) CIFAR10 with random labels, (B) CIFAR10 with true labels, and (C) MNIST with true labels. (D) The $\mathcal{H}^{(t)}$ (black dots above) and $\mathcal{H}^{(v)}$ (blue dots, below) values and respective kernel-based density functions (orange = training, blue = validation) for each task which illustrate that the estimated class separation for each task in their respective ambient representations are quite distinct.

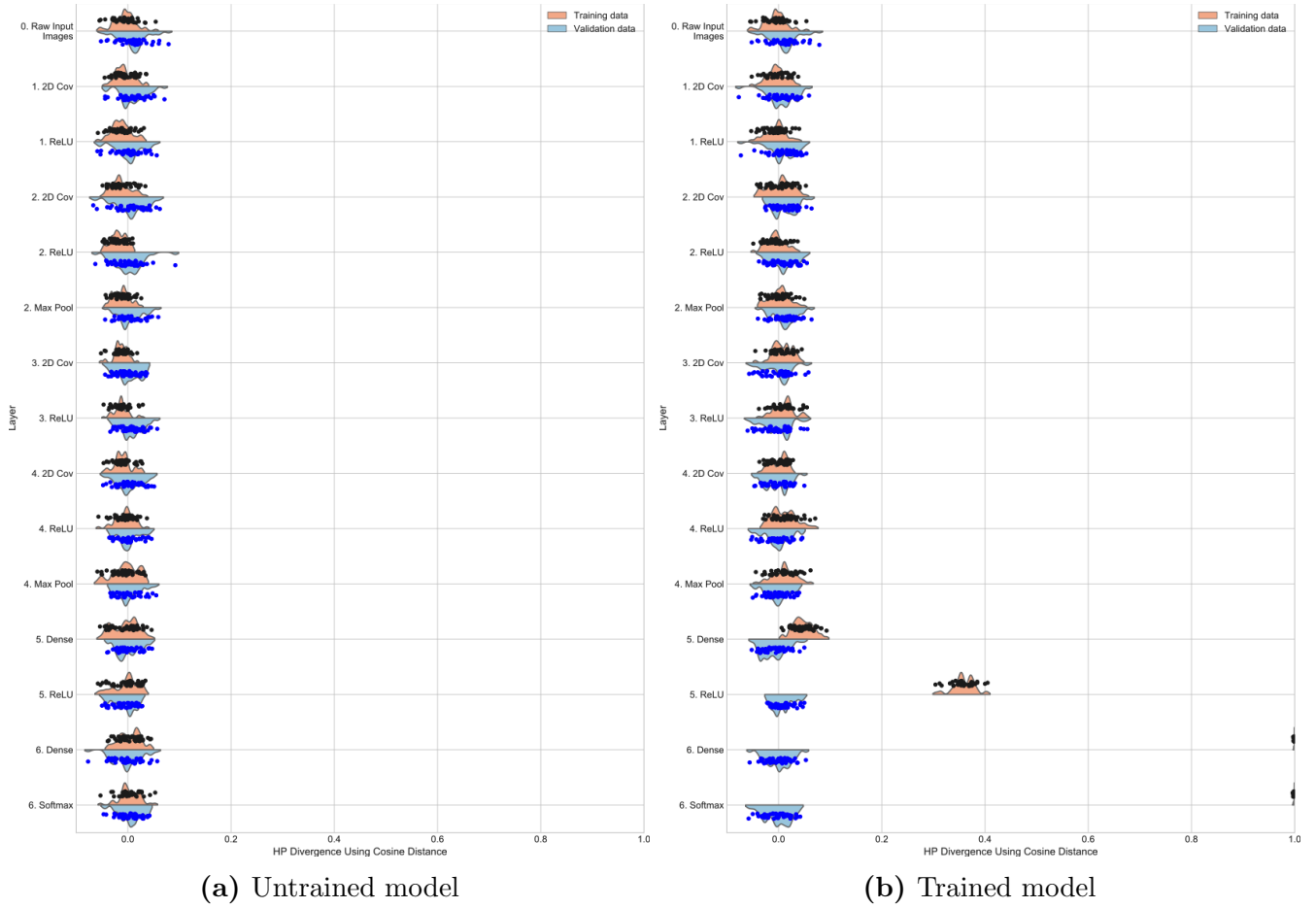


Figure S-18: \mathcal{H} class-pair statistics at each layer for instance 1 of the model for CIFAR10 with random class labels. (a) shows results for the data for passing through the randomly initialized model (epoch 0 state). (b) shows the results for the data passing through the fully trained model (epoch 200 state). (Note: Cosine distance is used as the proximity measure.)

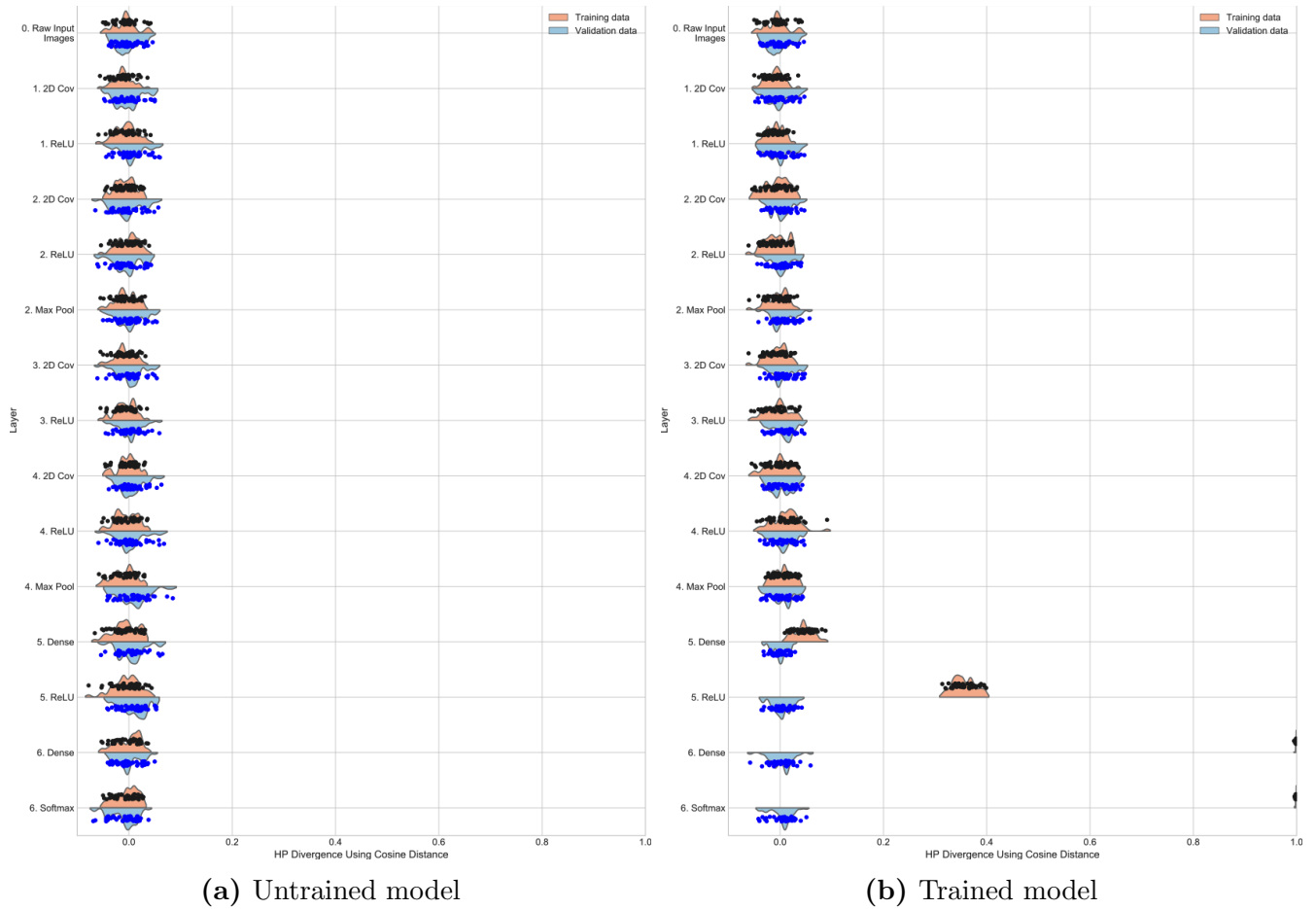


Figure S-19: \mathcal{H} class-pair statistics at each layer for instance 2 of the model for CIFAR10 with random class labels. (a) shows results for the data for passing through the randomly initialized model (epoch 0 state). (b) shows the results for the data passing through the fully trained model (epoch 200 state). (Note: Cosine distance is used as the proximity measure.)

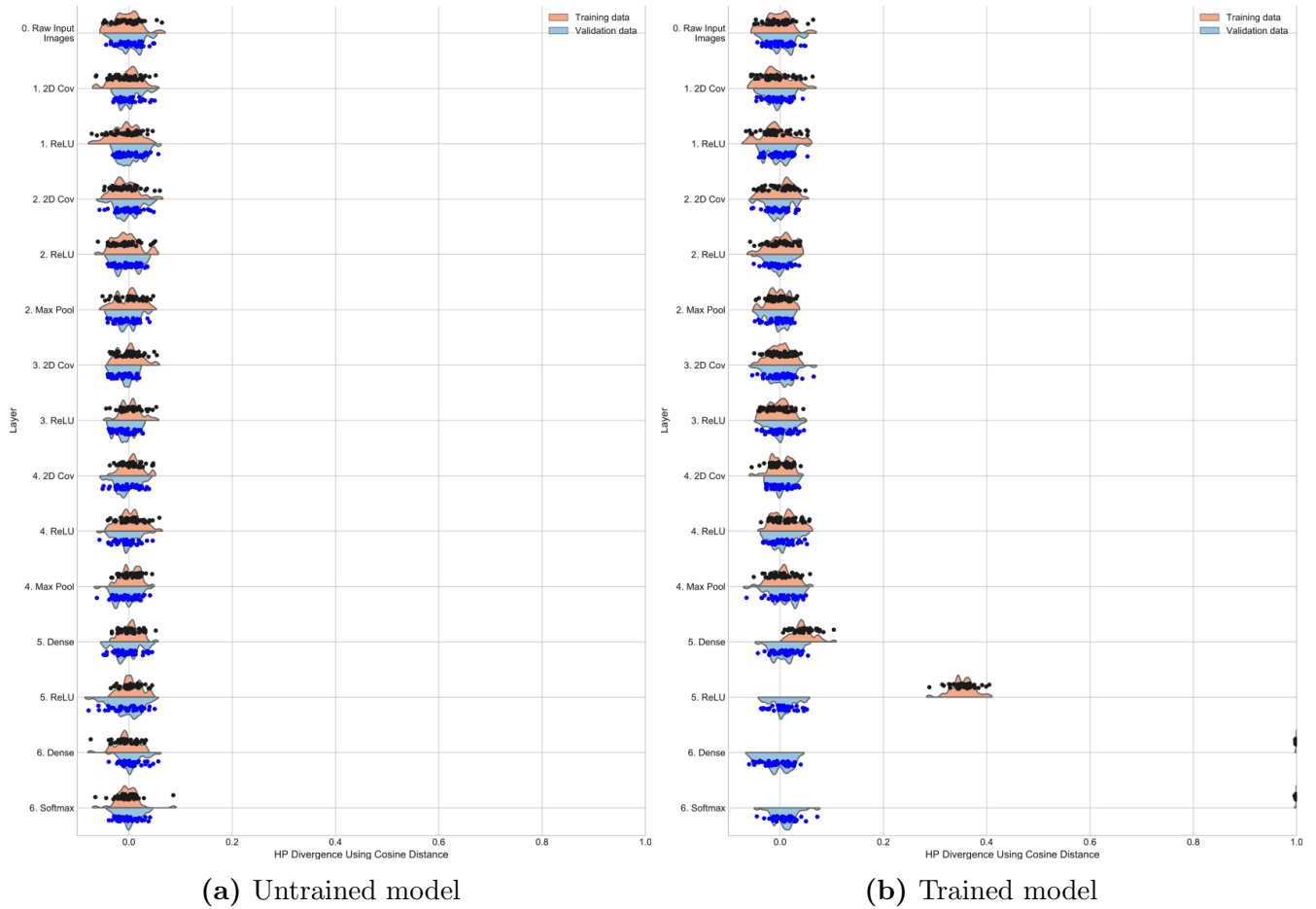


Figure S-20: \mathcal{H} class-pair statistics at each layer for instance 3 of the model for CIFAR10 with random class labels. (a) shows results for the data for passing through the randomly initialized model (epoch 0 state). (b) shows the results for the data passing through the fully trained model (epoch 200 state). (Note: Cosine distance is used as the proximity measure.)

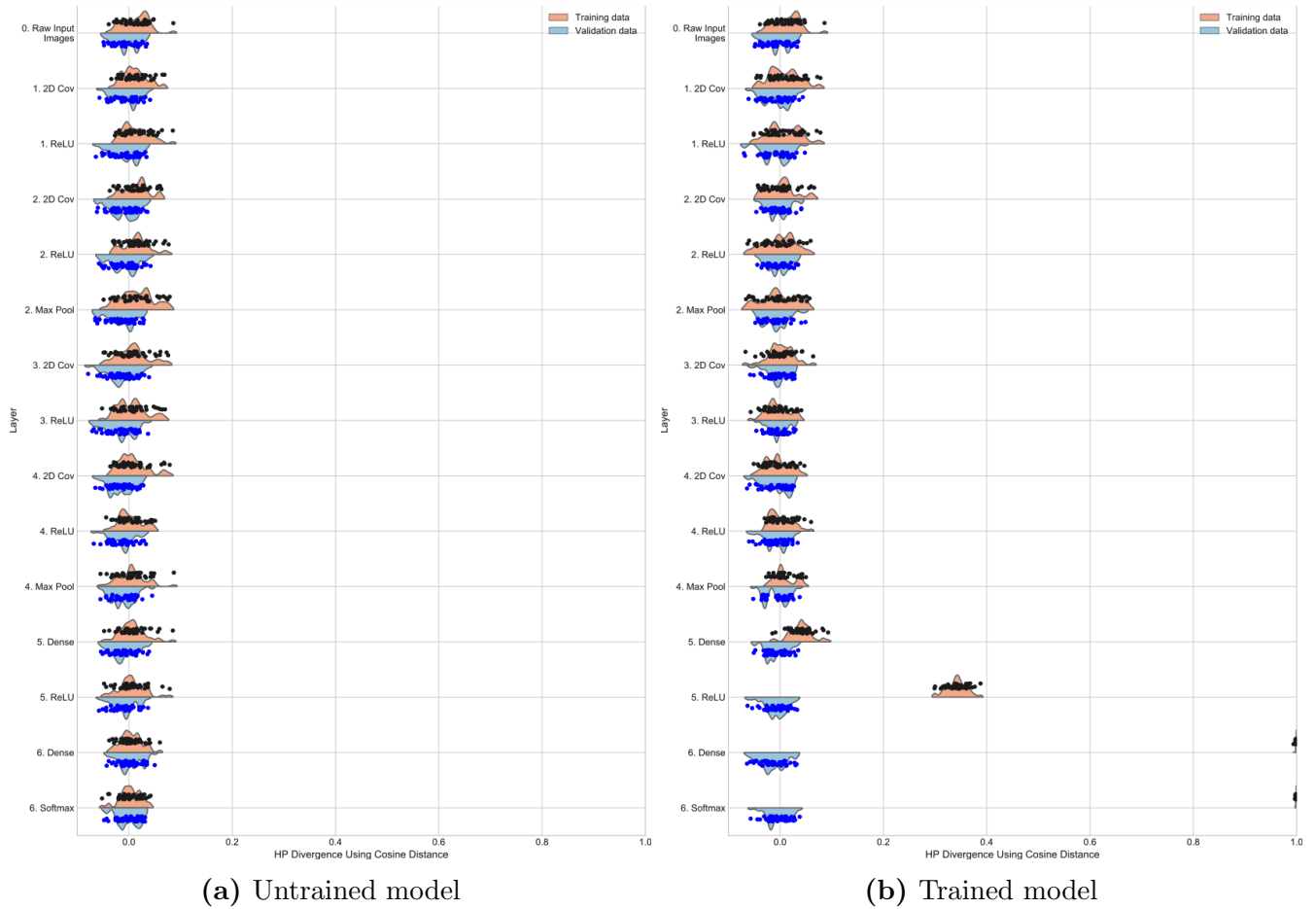


Figure S-21: \mathcal{H} class-pair statistics at each layer for instance 4 of the model for CIFAR10 with random class labels. (a) shows results for the data for passing through the randomly initialized model (epoch 0 state). (b) shows the results for the data passing through the fully trained model (epoch 200 state). (Note: Cosine distance is used as the proximity measure.)

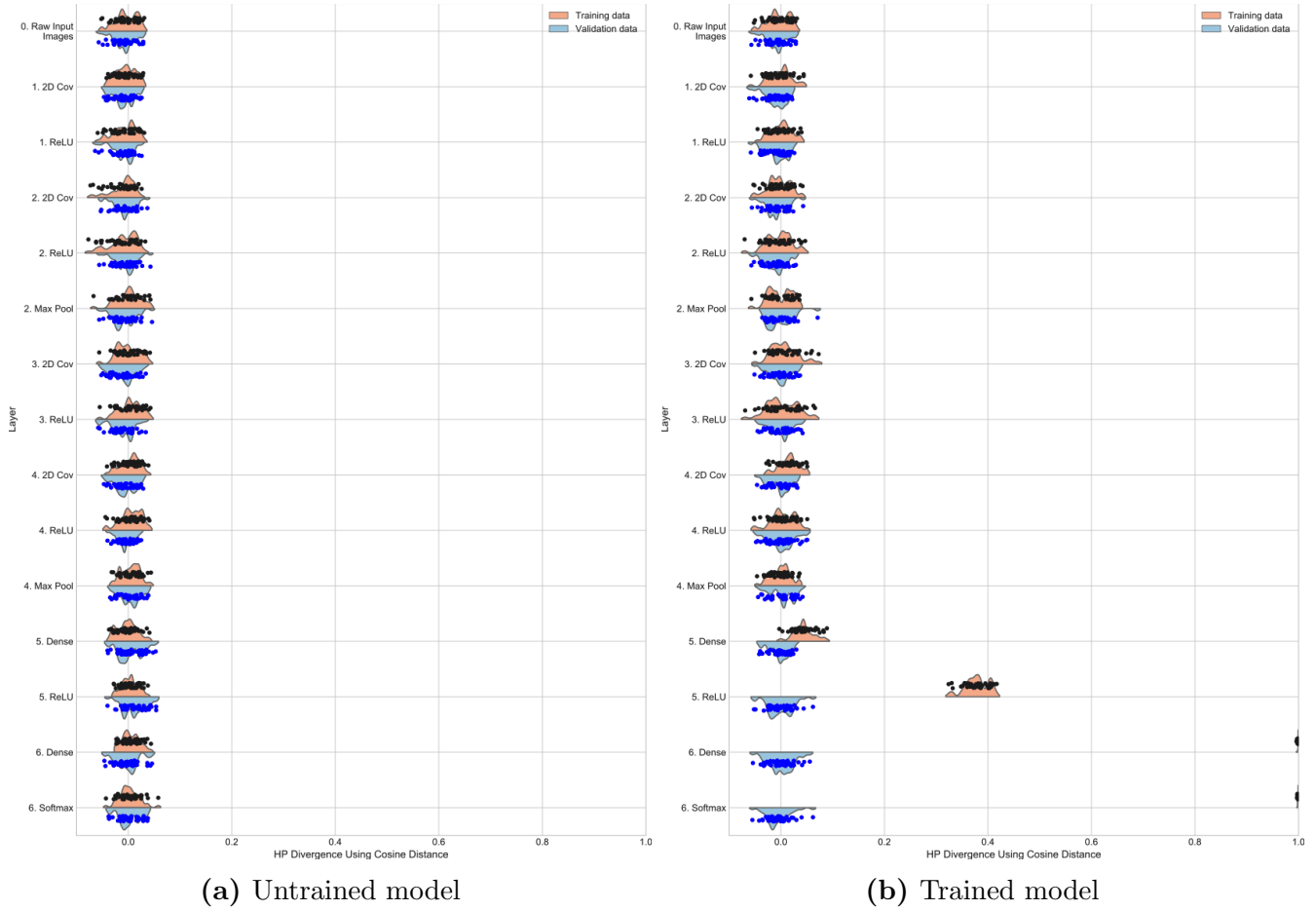


Figure S-22: \mathcal{H} class-pair statistics at each layer for instance 5 of the model for CIFAR10 with random class labels. (a) shows results for the data for passing through the randomly initialized model (epoch 0 state). (b) shows the results for the data passing through the fully trained model (epoch 200 state). (Note: Cosine distance is used as the proximity measure.)

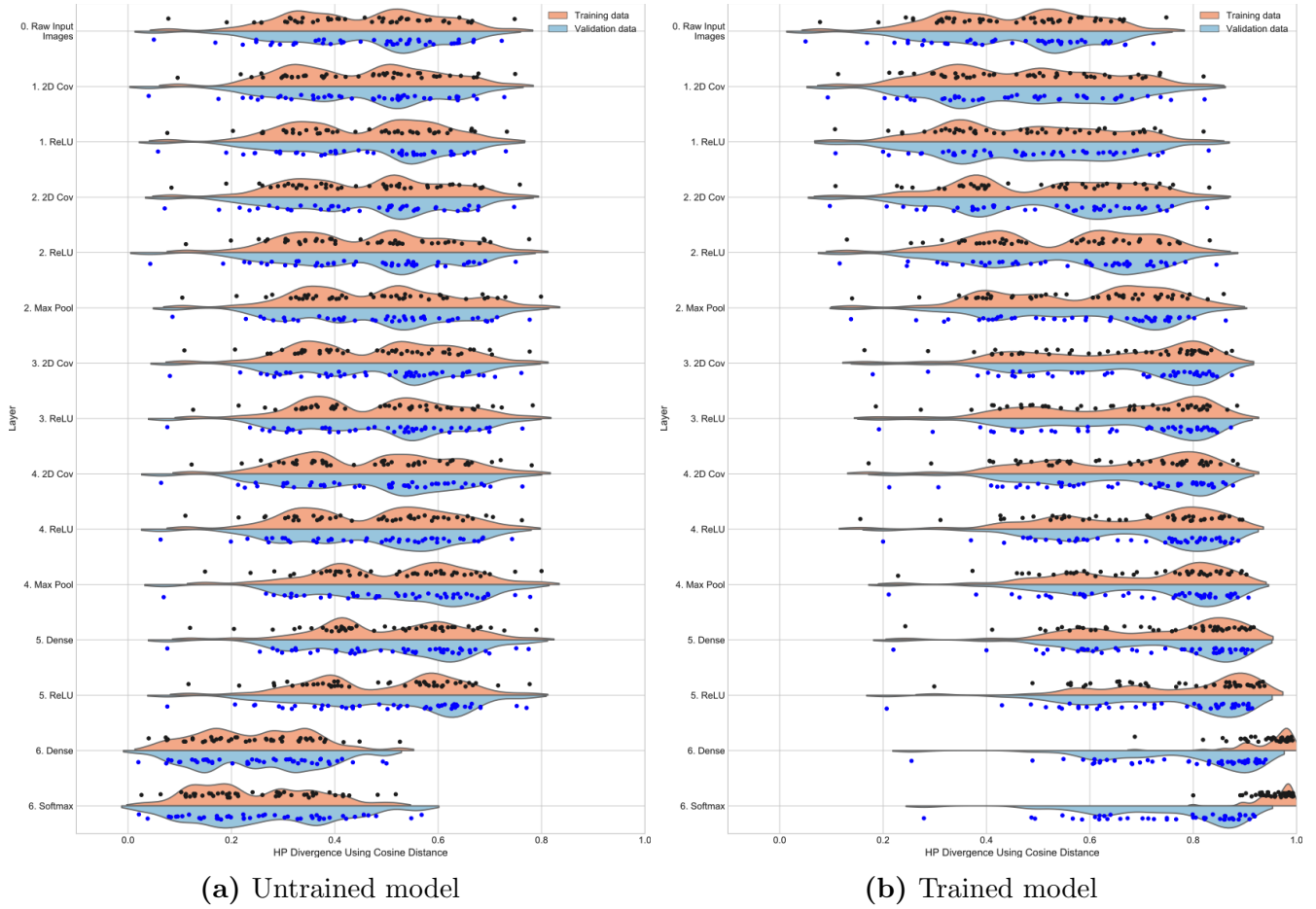


Figure S-23: \mathcal{H} class-pair statistics at each layer for instance 1 of the model for CIFAR10 with true class labels. (a) shows results for the data for passing through the randomly initialized model (epoch 0 state). (b) shows the results for the data passing through the fully trained model (stopping at peak validation set accuracy). (Note: Cosine distance is used as the proximity measure.)

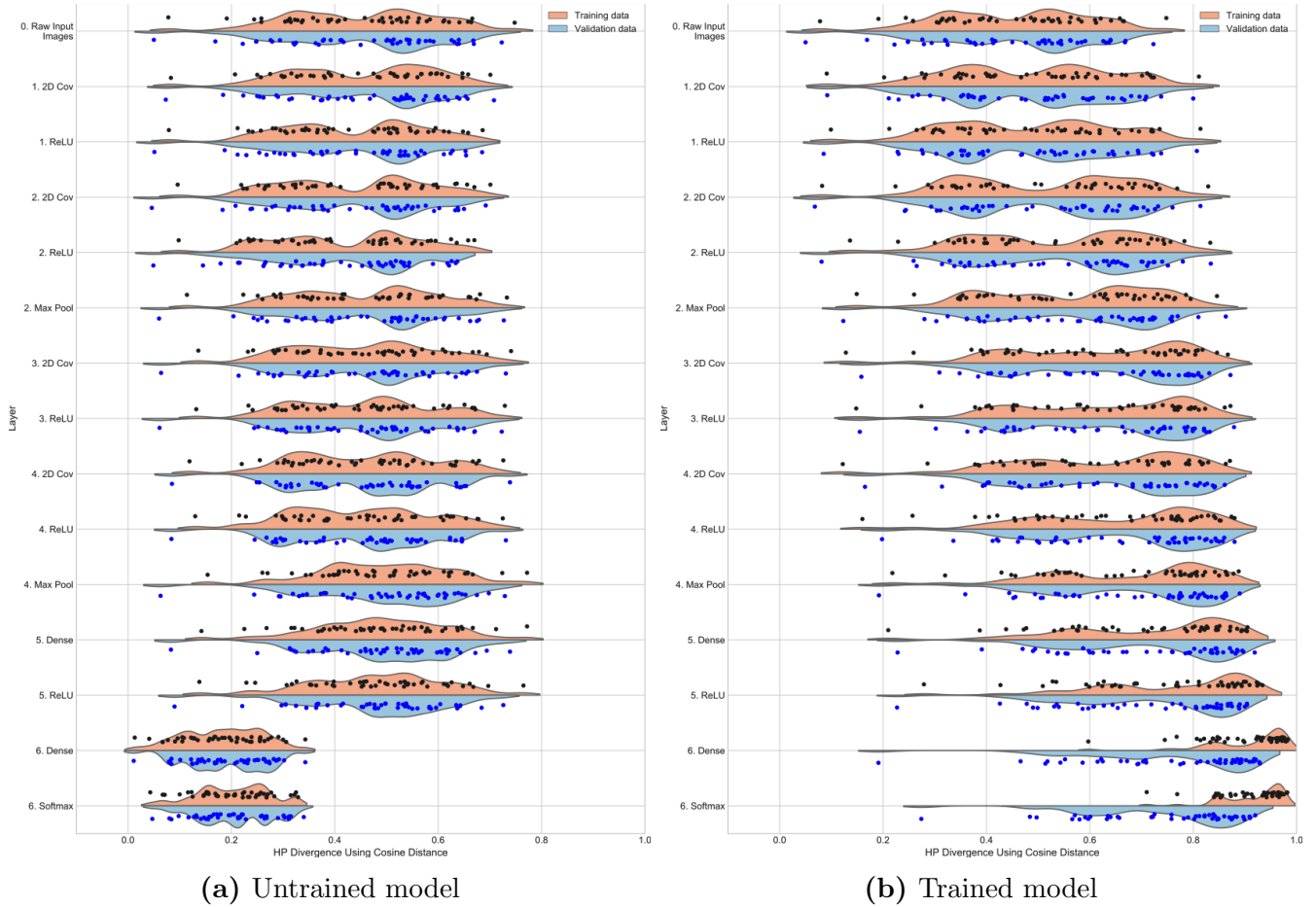


Figure S-24: \mathcal{H} class-pair statistics at each layer for instance 2 of the model for CIFAR10 with true class labels. (a) shows results for the data for passing through the randomly initialized model (epoch 0 state). (b) shows the results for the data passing through the fully trained model (stopping at peak validation set accuracy). (Note: Cosine distance is used as the proximity measure.)

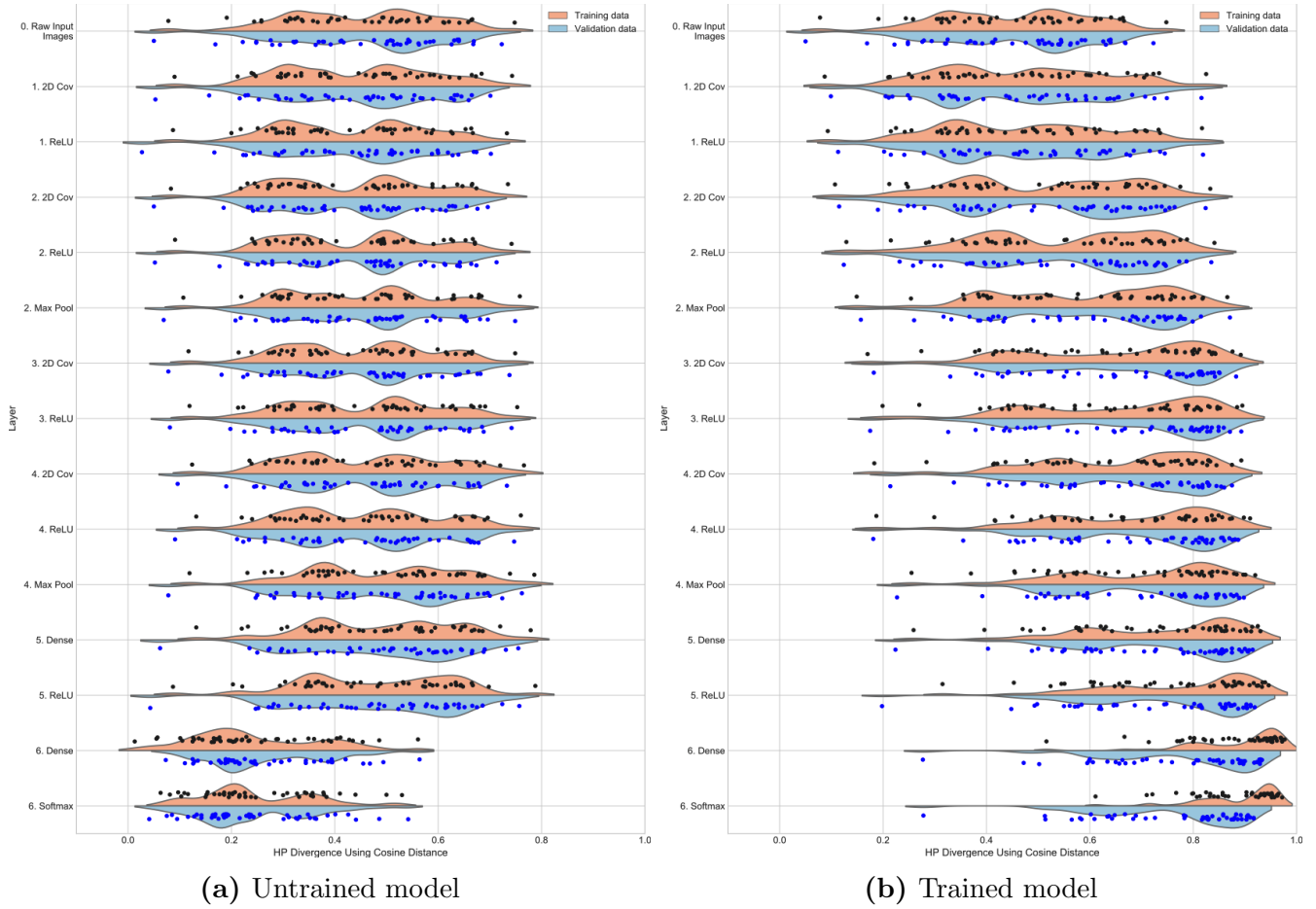


Figure S-25: \mathcal{H} class-pair statistics at each layer for instance 3 of the model for CIFAR10 with true class labels. (a) shows results for the data for passing through the randomly initialized model (epoch 0 state). (b) shows the results for the data passing through the fully trained model (stopping at peak validation set accuracy). (Note: Cosine distance is used as the proximity measure.)

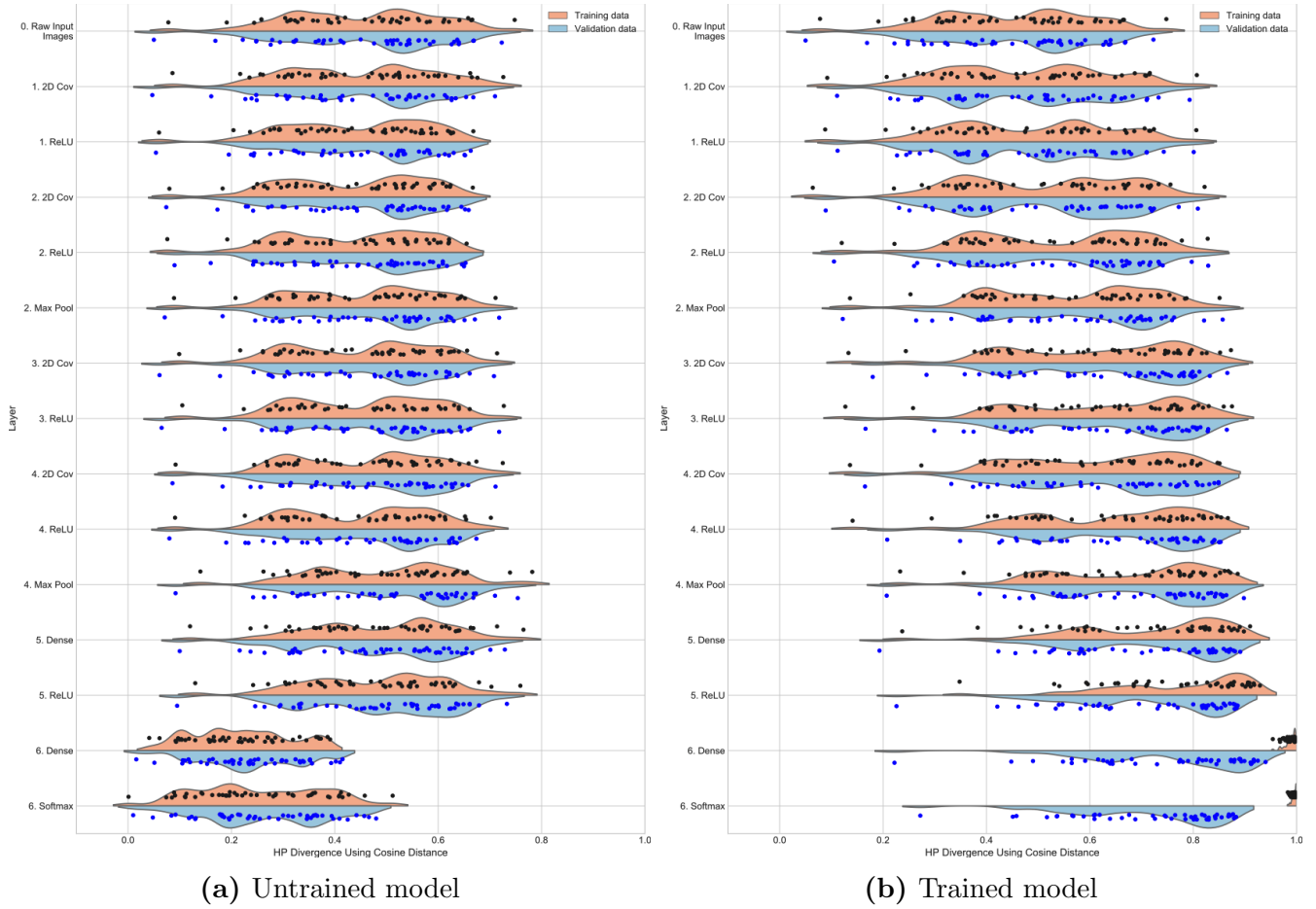


Figure S-26: \mathcal{H} class-pair statistics at each layer for instance 4 of the model for CIFAR10 with true class labels. (a) shows results for the data for passing through the randomly initialized model (epoch 0 state). (b) shows the results for the data passing through the fully trained model (stopping at peak validation set accuracy). (Note: Cosine distance is used as the proximity measure.)

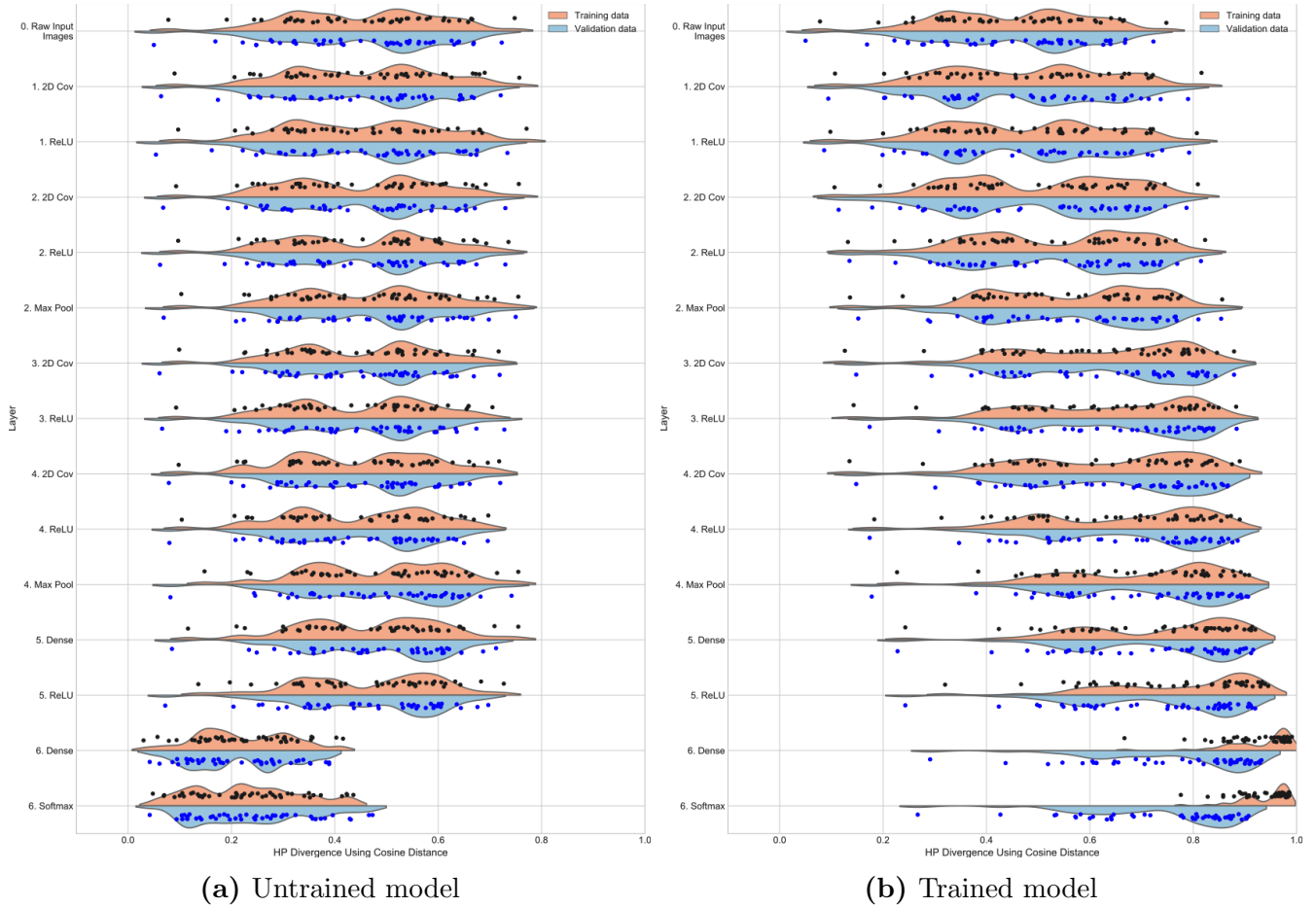


Figure S-27: \mathcal{H} class-pair statistics at each layer for instance 5 of the model for CIFAR10 with true class labels. (a) shows results for the data for passing through the randomly initialized model (epoch 0 state). (b) shows the results for the data passing through the fully trained model (stopping at peak validation set accuracy). (Note: Cosine distance is used as the proximity measure.)

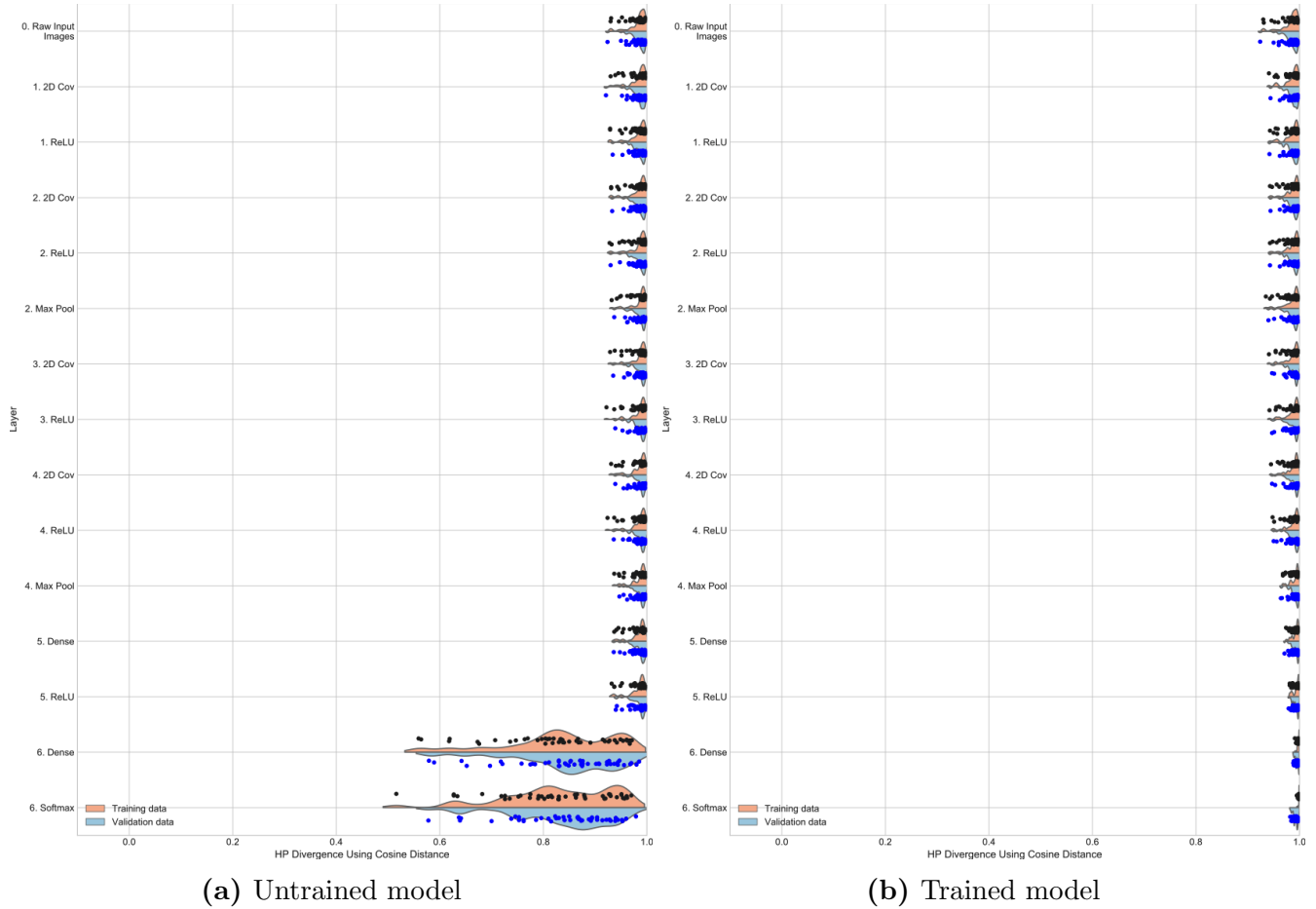


Figure S-28: \mathcal{H} class-pair statistics at each layer for instance 1 of the model for MNIST with true class labels. (a) shows results for the data for passing through the randomly initialized model (epoch 0 state). (b) shows the results for the data passing through the fully trained model (stopping at peak validation set accuracy). (Note: Cosine distance is used as the proximity measure.)

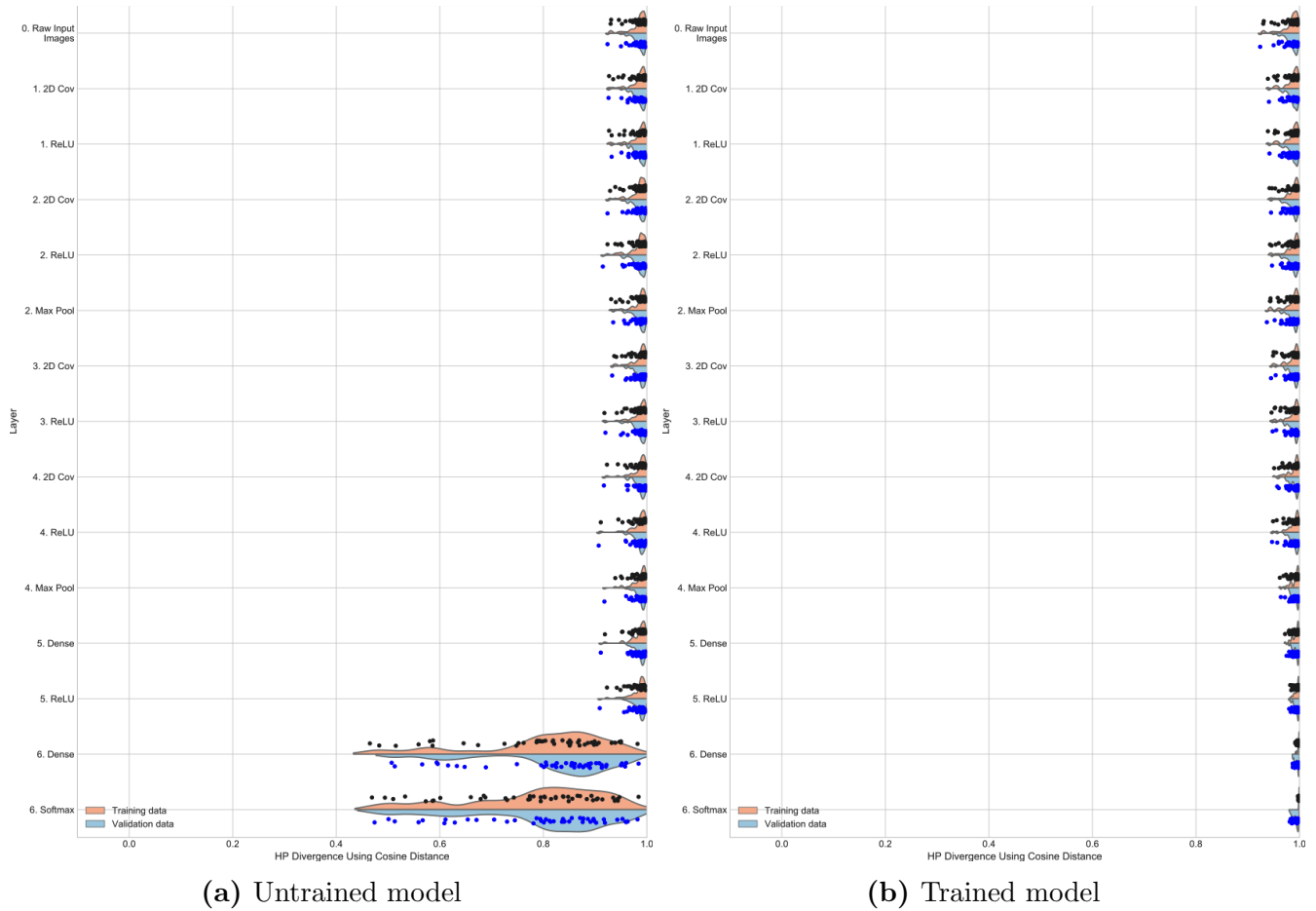


Figure S-29: \mathcal{H} class-pair statistics at each layer for instance 2 of the model for MNIST with true class labels. (a) shows results for the data for passing through the randomly initialized model (epoch 0 state). (b) shows the results for the data passing through the fully trained model (stopping at peak validation set accuracy). (Note: Cosine distance is used as the proximity measure.)

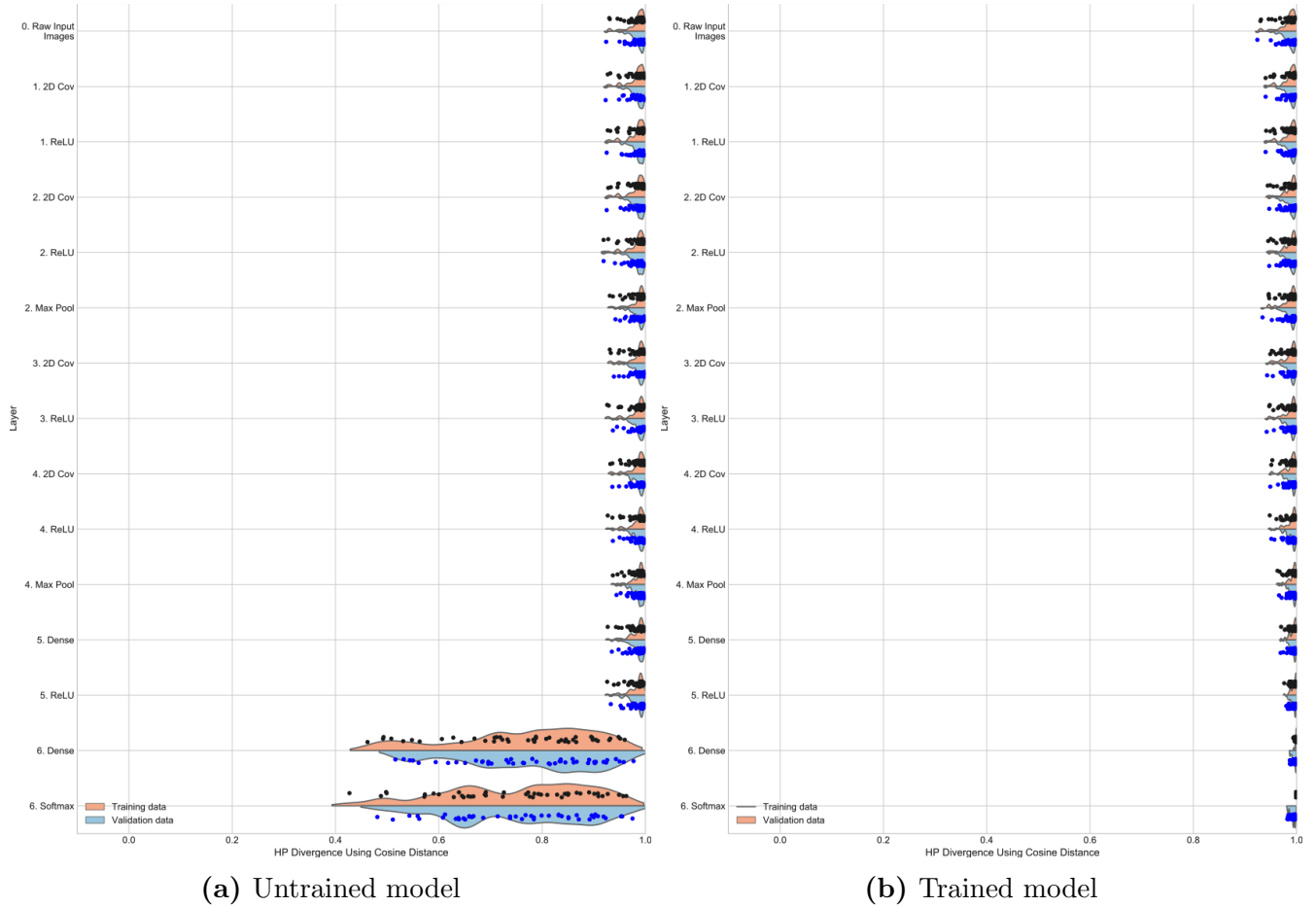


Figure S-30: \mathcal{H} class-pair statistics at each layer for instance 3 of the model for MNIST with true class labels. (a) shows results for the data for passing through the randomly initialized model (epoch 0 state). (b) shows the results for the data passing through the fully trained model (stopping at peak validation set accuracy). (Note: Cosine distance is used as the proximity measure.)

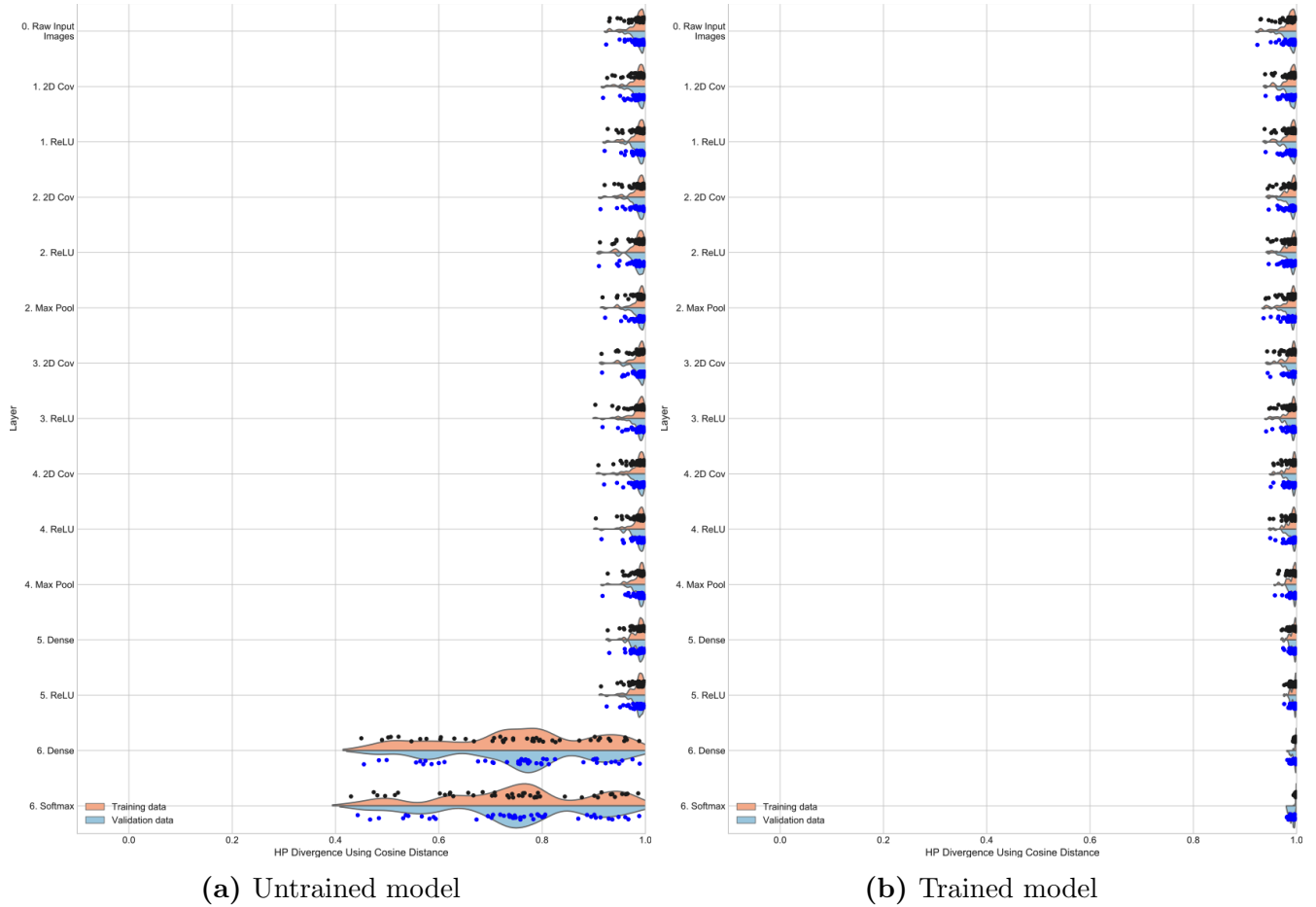


Figure S-31: \mathcal{H} class-pair statistics at each layer for instance 4 of the model for MNIST with true class labels. (a) shows results for the data for passing through the randomly initialized model (epoch 0 state). (b) shows the results for the data passing through the fully trained model (stopping at peak validation set accuracy). (Note: Cosine distance is used as the proximity measure.)

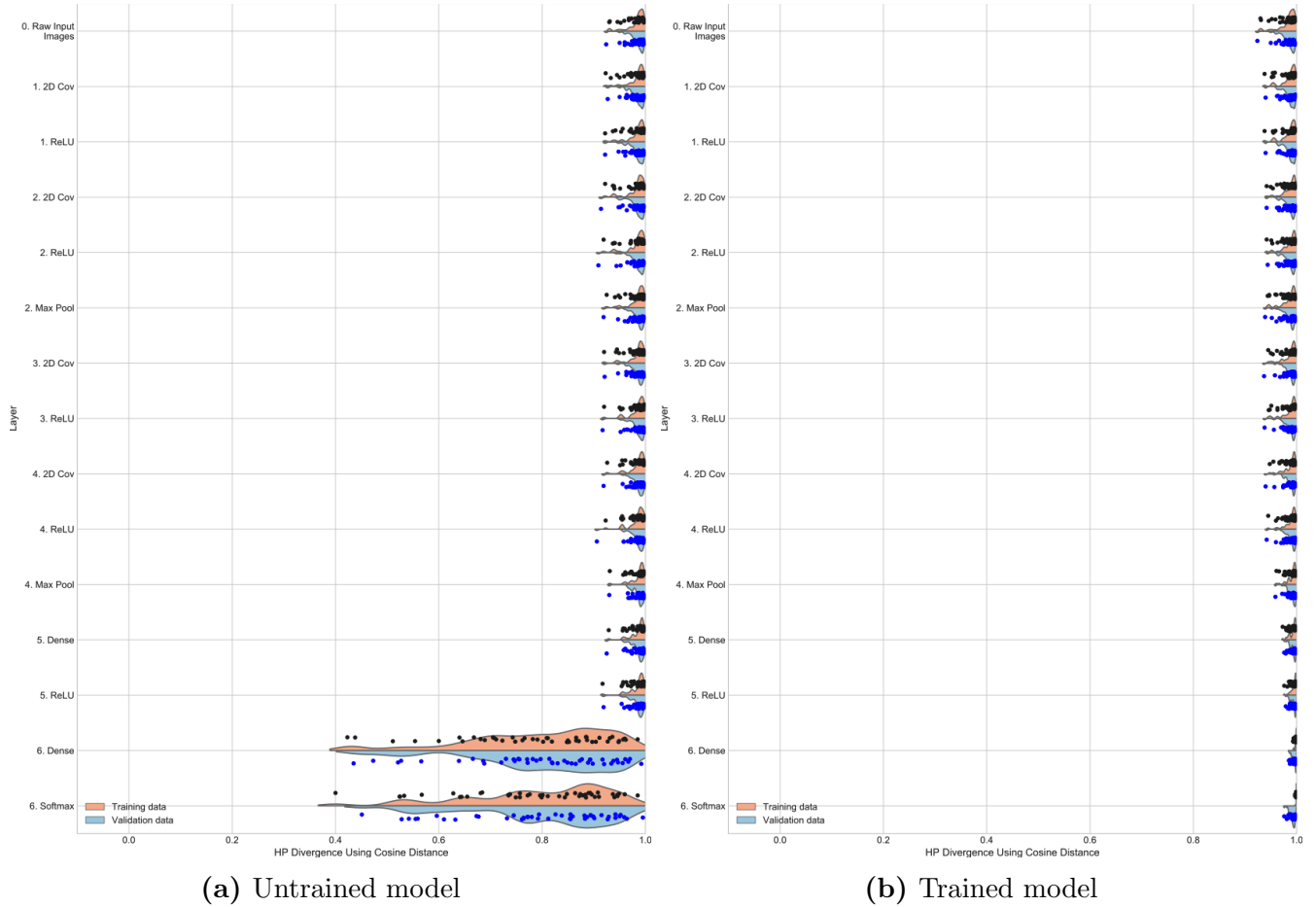


Figure S-32: \mathcal{H} class-pair statistics at each layer for instance 5 of the model for MNIST with true class labels. (a) shows results for the data for passing through the randomly initialized model (epoch 0 state). (b) shows the results for the data passing through the fully trained model (stopping at peak validation set accuracy). (Note: Cosine distance is used as the proximity measure.)

Table S-10: Two-sided permutation test of training data to detect change in $\bar{\mathcal{H}}$ between layers (before training) with critical value $\alpha = 0.025$. **Red font** denote layer instances for which we reject \mathbf{H}_0 , black font denotes layers for which we fail to reject \mathbf{H}_0 (Eq. 14 in paper). (Note: Cosine distance is used as the proximity measure. 50,000 Monte Carlo trials were used to estimate the p -values. $\Delta\bar{\mathcal{H}} = \bar{\mathcal{H}}_{(k,0)}^{(t)} - \bar{\mathcal{H}}_{(k-1,0)}^{(t)}$)

Input Space	Output Space	CIFAR10 w Random		CIFAR10 w True		MNIST w True	
		$\Delta\bar{\mathcal{H}}$	p -values	$\Delta\bar{\mathcal{H}}$	p -values	$\Delta\bar{\mathcal{H}}$	p -values
0.Input	1.Conv	-.001; -.004; -.001; -.002; -.001	.855; .302; .923; .736; .838	-.004; .002; -.011; -.002; .003	.901; .956; .725; .942; .932	-.001; .000; -.001; -.000; -.000	.827; .978; .793; .991; .994
1.Conv	1.ReLU	-.006; .005; -.003; .002; -.002	.158; .211; .619; .675; .719	.007; -.017; -.006; -.007; -.001	.828; .567; .843; .806; .973	-.000; .001; .000; .001; .000	.958; .870; .901; .754; .936
1.ReLU	2.Conv	-.001; -.002; .001; .001; -.003	.745; .725; .830; .893; .536	.005; -.001; -.000; -.007; -.004	.871; .984; .991; .821; .893	.000; -.000; -.000; -.001; -.001	.962; .948; .977; .854; .870
2.Conv	2.ReLU	-.004; .006; .001; .001; .000	.298; .148; .866; .924; .995	.002; -.014; .006; .001; .002	.947; .642; .848; .973; .940	.000; -.000; -.001; -.002; .000	.940; .905; .816; .644; .942
2.ReLU	2.MaxPool	.005; -.004; .006; .000; .010	.129; .337; .283; .960; .071	.016; .036; .011; .018; .012	.623; .236; .721; .537; .698	.001; .002; .003; .002; .001	.775; .658; .366; .522; .703
2.MaxPool	3.Conv	-.001; -.002; .001; -.008; -.000	.833; .627; .895; .220; .922	-.002; -.001; -.004; -.002; -.012	.958; .981; .897; .951; .690	-.000; .001; -.001; -.000; -.001	.984; .865; .876; .959; .836
3.Conv	3.ReLU	.000; .000; .003; -.002; .004	.899; .913; .519; .788; .405	.005; -.006; .008; .005; -.006	.883; .846; .793; .876; .832	-.001; -.001; -.001; -.001; .001	.844; .843; .851; .768; .827
3.ReLU	4.Conv	.003; .004; .003; .002; -.001	.403; .363; .525; .730; .811	-.008; .005; .005; .001; .004	.799; .863; .885; .974; .888	.001; .001; .000; .001; .001	.884; .783; .889; .872; .846
4.Conv	4.ReLU	.004; -.002; -.003; -.004; .003	.252; .692; .449; .411; .481	-.001; -.005; -.005; -.009; -.003	.983; .852; .868; .771; .931	-.001; -.001; -.000; .000; -.001	.880; .778; .920; .972; .862
4.ReLU	4.MaxPool	.002; -.005; .001; .002; -.001	.728; .280; .733; .660; .779	.041; .044; .034; .043; .037	.187; .120; .281; .143; .218	.000; .001; .001; .002; .002	.894; .711; .800; .643; .595
4.MaxPool	5.Dense	-.001; .004; -.001; .001; -.007	.796; .431; .828; .860; .096	-.010; -.007; .000; -.004; -.016	.734; .794; .997; .900; .594	-.001; -.001; -.002; -.001; -.001	.736; .742; .597; .828; .743
5.Dense	5.ReLU	.003; .002; .001; -.001; .005	.583; .773; .811; .856; .153	-.013; -.007; -.011; -.009; -.000	.673; .805; .730; .764; .993	-.001; -.002; -.001; -.001; -.001	.735; .575; .672; .664; .721
5.ReLU	6.Dense	-.006; .003; -.009; -.001; .001	.205; .571; .058; .846; .812	-.243; -.297; -.231; -.261; -.244	.000; .000; .000; .000; .000	-.152; -.188; -.221; -.232; -.193	.000; .000; .000; .000; .000
6.Dense	6.Softmax	.000; -.004; .001; -.001; -.002	.997; .401; .827; .745; .661	.002; .020; .004; .035; .007	.942; .205; .885; .132; .726	-.003; -.015; -.011; -.001; -.001	.884; .594; .711; .963; .966

Table S-11: Differences between the trained and initialized \mathcal{H} class-pair statistics of a layer, and respective p -values for the corresponding one-sided permutation test (Eq. 15 in paper). **Red font** denotes layer instances for which we reject \mathbf{H}_0 , and **black font** denotes layers for which we fail to reject \mathbf{H}_0 . (Note: Cosine distance is used as the proximity measure. 50,000 Monte Carlo trials to estimate the p -values. $\Delta\bar{\mathcal{H}} = \bar{\mathcal{H}}_{(k,T)}^{(t)} - \bar{\mathcal{H}}_{(k,0)}^{(t)}$)

Output Space	CIFAR10 w Random		CIFAR10 w True		MNIST w True	
	$\Delta\bar{\mathcal{H}}$	p -values	$\Delta\bar{\mathcal{H}}$	p -values	$\Delta\bar{\mathcal{H}}$	p -values
1.Conv	.003; .001; -.002; -.003; .003	.220; .394; .631; .674; .220	.020; .031; .022; .026; .020	.269; .173; .254; .211; .277	.002; .002; .003; .002; .003	.288; .241; .160; .231; .222
1.ReLU	.007; -.004; .001; -.006; .006	.055; .807; .409; .853; .094	.018; .050; .035; .042; .025	.297; .061; .147; .096; .222	.002; .002; .003; .002; .002	.275; .282; .183; .310; .227
2.Conv	.017 ; .001; .006 ; -.013; .006	.000 ; .406; .115; .989; .098	.049; .075 ; .076 ; .075 ; .050	.076; .014 ; .016 ; .013 ; .071	.002; .002; .004; .003; .003	.246; .229; .135; .209; .166
2.ReLU	.012 ; -.007; .007; -.016; .006	.000 ; .945; .087; .997; .116	.081 ; .116 ; .106 ; .100 ; .082	.008 ; .000 ; .001 ; .001 ; .008	.002; .003; .005; .004; .003	.271; .199; .095; .099; .177
2.MaxPool	.014 ; .001; -.003; -.017; -.001	.000 ; .441; .726; .993; .607	.105 ; .108 ; .139 ; .111 ; .101	.001 ; .001 ; .000 ; .001 ; .001	-.000; .000; -.000; .001; .001	.550; 473; .505; 436; .393
3.Conv	.021 ; .001; -.001; -.005; .007	.000 ; .430; .585; .822; .080	.164 ; .154 ; .196 ; .158 ; .168	.000 ; .000 ; .000 ; .000 ; .000	.001; .001; .002; .003; .003	.327; .343; .270; .213; .203
3.ReLU	.023 ; .002; -.008; -.011; -.001	.000 ; .348; .966; .972; .552	.164 ; .169 ; .199 ; .162 ; .188	.000 ; .000 ; .000 ; .000 ; .000	.002; .002; .003; .004; .002	.293; .269; .212; .155; .249
4.Conv	.010 ; -.000; -.005; -.012; .012	.003 ; .506; .892; .984; .002	.178 ; .164 ; .193 ; .154 ; .186	.000 ; .000 ; .000 ; .000 ; .000	.002; .002; .004; .005; .003	.245; .219; .105; .066; .168
4.ReLU	.016 ; .015 ; .008; -.002; -.001	.000 ; .002 ; .051; .633; .597	.203 ; .200 ; .224 ; .194 ; .212	.000 ; .000 ; .000 ; .000 ; .000	.003; .004; .005; .005; .004	.149; .114; .061; .061; .074
4.MaxPool	.014 ; .016 ; .001; .003; -.006	.002 ; .000 ; .428; .255; .930	.188 ; .183 ; .214 ; .185 ; .214	.000 ; .000 ; .000 ; .000 ; .000	.006 ; .005 ; .006 ; .006 ; .005	.012 ; .020 ; .004 ; .007 ; .024
5.Dense	.052 ; .051 ; .041 ; .033 ; .046	.000 ; .000 ; .000 ; .000 ; .000	.231; .227; .244; .227; .264	.000 ; .000 ; .000 ; .000 ; .000	.008 ; .008 ; .009 ; .008 ; .007	.000 ; .001 ; .000 ; .000 ; .001
5.ReLU	.362 ; .360 ; .350 ; .337 ; .375	.000 ; .000 ; .000 ; .000 ; .000	.286 ; .277 ; .293 ; .297 ; .309	.000 ; .000 ; .000 ; .000 ; .000	.011 ; .011 ; .012 ; .010 ; .010	.000 ; .000 ; .000 ; .000 ; .000
6.Dense	.995; 1.000; 1.003 ; .994; .995	.000 ; .000 ; .000 ; .000 ; .000	.698; .725; .637 ; .770; .706	.000 ; .000 ; .000 ; .000 ; .000	.167; .203; .238 ; .247 ; .207	.000 ; .000 ; .000 ; .000 ; .000
6.Softmax	.995 ; 1.004 ; 1.002 ; .996 ; .997	.000 ; .000 ; .000 ; .000 ; .000	.709 ; .714 ; .638 ; .741 ; .709	.000 ; .000 ; .000 ; .000 ; .000	.171 ; .219 ; .250 ; .249 ; .209	.000 ; .000 ; .000 ; .000 ; .000

Table S-12: Training data difference between input and output of each layer’s \mathcal{H} class-pair statistics for the trained models, and respective p -values for the one sided permutation test (Eq. 17 in paper). **Red font** denotes layer instances for which we reject \mathbf{H}_0 , and black font denotes layers for which we fail to reject \mathbf{H}_0 . (Note: Cosine distance is used as the proximity measure. 50,000 Monte Carlo trials used to estimate the p -values. $\Delta \bar{\mathcal{H}} = \bar{\mathcal{H}}_{(k,T)}^{(t)} - \bar{\mathcal{H}}_{(k-1,T)}^{(t)}$)

Input Space	Output Space	CIFAR10 w Random		CIFAR10 w True		MNIST w True	
		$\Delta \bar{\mathcal{H}}$	p -values	$\Delta \bar{\mathcal{H}}$	p -values	$\Delta \bar{\mathcal{H}}$	p -values
0.Input	1.Conv	.002; -.003; -.002; -.004; .002	.296; .794; .667; .767; .292	.016; .032; .011; .024; .023	.312; .163; .366; .231; .247	.003; .002; .002; .002; .003	.214; .230; .237; .231; .220
1.Conv	1.ReLU	-.002; .001; .001; -.002; .001	.686; .408; .467; .603; .414	.004; .003; .007; .008; .004	.457; .468; .422; .398; .459	-.000; .000; .000; .000; .000	.511; .487; .465; .469; .477
1.ReLU	2.Conv	.009; .003; .006; -.006; -.003	.028; .236; .154; .825; .731	.037; .024; .040; .027; .021	.153; .249; .133; .221; .271	.000; .000; .000; .000; .000	.441; .467; .440; .450; .466
2.Conv	2.ReLU	-.008; -.002; .002; -.003; .000	.969; .685; .368; .667; .478	.034; .027; .036; .026; .034	.169; .221; .161; .235; .169	-.000; .000; -.000; .000; .000	.494; .501; .499; .491; .480
2.ReLU	2.MaxPool	.007; .004; -.004; -.001; .002	.050; .193; .818; .544; .361	.040; .028; .043; .028; .031	.132; .216; .121; .205; .186	-.001; -.001; -.001; -.001; -.001	.669; .630; .669; .682; .617
2.MaxPool	3.Conv	.006; -.002; .002; .004; .008	.065; .683; .291; .257; .063	.057; .045; .053; .045; .054	.060; .108; .081; .103; .063	.002; .002; .001; .002; .001	.289; .302; .307; .268; .359
3.Conv	3.ReLU	.002; .002; -.004; -.007; -.004	.290; .368; .826; .919; .745	.005; .009; .012; .009; .014	.443; .399; .379; .404; .357	-.000; .000; -.000; -.000; .000	.548; .487; .498; .524; .463
3.ReLU	4.Conv	-.010; .002; .006; .001; .012	.994; .350; .103; .424; .016	.006; .000; -.001; -.007; .002	.437; .501; .509; .581; .475	-.001; .001; .002; .002; .001	.375; .318; .279; .246; .315
4.Conv	4.ReLU	.010; .013; .010; .006; -.010	.011; .006; .017; .118; .987	.024; .031; .025; .031; .024	.250; .204; .240; .193; .263	.001; .000; .001; .000; .001	.398; .431; .405; .459; .373
4.ReLU	4.MaxPool	-.000; -.005; -.006; .007; -.006	.504; .832; .885; .051; .903	.026; .028; .024; .034; .039	.227; .217; .247; .162; .133	.003; .003; .003; .003; .002	.089; .116; .107; .095; .155
4.MaxPool	5.Dense	.037; .040; .039; .031; .046	.000; .000; .000; .000; .000	.032; .036; .030; .037; .034	.170; .150; .184; .128; .153	.002; .002; .001; .001; .002	.176; .169; .224; .258; .157
5.Dense	5.ReLU	.312; .310; .310; .303; .334	.000; .000; .000; .000; .000	.043; .043; .038; .062; .044	.091; .102; .124; .022; .085	.001; .002; .001; .001; .002	.161; .065; .127; .163; .091
5.ReLU	6.Dense	.640; .643; .645; .657; .620	.000; .000; .000; .000; .000	.169; .151; .113; .211; .153	.000; .000; .000; .000; .000	.004; .003; .004; .004; .004	.000; .000; .000; .000; .000
6.Dense	6.Softmax	-.000; -.000; -.000; .000; -.000	.945; .809; .515; .523; .652	.013; .009; .005; .007; .010	.102; .267; .398; .000; .206	.001; .001; .001; .001; .001	.000; .000; .000; .016; .000

Table S-13: Training data difference between multi-layer component input and output \mathcal{H} class-pair statistics for the trained models, and respective p -values for the one sided permutation test (Eq. 17 in paper). **Red font** denotes layer instances for which we reject \mathbf{H}_0 , and black font denotes layers for which we fail to reject \mathbf{H}_0 . (Note: Cosine distance is used as the proximity measure. 50,000 Monte Carlo trials used to estimate the p -values. $\Delta \bar{\mathcal{H}} = \bar{\mathcal{H}}_{(k_2,T)}^{(t)} - \bar{\mathcal{H}}_{(k_1,T)}^{(t)}$)

Input Space	Output Space	CIFAR10 w Random		CIFAR10 w True		MNIST w True	
		$\Delta \bar{\mathcal{H}}$	p -values	$\Delta \bar{\mathcal{H}}$	p -values	$\Delta \bar{\mathcal{H}}$	p -values
0.Input	1.ReLU	.000; -.003; -.002; -.006; .004	.472; .739; .629; .838; .214	.020; .035; .018; .032; .026	.267; .145; .289; .165; .209	.003; .003; .003; .003; .003	.224; .214; .209; .210; .199
1.ReLU	2.ReLU	.000; .001; .008; -.009; -.003	.457; .426; .091; .910; .702	.071; .052; .077; .053; .056	.024; .071; .017; .066; .055	.000; .000; .000; .000; .000	.438; .466; .447; .438; .450
2.ReLU	2.MaxPool	.007; .004; -.004; -.001; .002	.049; .192; .819; .548; .353	.040; .028; .043; .028; .031	.135; .217; .118; .208; .184	-.001; -.001; -.001; -.001; -.001	.672; .628; .666; .684; .617
2.MaxPool	3.ReLU	.009; -.000; -.002; -.003; .004	.023; .545; .669; .695; .238	.062; .054; .064; .054; .068	.043; .068; .043; .064; .029	.001; .002; .001; .002; .001	.322; .292; .313; .293; .329
3.ReLU	4.ReLU	.000; .015; .016; .007; .001	.491; .002; .001; .078; .405	.030; .031; .024; .024; .026	.210; .202; .252; .252; .241	.002; .002; .002; .002; .002	.284; .256; .210; .217; .218
4.ReLU	4.MaxPool	-.000; -.005; -.006; .007; -.006	.507; .830; .882; .054; .902	.026; .028; .024; .034; .039	.224; .218; .248; .159; .133	.003; .003; .003; .003; .002	.087; .117; .106; .096; .154
4.MaxPool	5.ReLU	.349; .350; .349; .334; .380	.000; .000; .000; .000; .000	.075; .079; .068; .100; .079	.011; .010; .019; .001; .008	.003; .003; .003; .002; .003	.034; .011; .037; .059; .015
5.ReLU	6.Softmax	.639; .643; .645; .657; .620	.000; .000; .000; .000; .000	.182; .160; .118; .218; .163	.000; .000; .000; .000; .000	.005; .004; .005; .005; .004	.000; .000; .000; .000; .000

Table S-14: Training data difference between between multi-layer component input and output \mathcal{H} class-pair statistics for the trained models, and respective p -values for the one sided permutation test (Eq. 17 in paper). **Red font** denotes layer instances for which we reject \mathbf{H}_0 , and black font denotes layers for which we fail to reject \mathbf{H}_0 . (Note: Cosine distance is used as the proximity measure. 50,000 Monte Carlo trials used to estimate the p -values.

$$\Delta\bar{\mathcal{H}} = \bar{\mathcal{H}}_{(k_2, T)}^{(t)} - \bar{\mathcal{H}}_{(k_1, T)}^{(t)}$$

Input Space	Output Space	CIFAR10 w Random		CIFAR10 w True		MNIST w True	
		$\Delta\bar{\mathcal{H}}$	p -values	$\Delta\bar{\mathcal{H}}$	p -values	$\Delta\bar{\mathcal{H}}$	p -values
0.Input	2.MaxPool	.008; .002; .002; -.015; .003	.047; .328; .371; .992; .271	.131; .114; .139; .114; .113	.000; .000; .000; .000; .001	.002; .002; .002; .002; .002	.316; .295; .298; .314; .251
2.MaxPool	4.MaxPool	.009; .010; .008; .011; -.000	.031; .006; .046; .033; .537	.119; .112; .113; .113; .133	.000; .001; .001; .001; .000	.006; .006; .006; .006; .006	.012; .013; .007; .006; .013
4.MaxPool	5.ReLU	.349; .350; .349; .334; .380	.000; .000; .000; .000; .000	.075; .079; .068; .100; .079	.012; .010; .019; .001; .009	.003; .003; .003; .002; .003	.033; .011; .037; .059; .014
5.ReLU	6.Softmax	.639; .643; .645; .657; .620	.000; .000; .000; .000; .000	.182; .160; .118; .218; .163	.000; .000; .000; .000; .000	.005; .004; .005; .005; .004	.000; .000; .000; .000; .000

Table S-15: Validation data differences in mean of \mathcal{H} class-pair statistics between the input and output representations of a layer, and respective one-sided permutation test p -values. **Red font** denotes layer instances for which we reject \mathbf{H}_0 , and black font denotes layers for which we fail to reject \mathbf{H}_0 (Eq. 18 in paper). (Note: Note: Cosine distance is used as the proximity measure. 50,000 Monte Carlo trials used to estimate the p -values. $\Delta\bar{\mathcal{H}} = \bar{\mathcal{H}}_{(k, T)}^{(v)} - \bar{\mathcal{H}}_{(k-1, T)}^{(v)}$)

Input Space	Output Space	CIFAR10 w Random		CIFAR10 w True		MNIST w True	
		$\Delta\bar{\mathcal{H}}$	p -values	$\Delta\bar{\mathcal{H}}$	p -values	$\Delta\bar{\mathcal{H}}$	p -values
0.Input	1.Conv	-.002; .001; -.005; -.001; -.000	.669; .395; .886; .577; .524	.017; .032; .008; .022; .017	.309; .168; .410; .245; .307	.003; .002; .002; .002; .002	.161; .206; .193; .194; .205
1.Conv	1.ReLU	.002; .000; .001; -.000; .001	.381; .490; .417; .517; .447	.006; -.001; .012; .009; .004	.423; .512; .371; .396; .455	.000; .000; .000; .000; .000	.483; .477; .470; .475; .497
1.ReLU	2.Conv	.003; .003; -.002; .002; -.000	.287; .249; .640; .346; .501	.035; .026; .042; .025; .023	.164; .227; .124; .238; .264	.000; .000; .000; .000; .000	.432; .435; .453; .478; .461
2.Conv	2.ReLU	-.003; .001; .001; -.000; -.002	.754; .432; .399; .503; .717	.030; .024; .029; .028; .032	.200; .259; .229; .219; .188	-.000; .000; -.000; -.000; .000	.517; .499; .512; .505; .496
2.ReLU	2.MaxPool	.004; .003; -.001; -.006; .007	.219; .267; .578; .895; .050	.044; .030; .048; .030; .038	.112; .201; .099; .196; .136	-.001; -.001; -.001; -.001; -.001	.635; .692; .667; .670; .665
2.MaxPool	3.Conv	-.012; .000; .005; .006; .001	.989; .462; .127; .090; .396	.064; .054; .060; .053; .061	.040; .068; .057; .069; .045	.001; .002; .002; .002; .002	.302; .237; .275; .234; .266
3.Conv	3.ReLU	-.003; .002; .001; -.002; .001	.721; .311; .427; .650; .437	.003; .005; .009; .004; .012	.466; .443; .405; .448; .370	-.000; -.000; -.000; -.000; .000	.513; .520; .529; .531; .479
3.ReLU	4.Conv	-.001; -.004; .000; -.002; -.001	.556; .826; .498; .706; .593	.006; .004; .004; -.002; .003	.436; .452; .458; .523; .474	.000; .001; .001; .001; .001	.448; .337; .340; .344; .410
4.Conv	4.ReLU	.002; .002; .003; -.000; .003	.313; .308; .273; .525; .267	.024; .030; .023; .032; .030	.245; .203; .252; .176; .211	.001; -.000; .000; .000; .001	.383; .509; .472; .427; .408
4.ReLU	4.MaxPool	-.001; -.001; .005; .002; .004	.598; .605; .180; .355; .204	.018; .024; .017; .028; .031	.295; .253; .309; .204; .192	.002; .003; .003; .002; .002	.143; .104; .084; .132; .118
4.MaxPool	5.Dense	-.007; -.005; -.002; -.003; -.006	.931; .881; .624; .719; .932	.025; .029; .023; .025; .020	.233; .204; .246; .231; .283	.001; .001; .001; .001; .002	.203; .156; .298; .178; .160
5.Dense	5.ReLU	.017; .003; -.000; .001; .001	.000; .166; .543; .450; .417	.009; .009; .012; .003; .009	.398; .400; .357; .461; .390	.001; .001; .001; .001; .001	.239; .201; .167; .271; .283
5.ReLU	6.Dense	-.007; -.001; -.013; -.007; .002	.938; .552; .996; .932; .371	.040; .039; .035; .041; .035	.112; .125; .145; .106; .143	.002; .001; .002; .001; .002	.009; .144; .046; .112; .057
6.Dense	6.Softmax	-.002; .003; .015; .010; -.008	.658; .274; .002; .020; .946	-.026; -.012; -.019; -.038; -.025	.793; .644; .727; .883; .787	-.003; -.002; -.003; -.004; -.003	.999; .990; .999; 1.000; 1.000

Table S-16: Validation data differences in mean of \mathcal{H} class-pair statistics between the input and output representations of multilayer layer components, and respective one-sided permutation test p -values. **Red font** denotes layer instances for which we reject \mathbf{H}_0 , and black font denotes layers for which we fail to reject \mathbf{H}_0 (Eq. 18 in paper). (Note: Note: Cosine distance is used as the proximity measure. 50,000 Monte Carlo trials used to estimate the p -values. $\Delta\bar{\mathcal{H}} = \bar{\mathcal{H}}_{(k_2, T)}^{(v)} - \bar{\mathcal{H}}_{(k_1, T)}^{(v)}$)

Input Space	Output Space	CIFAR10 w Random		CIFAR10 w True		MNIST w True	
		$\Delta\bar{\mathcal{H}}$	p -values	$\Delta\bar{\mathcal{H}}$	p -values	$\Delta\bar{\mathcal{H}}$	p -values
0.Input	1.ReLU	-.001; .001; -.005; -.001; .000	.555; .381; .838; .593; .472	.023; .031; .020; .031; .021	.249; .176; .283; .174; .271	.003; .002; .003; .003; .002	.156; .188; .174; .183; .203
1.ReLU	2.ReLU	-.000; .004; -.001; .002; -.002	.527; .203; .549; .344; .715	.065; .050; .071; .053; .055	.036; .082; .025; .064; .063	-.000; .000; .000; .000; .000	.451; .435; .467; .481; .460
2.ReLU	2.MaxPool	.004; .003; -.001; -.006; .007	.225; .272; .582; .892; .051	.044; .030; .048; .030; .038	.111; .199; .100; .198; .136	-.001; -.001; -.001; -.001; -.001	.638; .689; .670; .670; .658
2.MaxPool	3.ReLU	-.015; .003; .006; .005; .002	.997; .267; .079; .137; .341	.067; .059; .069; .057; .074	.034; .053; .034; .053; .021	.001; .002; .001; .002; .002	.318; .248; .300; .264; .251
3.ReLU	4.ReLU	.002; -.002; .003; -.003; .002	.380; .668; .275; .749; .354	.030; .034; .028; .030; .032	.198; .174; .223; .195; .186	.001; .001; .001; .001; .001	.331; .354; .319; .289; .323
4.ReLU	4.MaxPool	-.001; -.001; .005; .002; .004	.598; .603; .180; .349; .201	.018; .024; .017; .028; .031	.296; .248; .315; .205; .192	.002; .003; .003; .002; .002	.146; .105; .084; .131; .118
4.MaxPool	5.ReLU	-.009 ; -.001; -.002; -.002; -.005	.016 ; .627; .655; .667; .877	.034; .038; .035; .028; .029	.166; .136; .149; .203; .200	.002; .002; .002; .002; .002	.070; .035; .068; .069; .069
5.ReLU	6.Softmax	-.009; .002; .001; .003; -.006	.973; .297; .380; .254; .896	.014; .027; .016; .004; .010	.329; .203; .306; .453; .377	-.000; -.001; -.001; -.002; -.002	.635; .894; .909; .990; .941

Table S-17: Validation data differences in mean of \mathcal{H} class-pair statistics between the input and output representations of multilayer layer components, and respective one-sided permutation test p -values. **Red font** denotes layer instances for which we reject \mathbf{H}_0 , and black font denotes layers for which we fail to reject \mathbf{H}_0 (Eq. 18 in paper). (Note: Cosine distance is used as the proximity measure. 50,000 Monte Carlo trials used to estimate the p -values. $\Delta\bar{\mathcal{H}} = \bar{\mathcal{H}}_{(k_2, T)}^{(v)} - \bar{\mathcal{H}}_{(k_1, T)}^{(v)}$)

Input Space	Output Space	CIFAR10 w Random		CIFAR10 w True		MNIST w True	
		$\Delta\bar{\mathcal{H}}$	p -values	$\Delta\bar{\mathcal{H}}$	p -values	$\Delta\bar{\mathcal{H}}$	p -values
0.Input	2.MaxPool	.003; .008; -.006; -.005; .005	.309; .039; .907; .843; .119	.132 ; .111 ; .138 ; .115 ; .114	.000 ; .001 ; .000 ; .000 ; .001	.002; .002; .002; .002; .002	.215; .287; .279; .294; .298
2.MaxPool	4.MaxPool	-.014; -.000; .013 ; .004; .008	.999; .538; .003 ; .213; .049	.115 ; .117 ; .113 ; .115 ; .137	.000 ; .001 ; .001 ; .001 ; .000	-.004 ; .005 ; -.005 ; .005 ; .005	.022 ; .010 ; .009 ; .009 ; .008
4.MaxPool	5.ReLU	-.009 ; -.001; -.002; -.002; -.005	.016 ; .624; .657; .670; .874	.034; .038; .035; .028; .029	.162; .139; .149; .200; .201	.002; .002; .002; .002; .002	.069; .036; .066; .069; .069
5.ReLU	6.Softmax	-.009; .002; .001; .003; -.006	.973; .300; .380; .264; .898	.014; .027; .016; .004; .010	.333; .202; .307; .451; .381	-.000; -.001; -.001; -.002; -.002	.634; .891; .909; .989; .942

Table S-18: Two-sided permutation test (Eq. 20 in paper) comparing the differences in the mean change induced on the training and validation statistics ($\Delta\mathcal{H}_{(k,k-1)}^{(t)}$ and $\Delta\mathcal{H}_{(k,k-1)}^{(v)}$). **Red font** denotes layer instances for which we reject \mathbf{H}_0 , and **black font** denotes layers for which we fail to reject \mathbf{H}_0 . (Note: Cosine distance is used as the proximity measure. 50,000 Monte Carlo trials used to estimate the p -values. $\Delta\mu = \overline{\Delta\mathcal{H}}_{(k,k-1)}^{(t)} - \overline{\Delta\mathcal{H}}_{(k,k-1)}^{(v)}$)

Input Space	Output Space	CIFAR10 w Random		CIFAR10 w True		MNIST w True	
		$\Delta\mu$	p -values	$\Delta\mu$	p -values	$\Delta\mu$	p -values
0.Input	1.Conv	.005; -.005; .003; -.003; .003	.201; .253; .467; .408; .472	-.000; -.000; .004; .001; .006	.961; .982; .694; .868; .442	-.000; .000; -.000; .000; .000	.914; .906; .948; .979; .776
1.Conv	1.ReLU	-.004; .001; -.000; -.001; .000	.046; .741; .833; .455; .805	-.002; -.004; -.005; -.000; -.000	.346; .133; .085; .835; .956	-.000; -.000; .000; .000; .000	.362; 1.000; .628; .881; .252
1.ReLU	2.Conv	.006; .000; .008; -.008; -.003	.244; .995; .089; .089; .560	.002; -.002; -.002; .002; -.001	.848; .774; .862; .821; .834	.000; -.000; .000; .000; .000	.911; .748; .772; .613; 1.000
2.Conv	2.ReLU	-.005; -.003; .001; -.003; .003	.128; .282; .825; .434; .382	.004; .004; .008; -.002; .002	.293; .293; .059; .574; .506	.000; .000; .000; .000; .000	.347; 1.000; .652; .436; .446
2.ReLU	2.MaxPool	.003; .001; -.004; .005; -.006	.436; .739; .332; .198; .160	-.004; -.002; -.004; -.002; -.007	.354; .575; .428; .654; .110	-.000; .000; -.000; -.000; .000	.483; .748; .831; .646; .841
2.MaxPool	3.Conv	.018 ; -.002; -.003; -.002; .007	.000 ; .541; .515; .605; .146	-.007; -.009; -.007; -.008; -.007	.446; .242; .393; .295; .404	.000; -.000; -.000; -.000; -.001	.430; .651; .927; .865; .319
3.Conv	3.ReLU	-.006; -.001; -.005; -.005; -.005	.085; .844; .120; .081; .208	.002; .004; .003; .005; .001	.215; .040; .197; .027; .613	-.000; .000; .000; .000; .000	.422; .610; .604; .943; .649
3.ReLU	4.Conv	-.009; .006; .006; .003; .013	.051; .171; .167; .474; .008	-.001; -.004; -.005; -.005; -.000	.888; .346; .412; .303; .944	.001; .000; .001; .001; .001	.394; .630; .366; .122; .202
4.Conv	4.ReLU	.008; .011; .007; .006; -.013	.082; .033; .181; .275; .008	.000; .001; .002; -.001; -.006	.967; .875; .652; .908; .232	-.000; .000; .000; -.000; .000	.965; .419; .420; .802; .568
4.ReLU	4.MaxPool	.001; -.003; -.011; .006; -.010	.822; .446; .033; .221; .055	.008; .004; .007; .007; .008	.050; .375; .057; .162; .049	.001; .000; -.000; .001; -.000	.384; 1.000; 1.000; .508; .740
4.MaxPool	5.Dense	.044 ; .044 ; .041 ; .033 ; .052	.000 ; .000 ; .000 ; .000 ; .000	.007 ; .007; .007 ; .013 ; .014	.013 ; .038; .046 ; .004 ; .000	.000; .000; .001; -.000; .000	.686; .936; .342; .548; .875
5.Dense	5.ReLU	.296 ; .307 ; .311 ; .302 ; .333	.000 ; .000 ; .000 ; .000 ; .000	.034 ; .034 ; .026 ; .059 ; .035	.000 ; .000 ; .000 ; .000 ; .000	.000; .001; .000; .001; .001	.386; .069; .650; .162; .015
5.ReLU	6.Dense	.647 ; .644 ; .658 ; .664 ; .619	.000 ; .000 ; .000 ; .000 ; .000	.129 ; .112 ; .079 ; .169 ; .118	.000 ; .000 ; .000 ; .000 ; .000	.002 ; .002 ; .002 ; .003 ; .002	.041 ; .000 ; .004 ; .000 ; .006
6.Dense	6.Softmax	-.002; -.003; -.015 ; -.010; .008	.664; .481; .004 ; .033; .129	.039 ; .021 ; .023 ; .045 ; .035	.000 ; .000 ; .000 ; .000 ; .000	.004 ; .003 ; .004 ; .004 ; .004	.000 ; .000 ; .000 ; .000 ; .000